STM et supra

Christian Lupien

Université de Sherbrooke

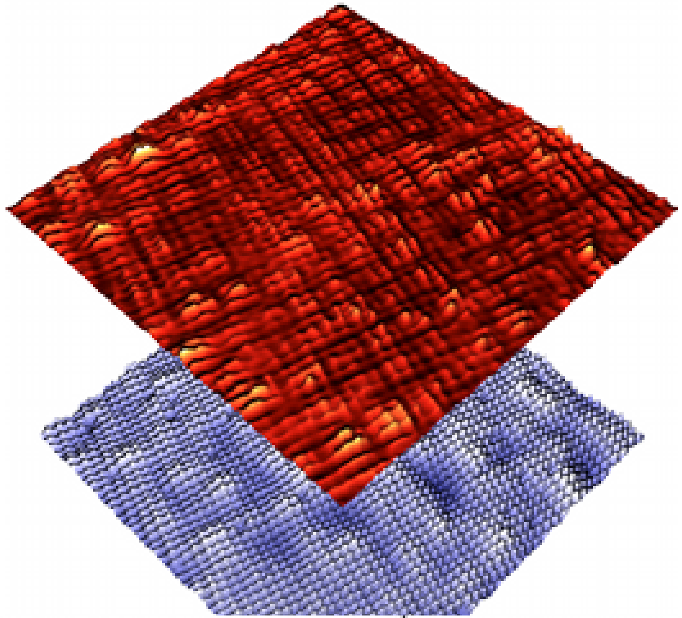

UNIVERSITÉ DE SHERBROOKE

Plan

- Théorie de STM/STS
  - Effet tunnel 1D
  - Tunnel dans STM/STS
- Mesures possibles
  - Effets de la pointe
  - Résolution atomique
  - Contrôle atomique
  - Spectroscopie
  - QPI

Questions générales

- Technique de surface:
  - Comme ARPES (sensibilité à la surface différente)
  - Plus simple pour systèmes 2D
    - En 3D surface et bulk peuvent être différent
      - Reconstruction de surface
      - États de surface (peuvent être à une énergie inopportune)
  - Bon pour systèmes 2D protégé
    - Couche isolante comme pour BSSCO et Na-CCOC
  - Excellent pour surface seulement (isolant topologique)
- Effet de la pointe (champ électrique fort, important pour semi-conducteurs, peu de porteur)

1D Tunneling: square potential barrier

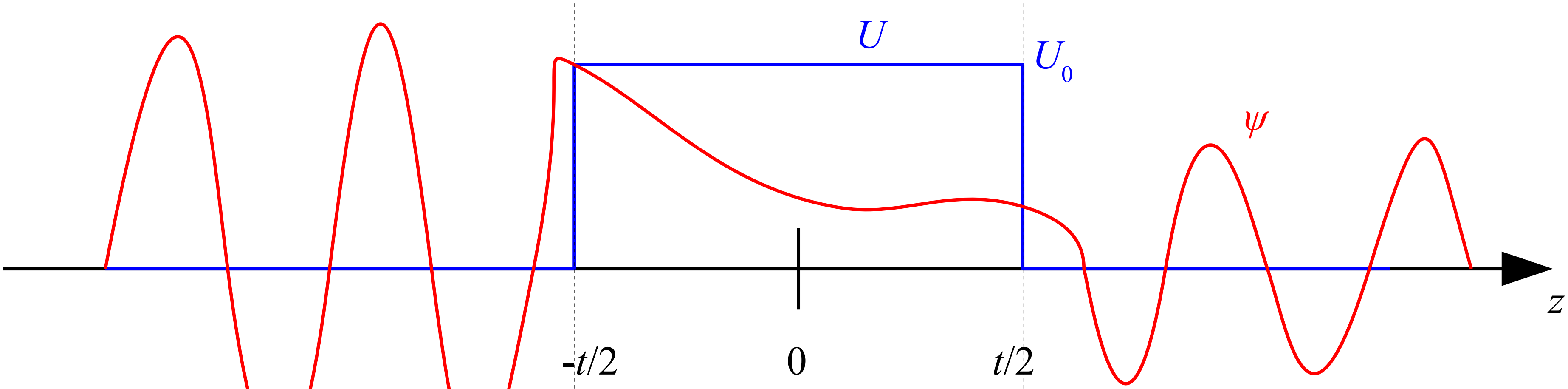

Solve with Schroedinger's equation

$$-\frac{\hbar^2}{2m}\frac{\partial^2\psi}{\partial z^2}-U\psi=E_z\psi$$

$$\psi=\exp(ik_z z)+R\exp(-ik_z z)$$

$$k_z=\sqrt{\frac{2m}{\hbar^2}E_z}$$

$$\psi=A\exp(\kappa z)+B\exp(-\kappa z)$$

$$\kappa=\sqrt{\frac{2m}{\hbar^2}(U_0-E_z)}$$

$$\psi=T\exp(ik_z z)$$

R: The reflected wave
T: The transmitted wave

$$1+|R^2|=|T^2|$$

Solve by having continuous

$$\psi,\ \frac{\partial\psi}{\partial z}$$

$$|(T)^2|=\frac{1}{1+\frac{(k_z^2+\kappa^2)^2}{4k_z^2\kappa^2}\sinh^2(\kappa t)}$$

$$|(T)^2|\approx\frac{16k_z^2\kappa^2}{(k_z^2+\kappa^2)^2}\exp(-2\kappa t)$$

For $\kappa t \gg 1$

Higher D, STM

- Change ψ to $\Psi = \psi \exp(ik_x x + ik_y y)$
- Answer stays the same.
- k_x, and k_y are conserved.
- The energy E is also conserved (elastic tunneling).
- U depends on work function of both ends and the applied voltage (not a constant anymore)
- $E_z = E - \frac{\hbar^2}{2\mathrm{m}}(k_x^2 + k_y^2)$
- Stronger tunneling if k_x, & k_y *are* small (for $E \sim U_0$).

Important results for a single electron

$$\left|(T)^2\right| \approx \boxed{\frac{16 k_z^2 \kappa^2}{(k_z^2+\kappa^2)^2}} \exp(-2\kappa t)$$

Fast Exponential decay
1 Å → ×10
Depends on work function

Matrix element
Depends on matching boundary conditions

For a more general potential

$$\left|(T)^2\right| = g \exp\left(-2\int_{z_1}^{z_2} dz \sqrt{\frac{2m}{\hbar^2}\left[U(z)-E_z\right]}\right)$$

Depending on approximations

$$g = \frac{16 k_z^2 \kappa^2}{(k_z^2+\kappa^2)^2} \quad \text{or} \quad g = 1 \quad \text{WKB approximation}$$

Théorie avec pointe

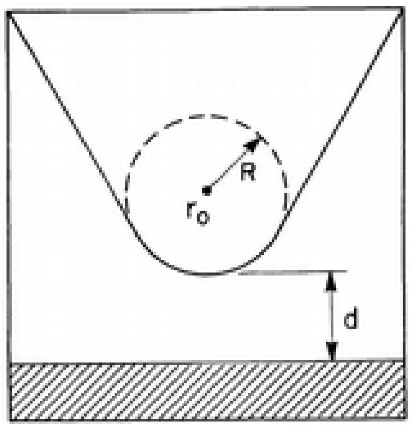

Pointe avec centre à r_o, rayon de courbure deR,

Distance de la surface de d.

Le plus simple: Géométrie sphérique des orbitales (s)
 (sinon type p, d, ...)

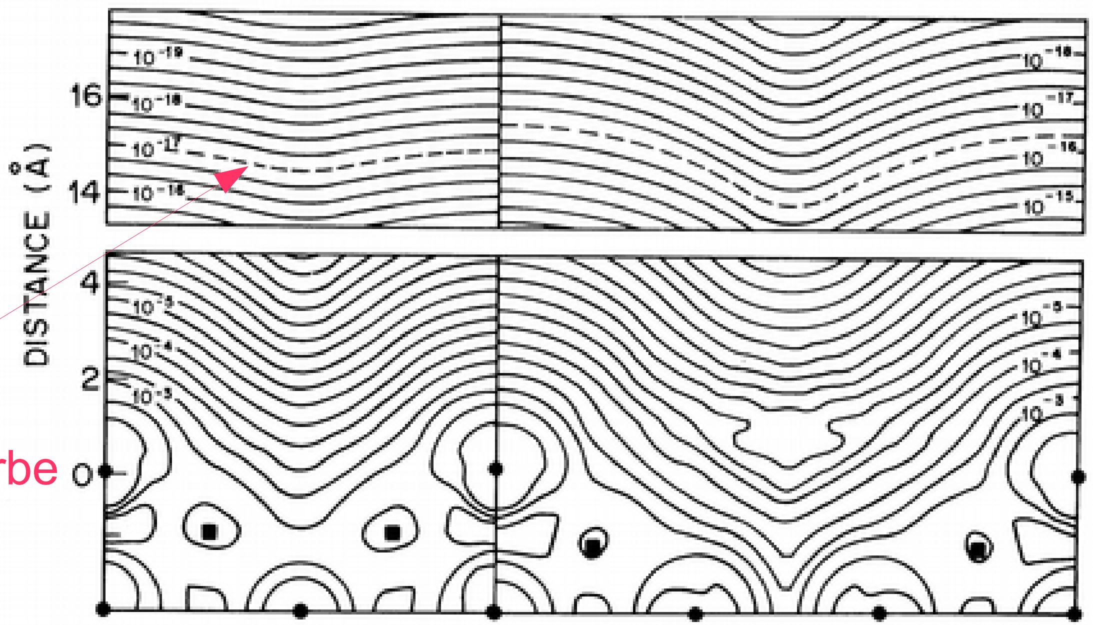

La pointe (r_o) suit une courbe de probabilité constante

FIG. 2. Calculated $\rho(r;E_F)$ for Au(110)(2×1) (left) and (3×1) (right) surfaces. Figure shows (1$\bar{1}$0) plane through outermost atoms. Positions of nuclei are indicated by solid circles (in plane) and squares (out of plane). Contours of constant $\rho(r;E_F)$ are labeled in units of a.u.$^{-3}$ eV^{-1}. Note break in distance scale. Peculiar structure around contour 10^{-5} of (3×1) is due to limitations of the plane-wave part of the basis in describing the exponential decay inside the deep troughs. Center of curvature of probe tip follows dashed line.

J. Tersoff, D. R. Hamann, PRL **50**, 1998 (1983), etPRB: **31,** 805 (1985)

Multiple electrons

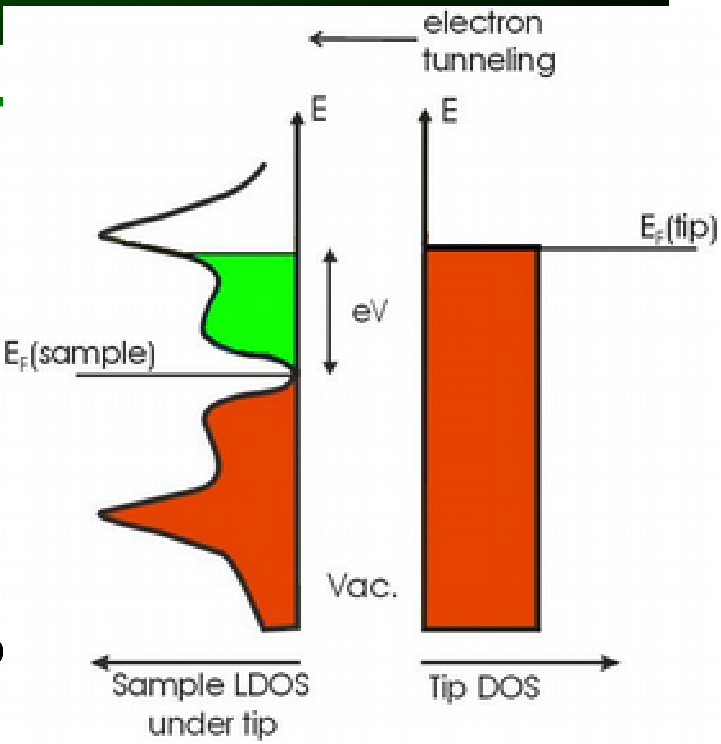

We need to insert the effect of the density of states and the temperature (Fermi function $f(E)$)

We assume small energy (vs work function) so κ is independent of energy.

Calculate the conventional current from sample to tip

$$I = M \exp(-2\kappa z) \int_{-\infty}^{+\infty} dE\, n_S(E+eV)\, n_T(E) \left[f(E) - f(E+eV) \right]$$

$$f(E) = \frac{1}{1+\exp\left(\frac{E-\mu}{k_B T}\right)}$$

n_S and n_T are the sample and tip density of states
M is a matrix element (could be inside the integral)
V is voltage applied on sample.

At T=0, the Fermi function disappear and change the integral limits to between -eV and 0

Spectra: conductance

The measured conductance G is given by:

$$G = \frac{dI}{dV} = M\exp(-2\kappa z)\, n_T(0) \int_{-\infty}^{+\infty} dE\, n_S(E+eV) \frac{1}{4k_B T \cosh^2\left(\frac{E}{2k_B T}\right)}$$

Where we assume n_T has a weak energy dependence (valid for small energies) and a good metallic tip

The smearing effect due to the temperature.
At T=0 $\rightarrow \delta(E)$
So $G \approx n_s(eV)$

<u>G can be measured directly with a lock-in</u>

Also from a I vs z curve, can extract κ hence the work function.

Inelastic tunneling

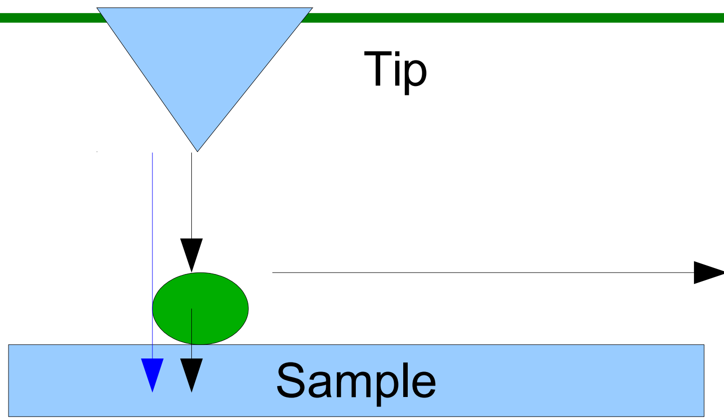

The electrons tunnel
But leave some energy in an excitation of energy E_e (molecular vibration, ...)

Only possible if $E>E_e$

Conductance spectra:

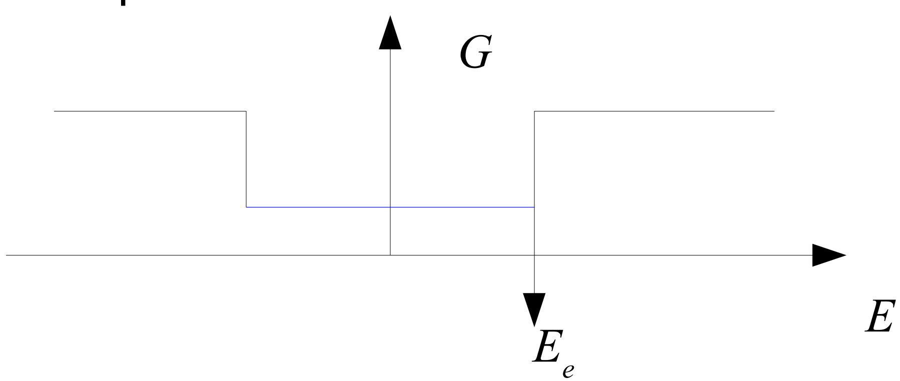

Make the effect evident by taking derivative of conductance. So look at

$$\frac{d^2 I}{dV^2}$$

Important

- Intégrales de densité d'états
  - Information angulaire (directionnel) perdu ou modifié (poids différent dans intégrale)
- Plusieurs bandes, couplage différent
- Effet tunnel historiquement important (gap supra, densité état affecté par phonons.)

Basics of STM technique

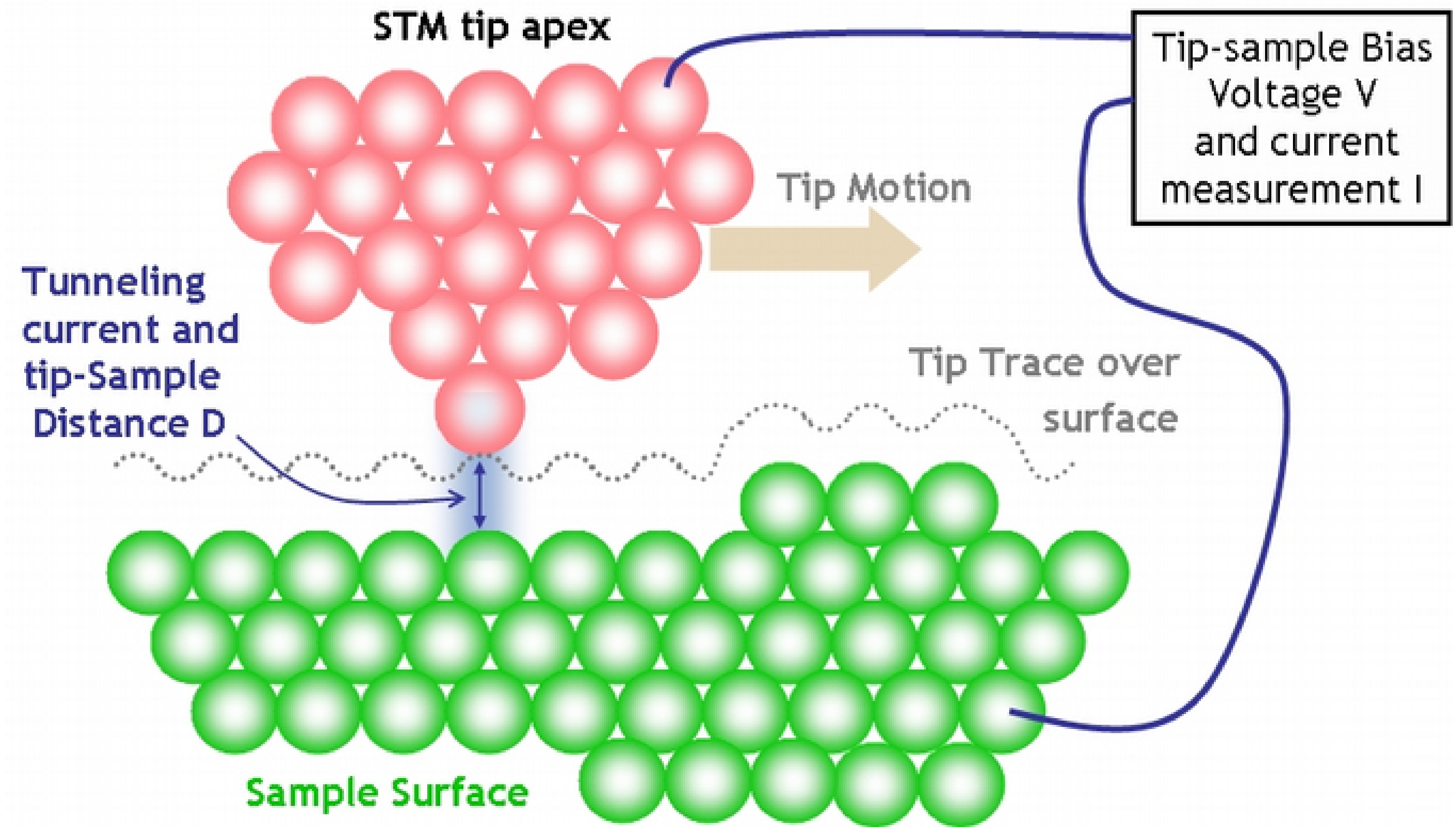

Ref: Opensource Handbook of Nanoscience and Nanotechnology
http://en.wikibooks.org/wiki/Nanotechnology

Constant current feedback

When measurement are taken with a feedback current of I_0 under a voltage of V_0 the conductance is (T=0):

$$G(\vec{r},V)=I_0\frac{n_S(\vec{r},eV)}{\int_0^{eV_0}dE\,n_S(\vec{r},E)}$$

So

$$G(\vec{r},V)\propto n_S(\vec{r},eV)$$

GREAT tool
STS (scanning tunneling spectroscopy)
But there are some approximations

But proportionality constant varies in space

In Fourier space:

$$\cancel{G(\vec{k},V)\propto n_S(\vec{k},eV)}$$

Z ratio map

To avoid problem with feedback (integral) in

$$G(\vec{r},V)=I_0\frac{n_S(\vec{r},eV)}{\int_0^{eV_0}dE\,n_S(\vec{r},E)}$$

Then use Z ratio instead:

$$Z(\vec{r},V)=\frac{G(\vec{r},V)}{G(\vec{r},-V)}$$

This removes integral
•Better contrast (sometimes)
•Extract energy asymmetry
•Loose energy symmetric part

STM equipment

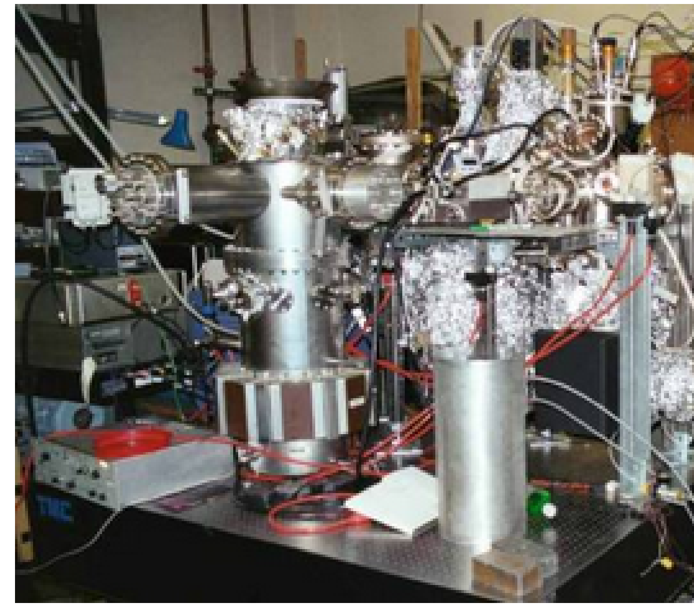

VT-UHV-STM, Zettl, Berkeley

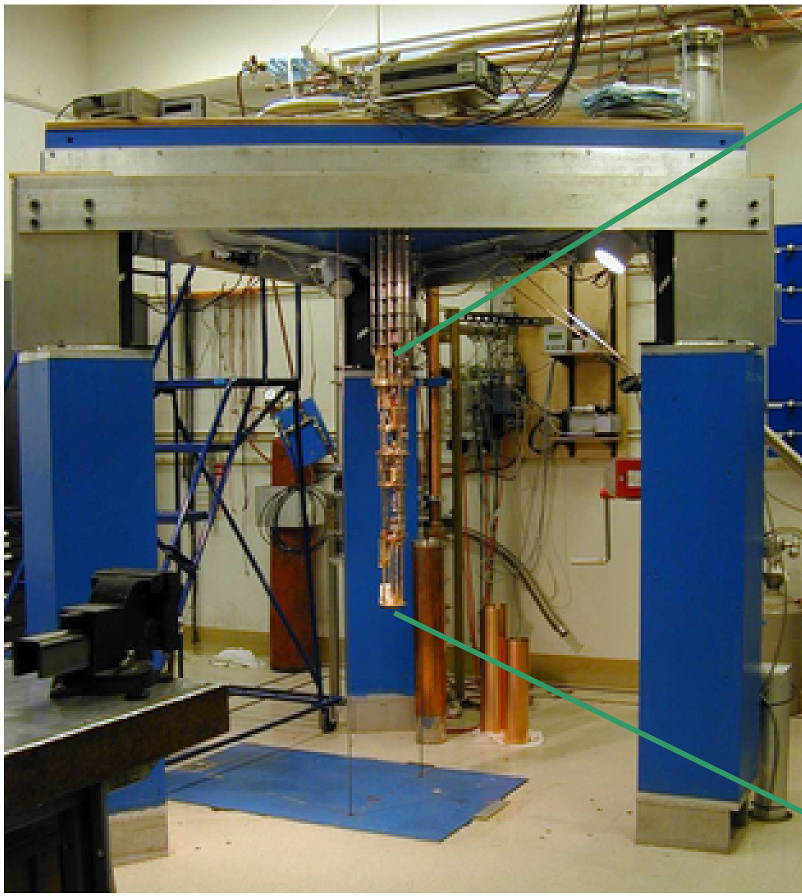

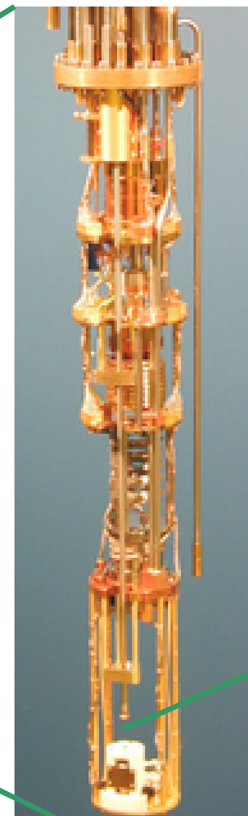

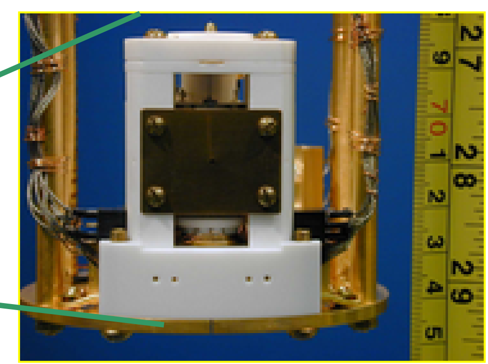

Very Low Temperature STM,Davis Berkeley-Cornell

Pour voir petit

GRANDE Destruction!!

Pour voir petit


Construction

« State of the Art » : floating room

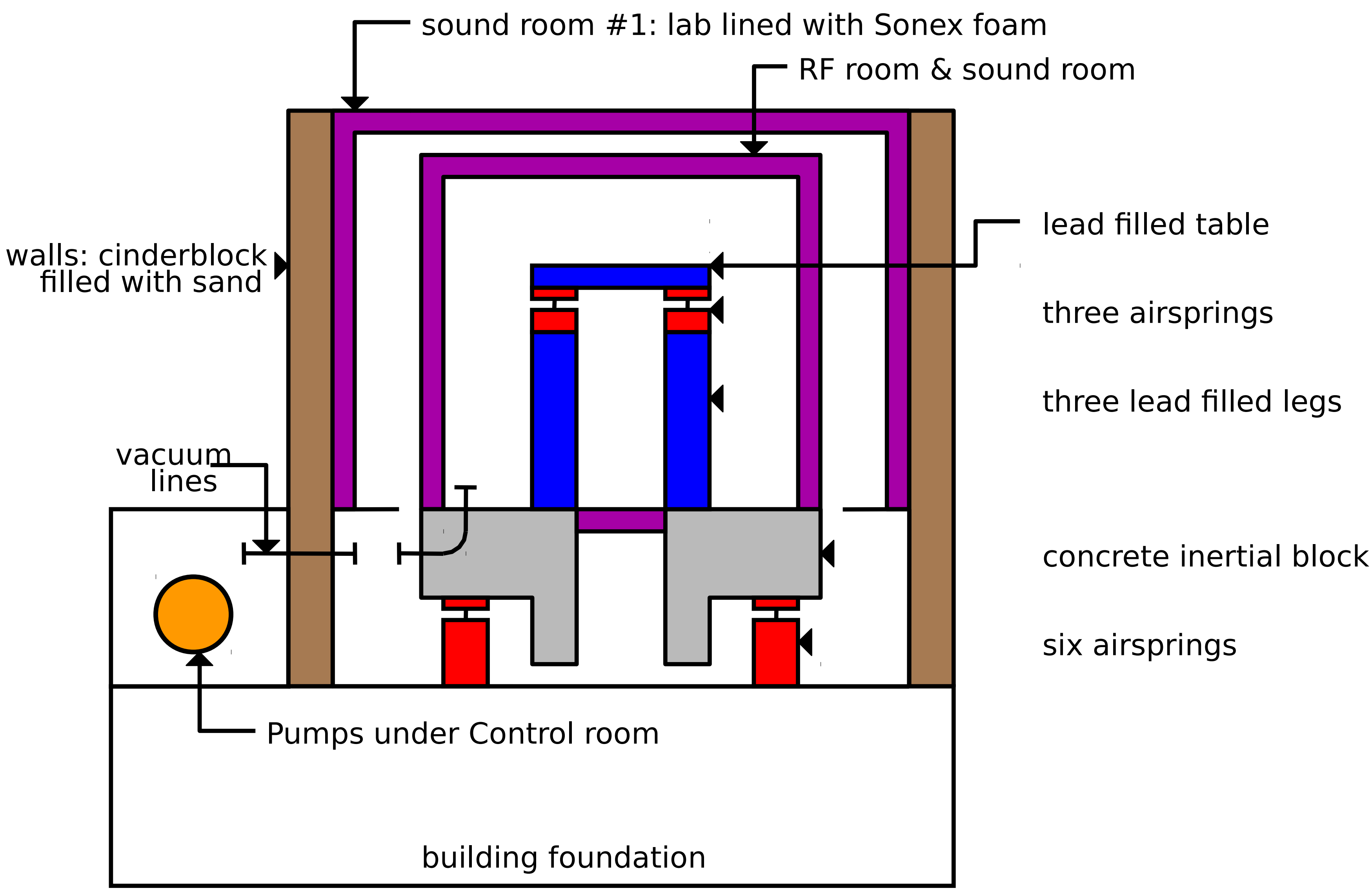

Chambre flottante insonorisée et cage faraday

Microscope assemblé

Cryostat

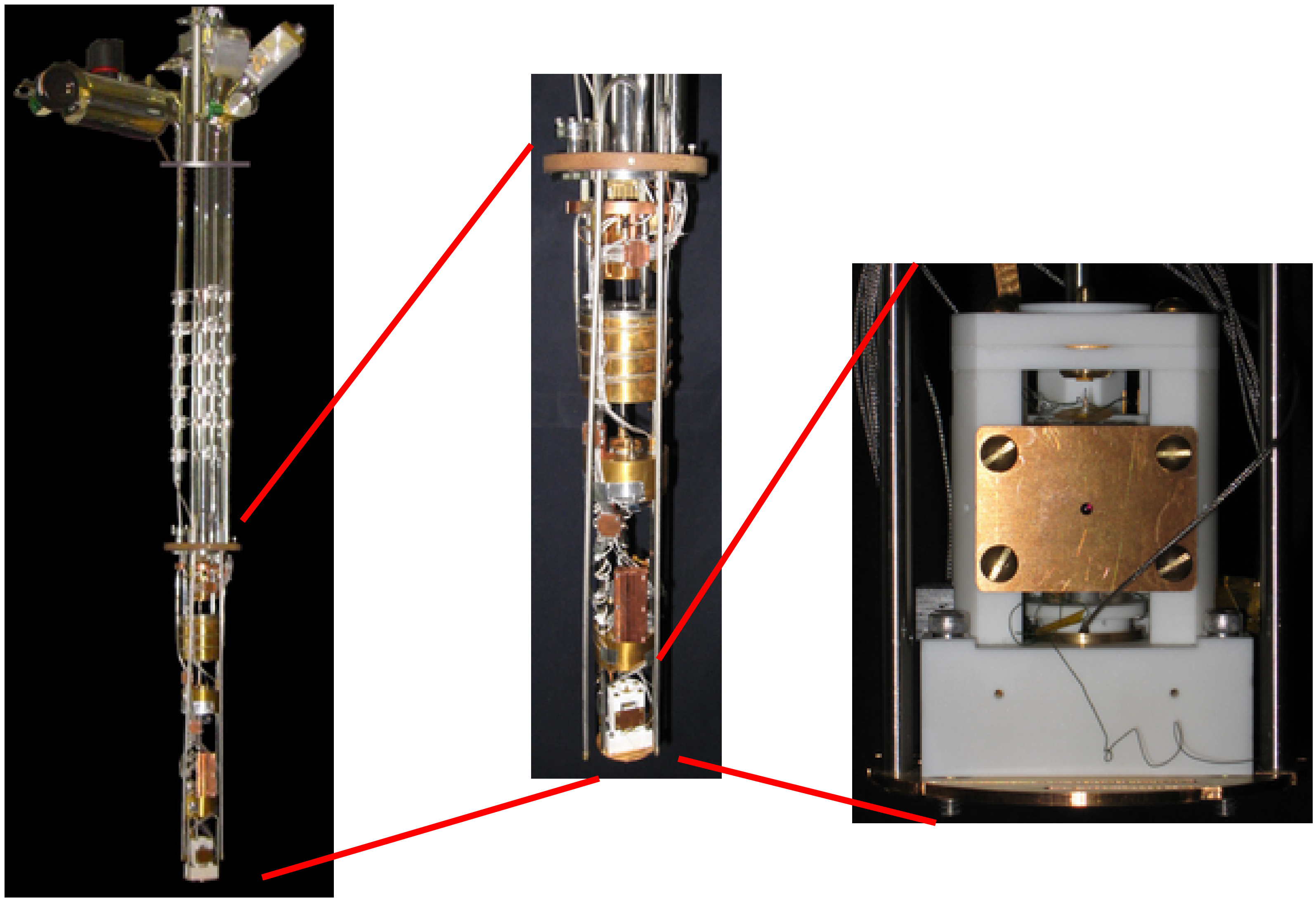

Sample preparation (cleaving)

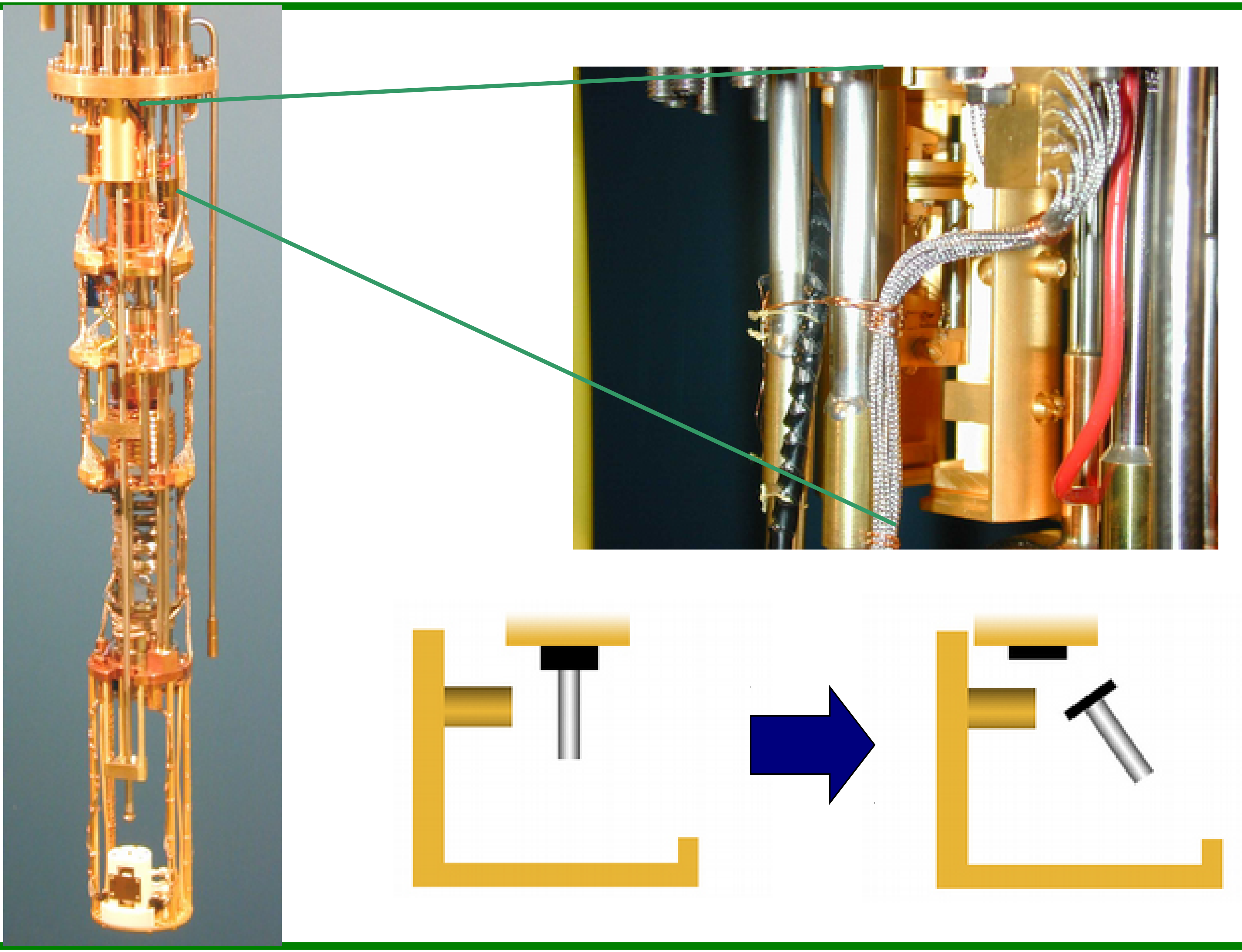

Design de l'instrument pour STM/STS

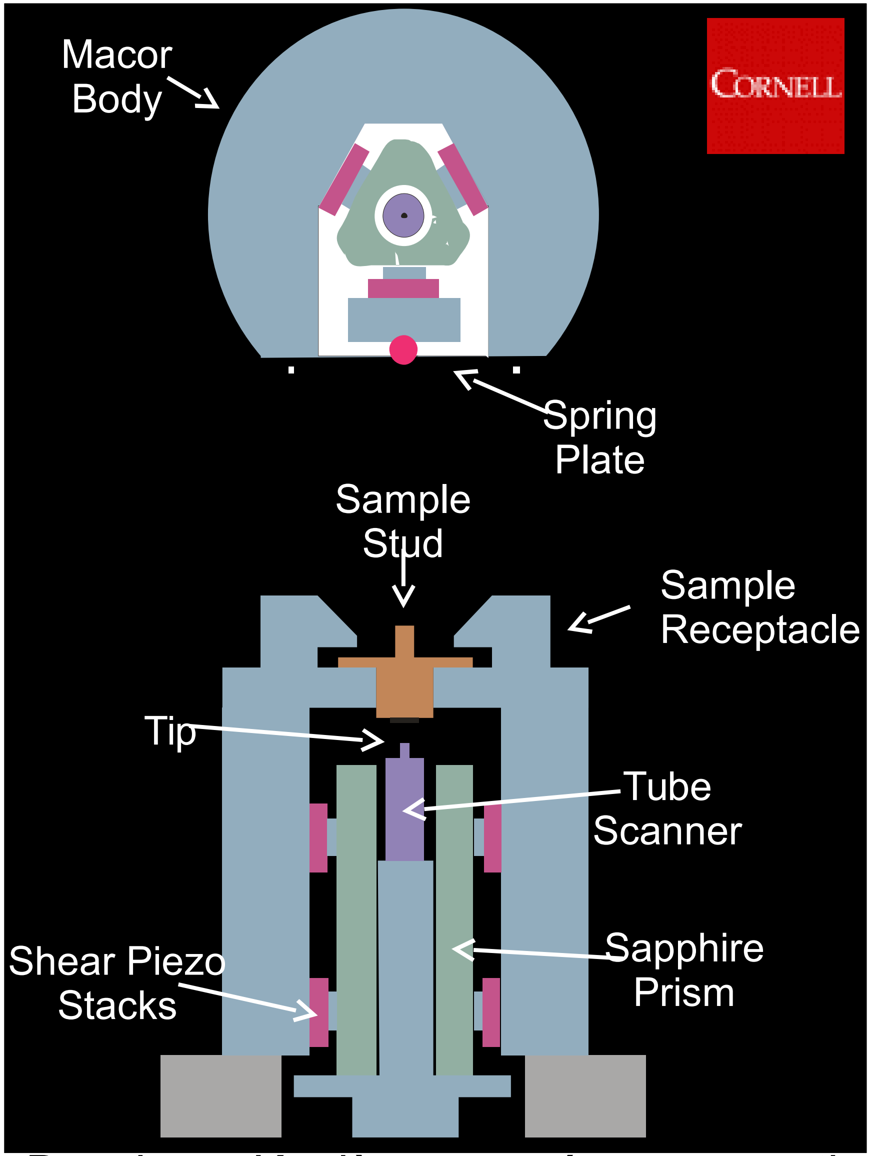

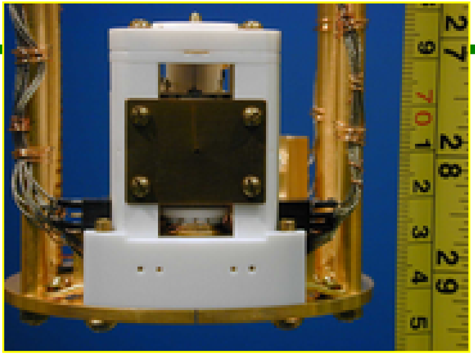

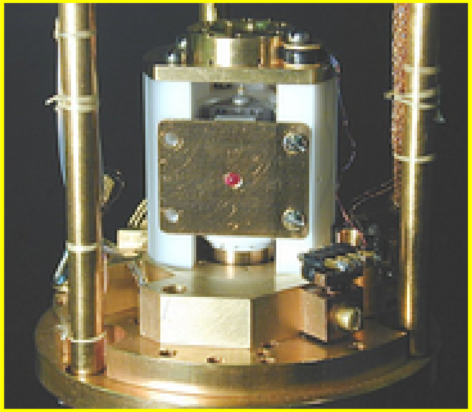

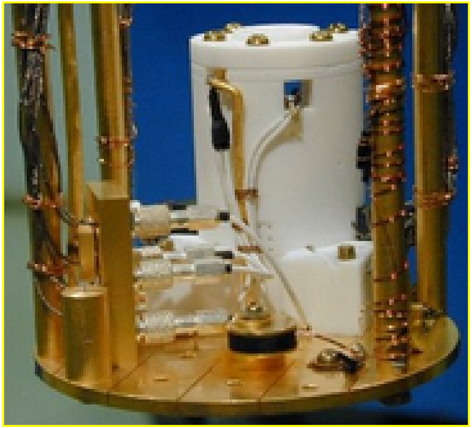

Besoin : mK, pièce avec écran acoustique/RF

Rev. Sci. Inst. **70**, 1459 (1999).

Microscope

Un microscope en morceux...

Microscope

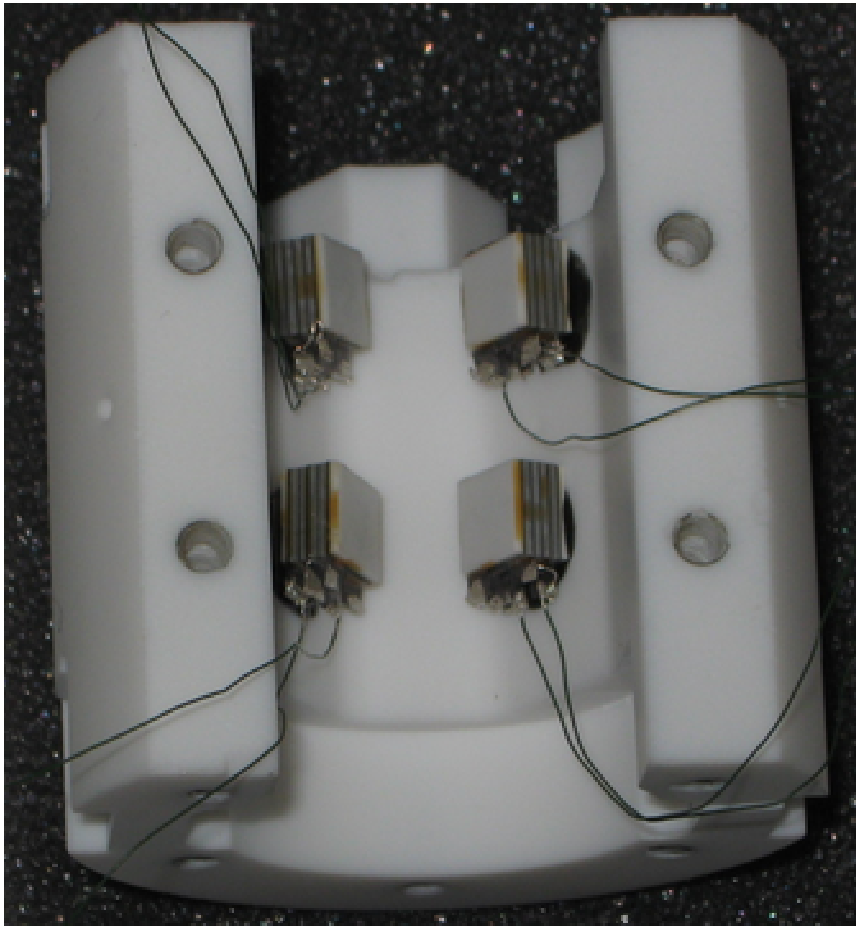

Corps du marcheur

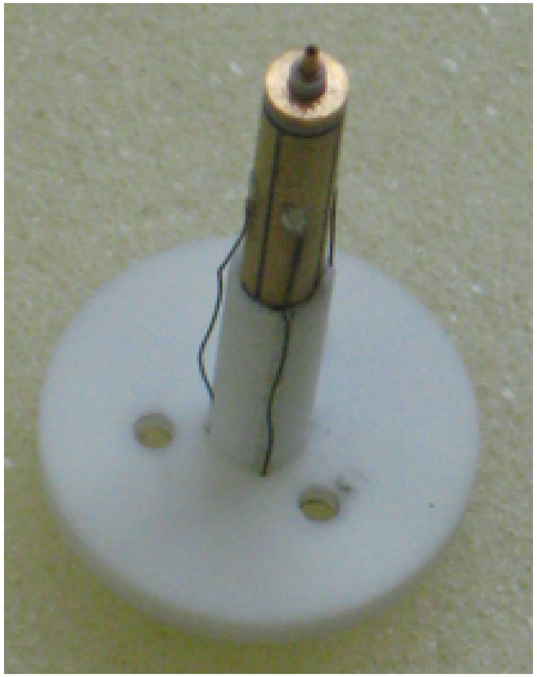

Coeur du microscope
Piezo XYZ et
porte-pointe

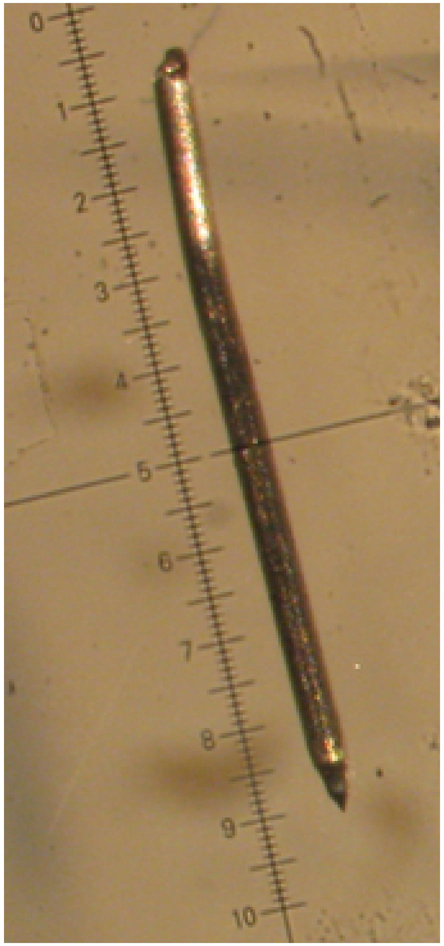

Pointe de Tungstène
8mm

Approche grossière

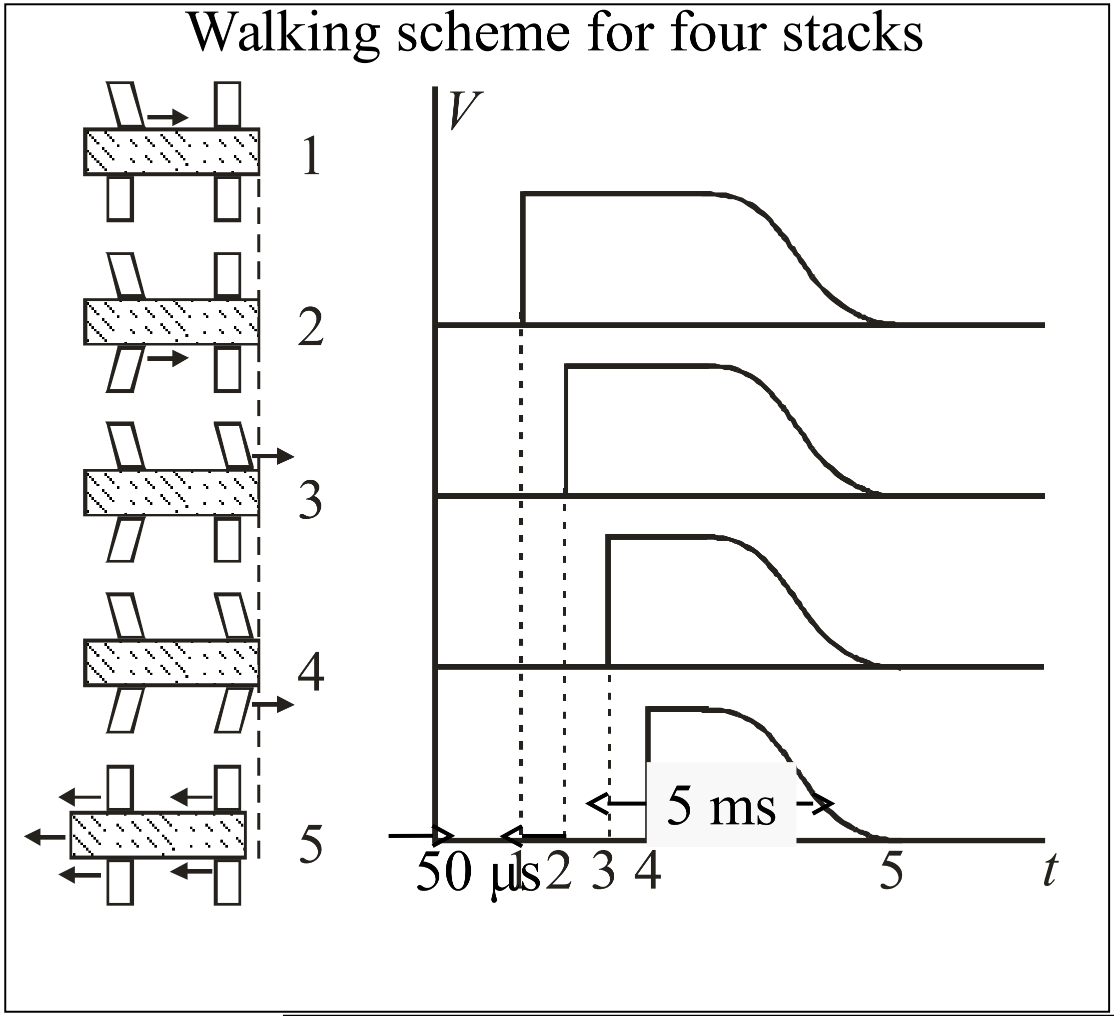

1 pas = 250 Å à Basse Temp
Déplacement Total = 5 mm
Reproductibilité horizontale = 100 Å

Déplacement Marcheur (bas)

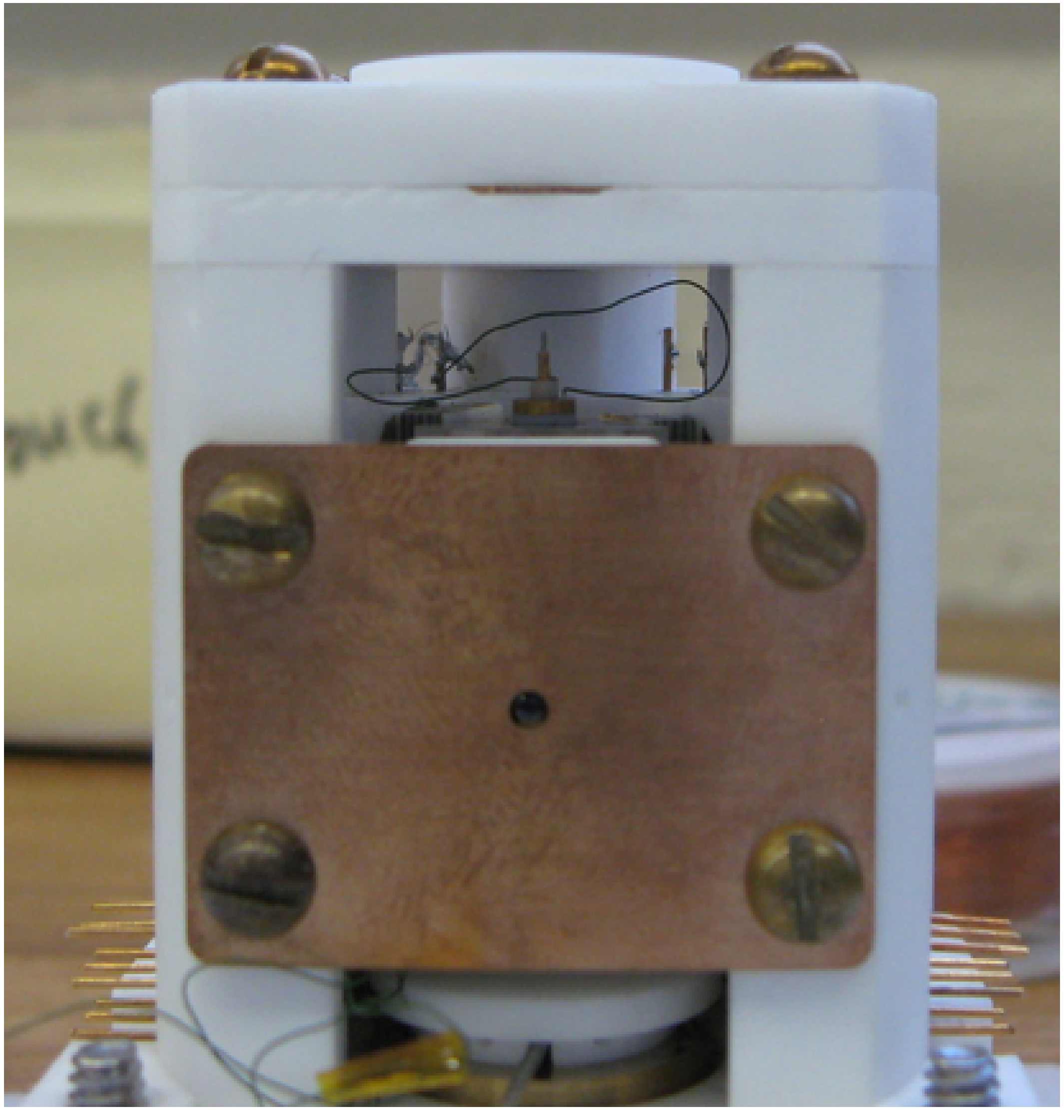

Déplacement Marcheur (haut)

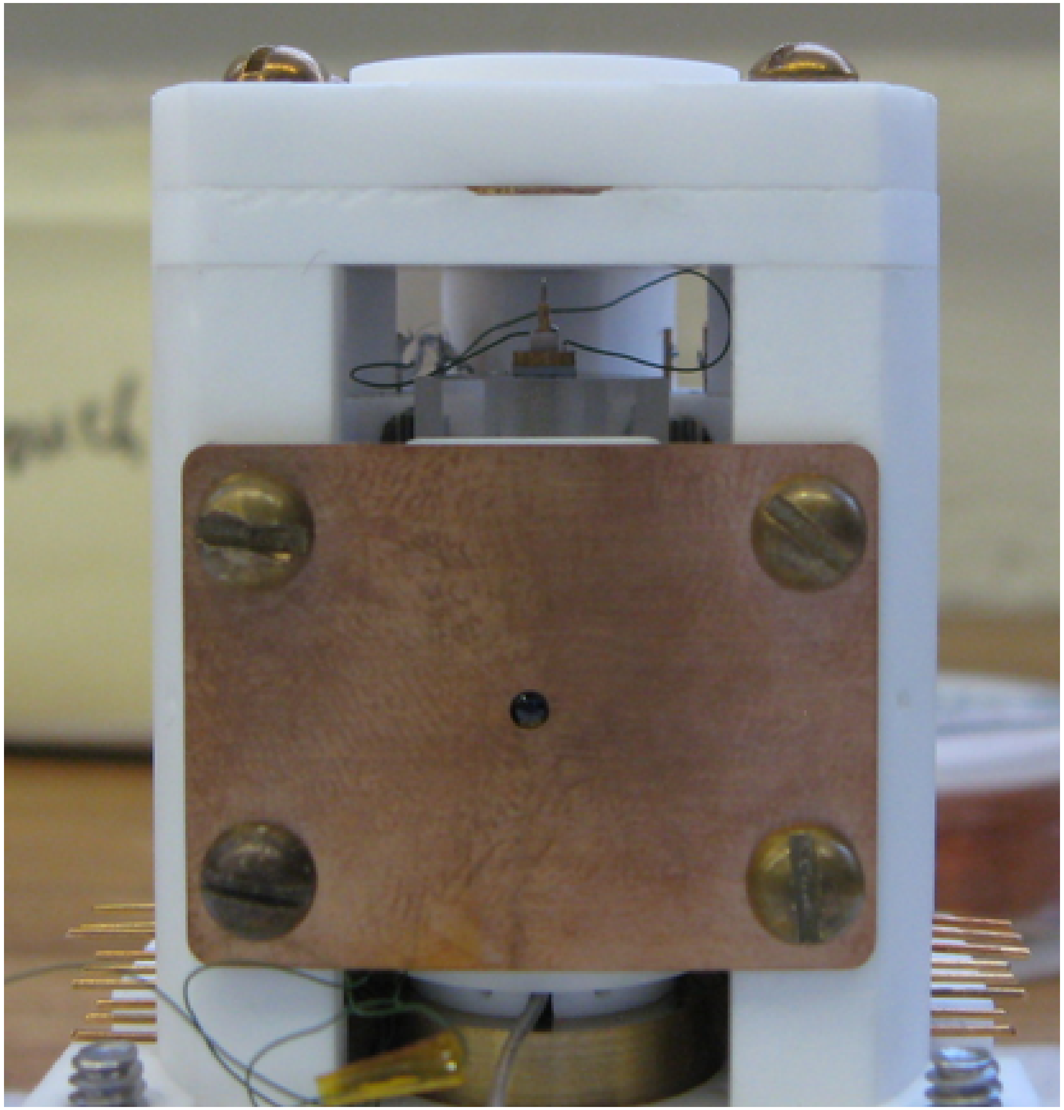

STM Technique

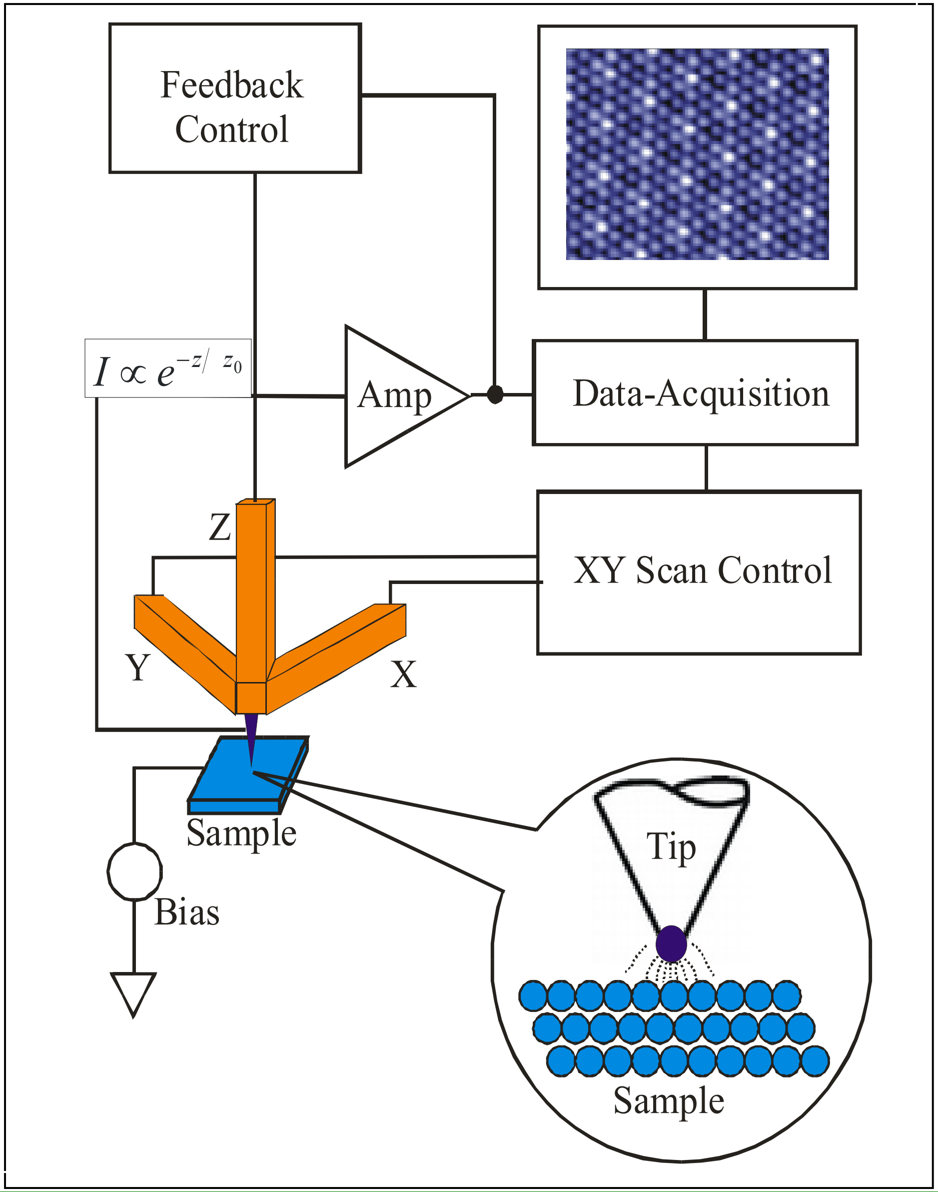

- In Vacuum (dirty)
- In air
  - UHV (variable T)
  - Cryogenic (great vacuum)
- Low T
  - Thermal stability
  - Surface stability

Scanning Tunneling Microscopy

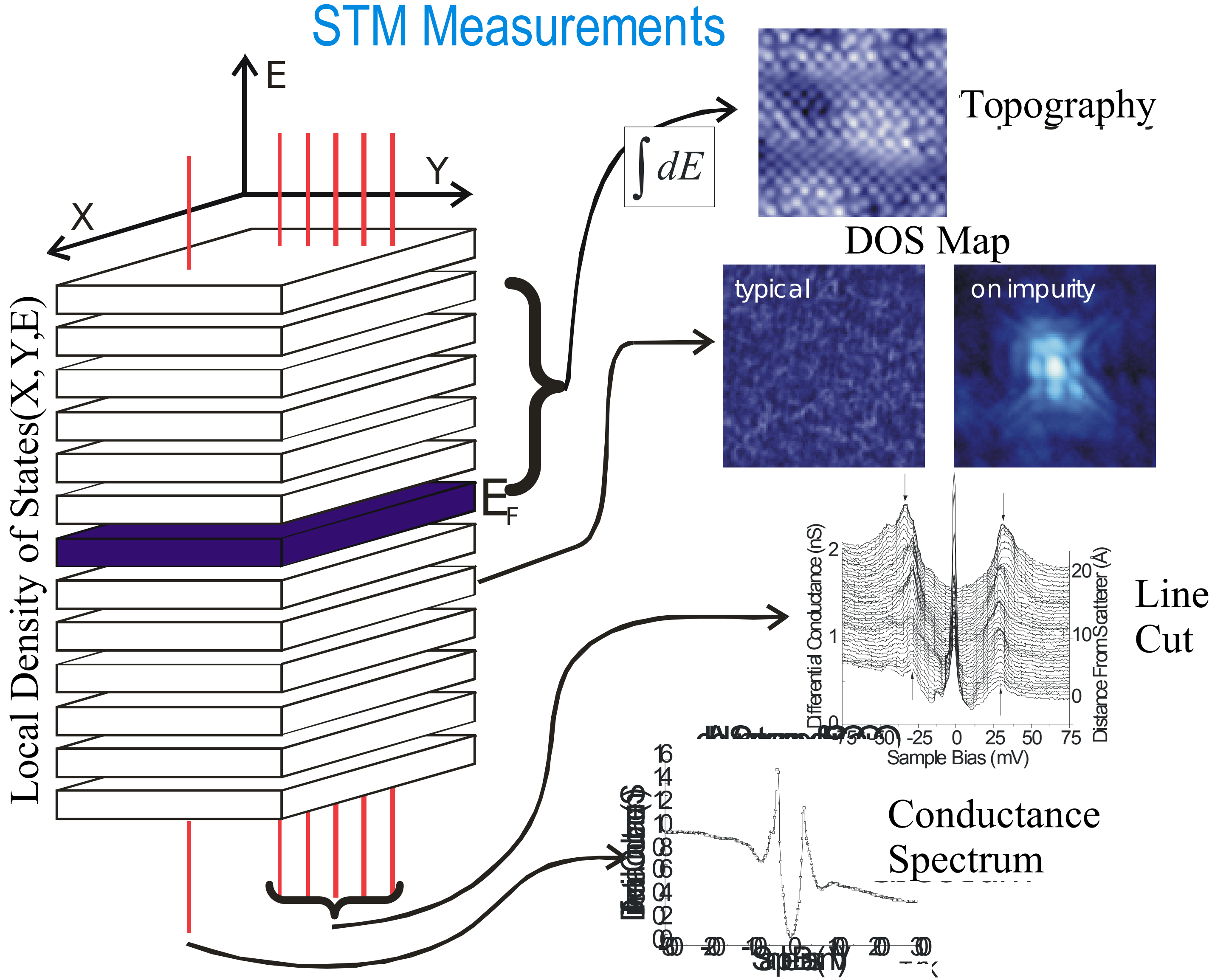

...Très Haute Résolution

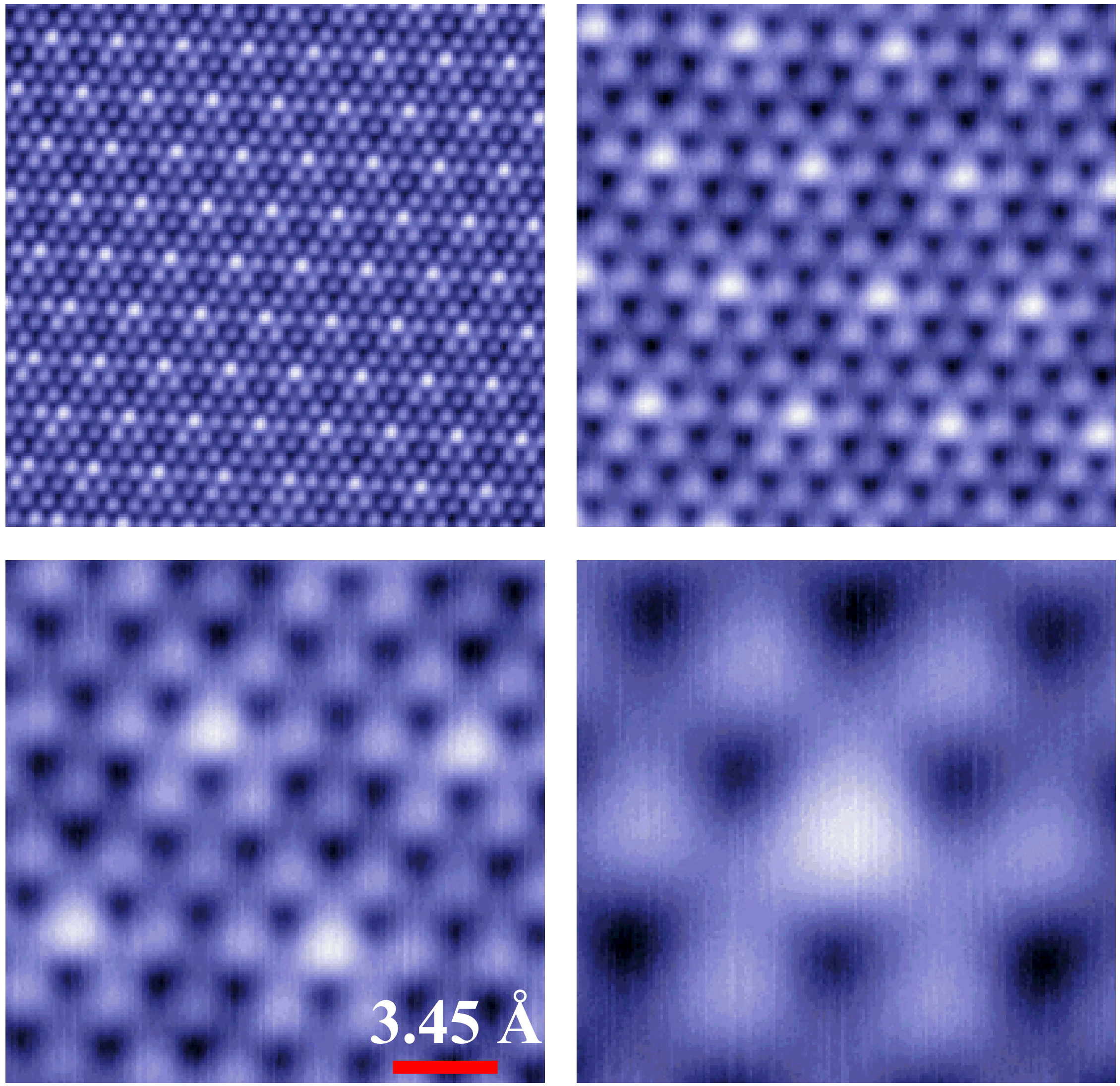

Zoom sur $NbSe_2$ (Onde de densité de charge)

250 mK
50 pA, 50 mV

STM Image les densité d'électrons – pas les atomes

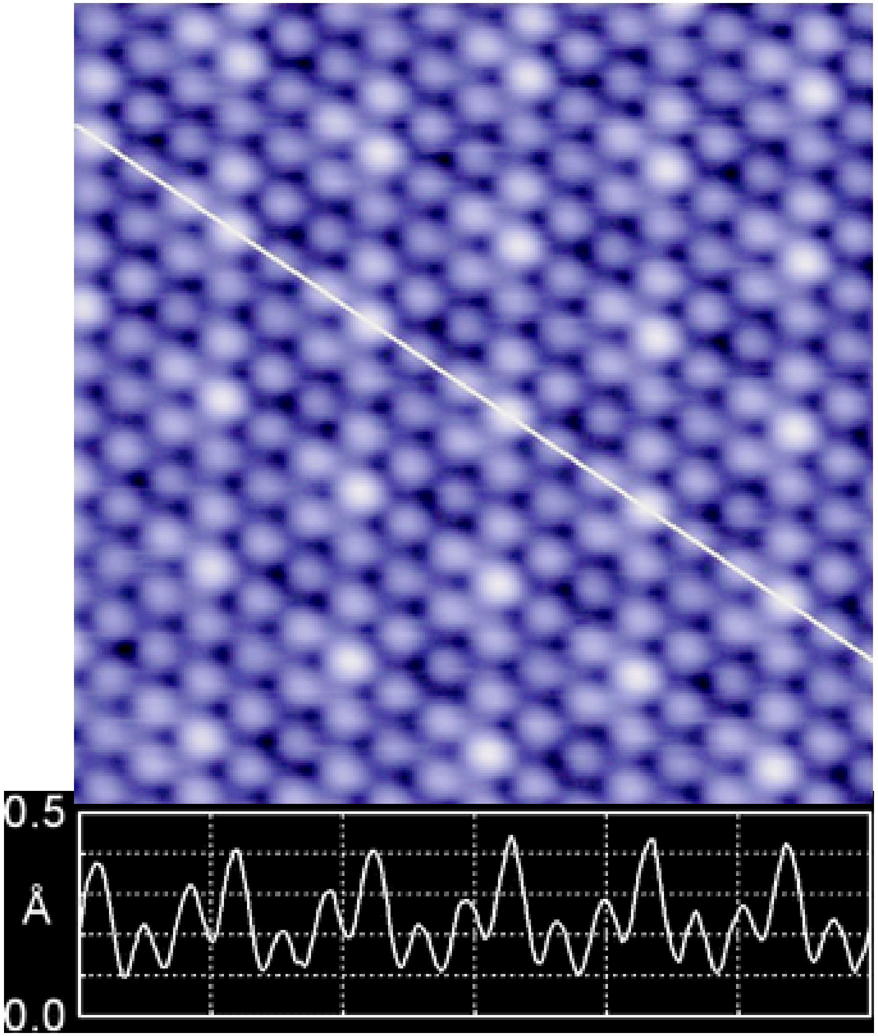

NbSe$_2$: Onde de densité de charge

250 mK
50 pA, 50 mV

Qu'est ce qui est sur la pointe?

Pointe avec C_{60} / défauts sur le graphite

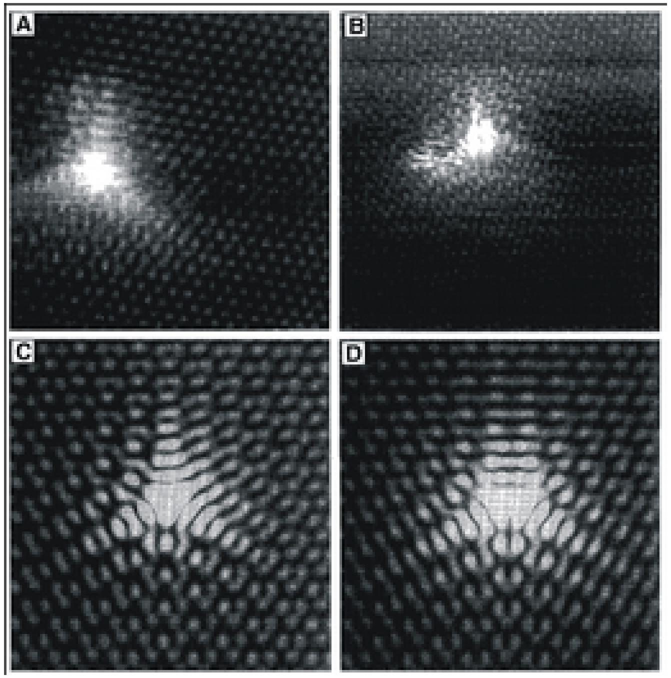

K.F. Kelly, Science: **273,** 1371 (1996)

Nanotube crû sur la pointe

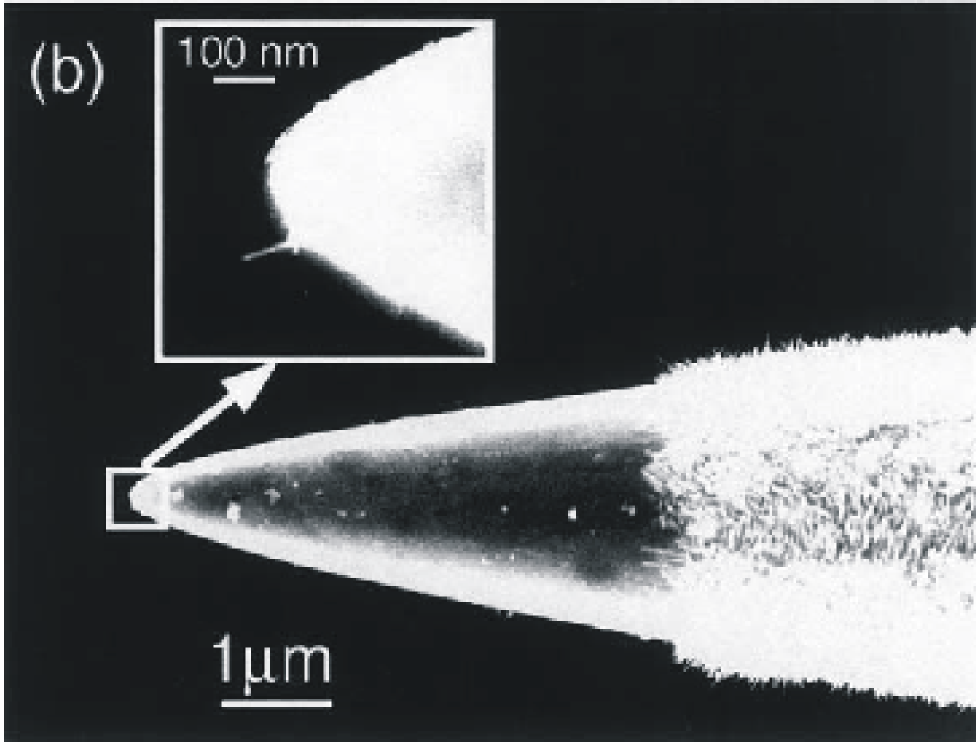

Y. Shingaya, Physica B **323**, 153 (2002)

Pointes standard :

- Fils coupé de PtIr
- Tungstène formé électrochimiquement, émission de champs

Graphite (pointes différentes)

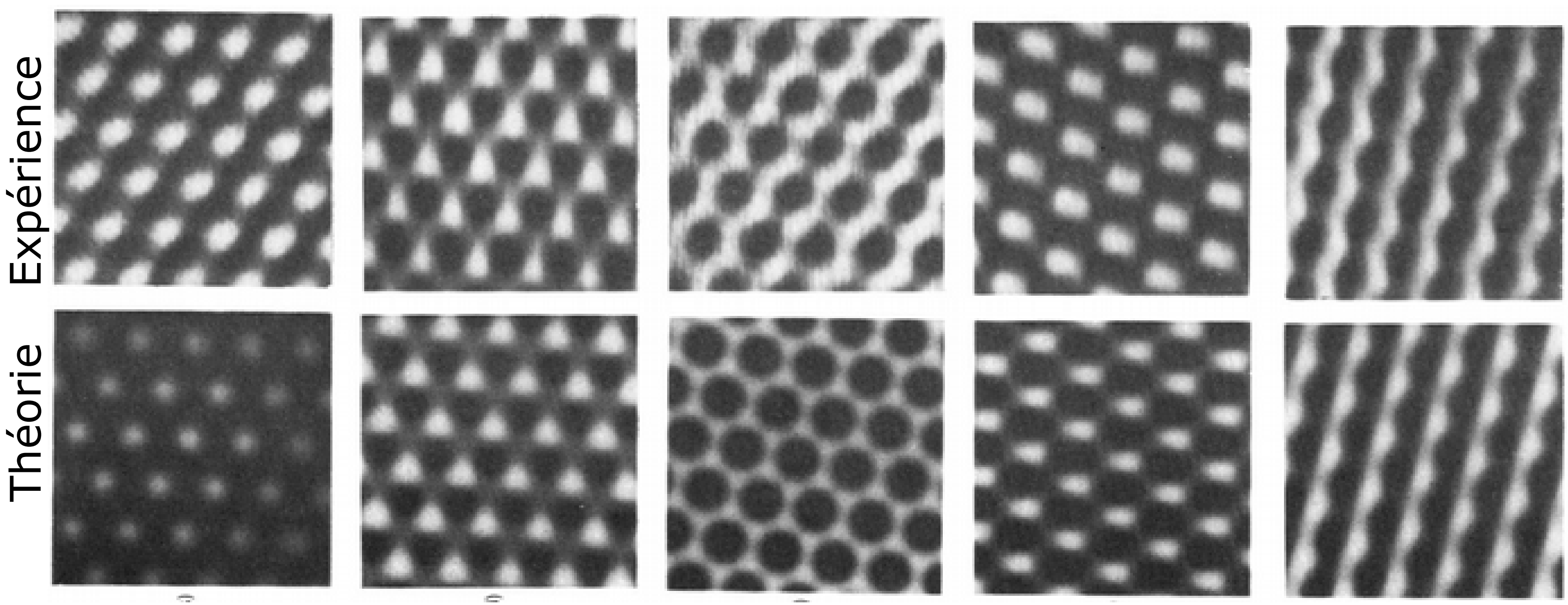

H.A. Mizes *et al.*, PRB **36**, 4491 (1987)

Reconstruction Au(111) Herringbone

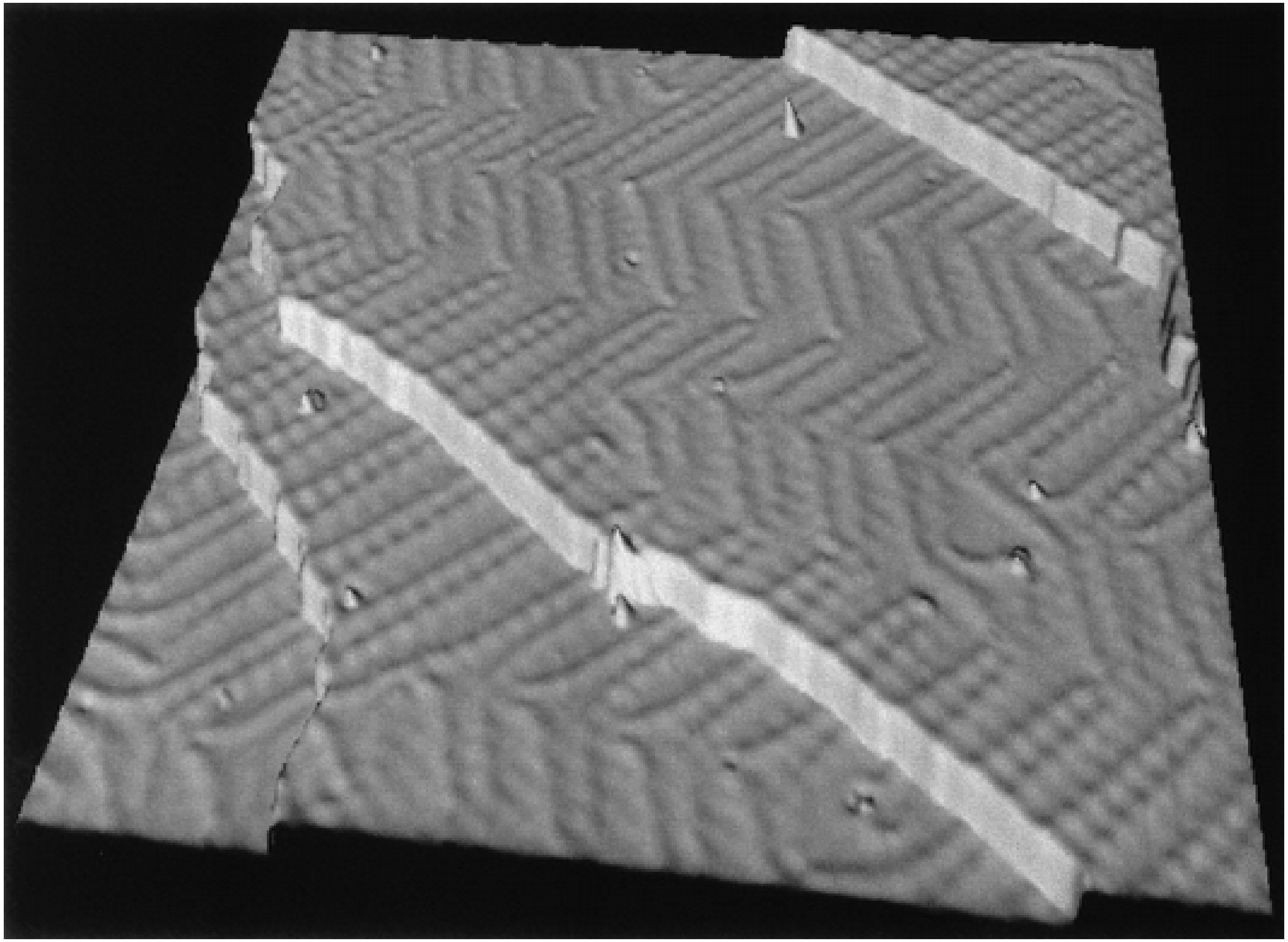

W. Chen *et al.*, PRL **80**, 1469 (1998)

Surface reconstruction: Si(111) 7x7

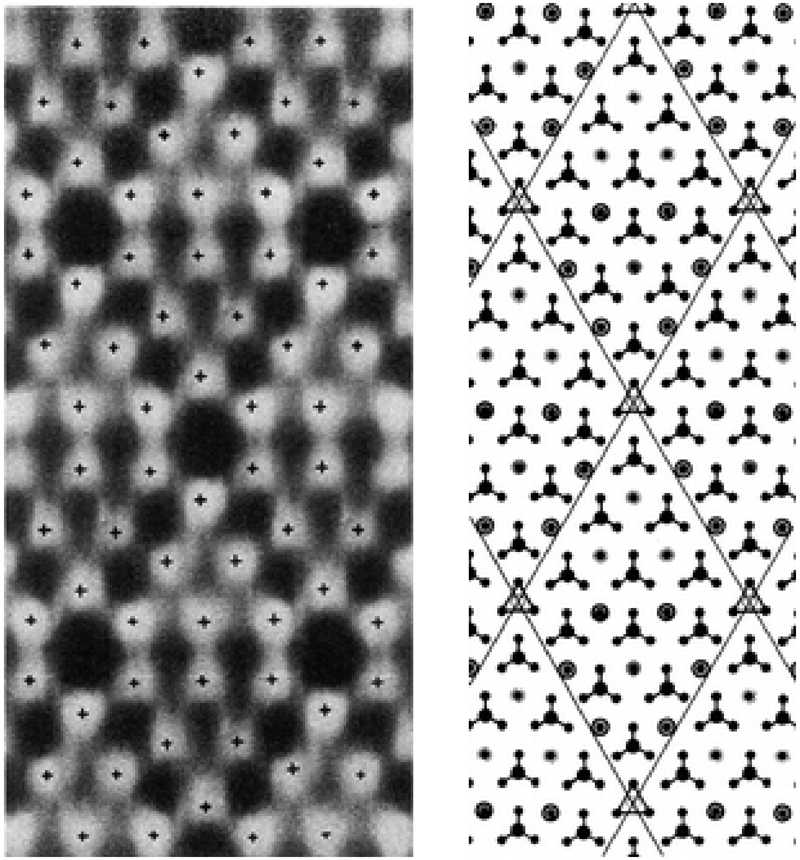

G. Binning *et al.*, PRL **50** ,120 (1983)

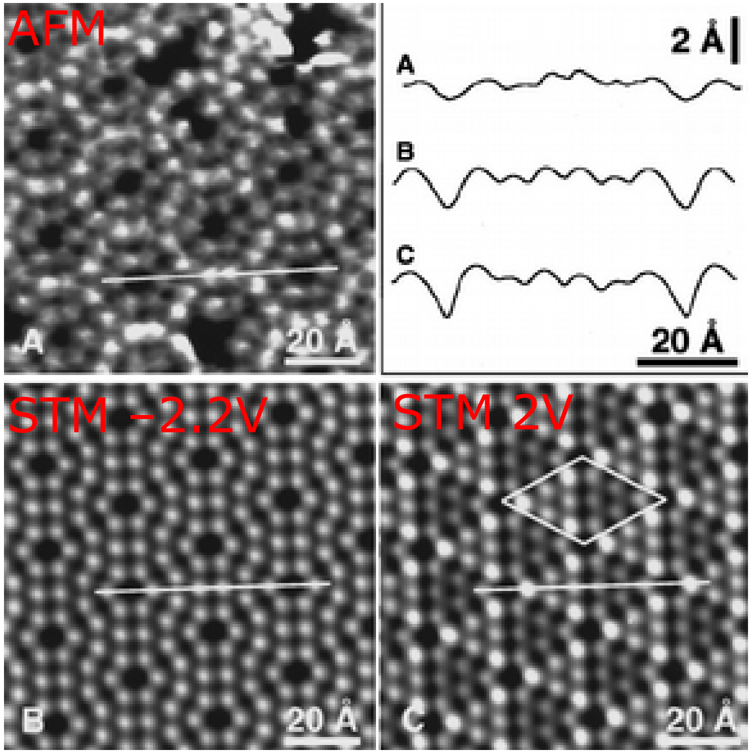

R. Erlandsson *et al.*, PRB **54**, R8309 (1996)

Reconstruction occurs at surfaces because of the broken bounds.
Another problem/advantage of surfaces is surface states.

Structure of $Bi_2Sr2CaCu_2O_{8+\delta}$

$a \approx b = 5.4$ Å

$c = 30.7$ Å

$T_c \sim 90$ K

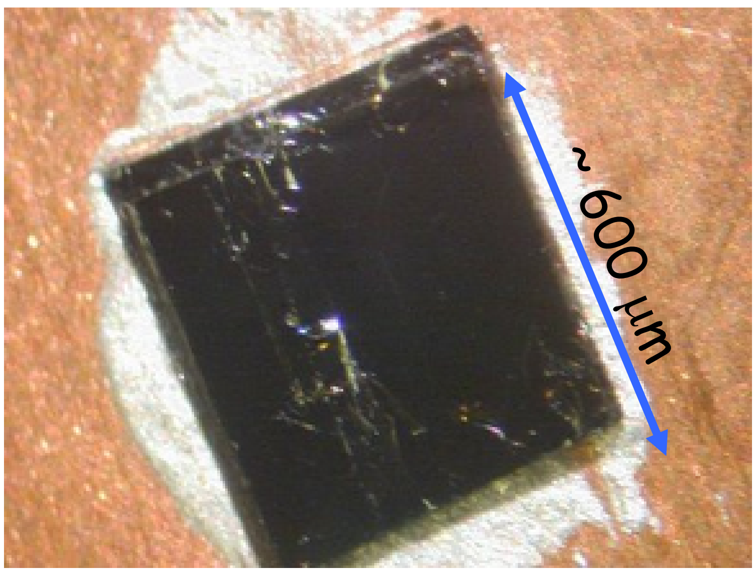

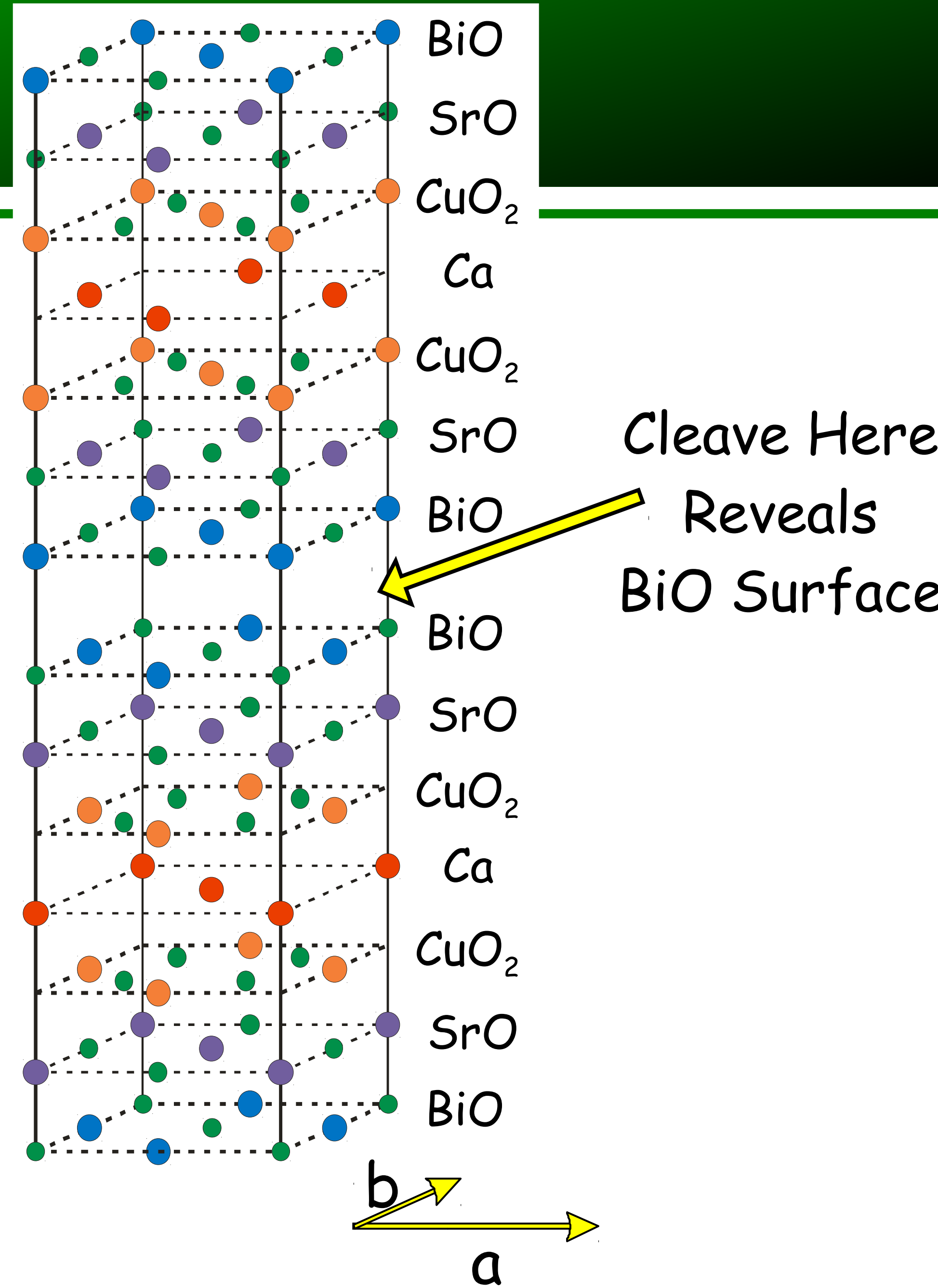

Terraces on a Cleaved BSCCO Surface

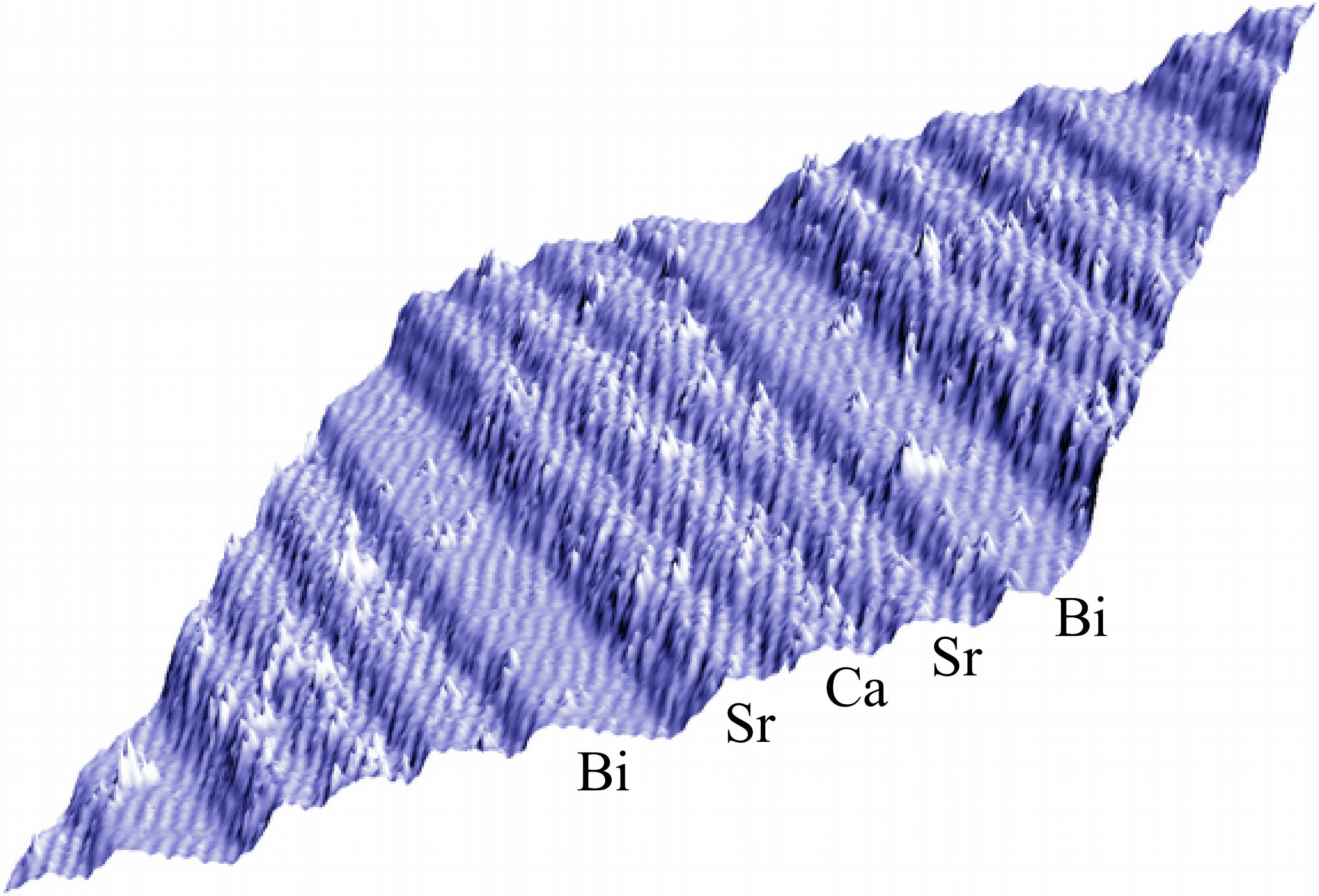

Applied Physics Letters **73** (1), 58-60 (1998).

Cuivre (111)

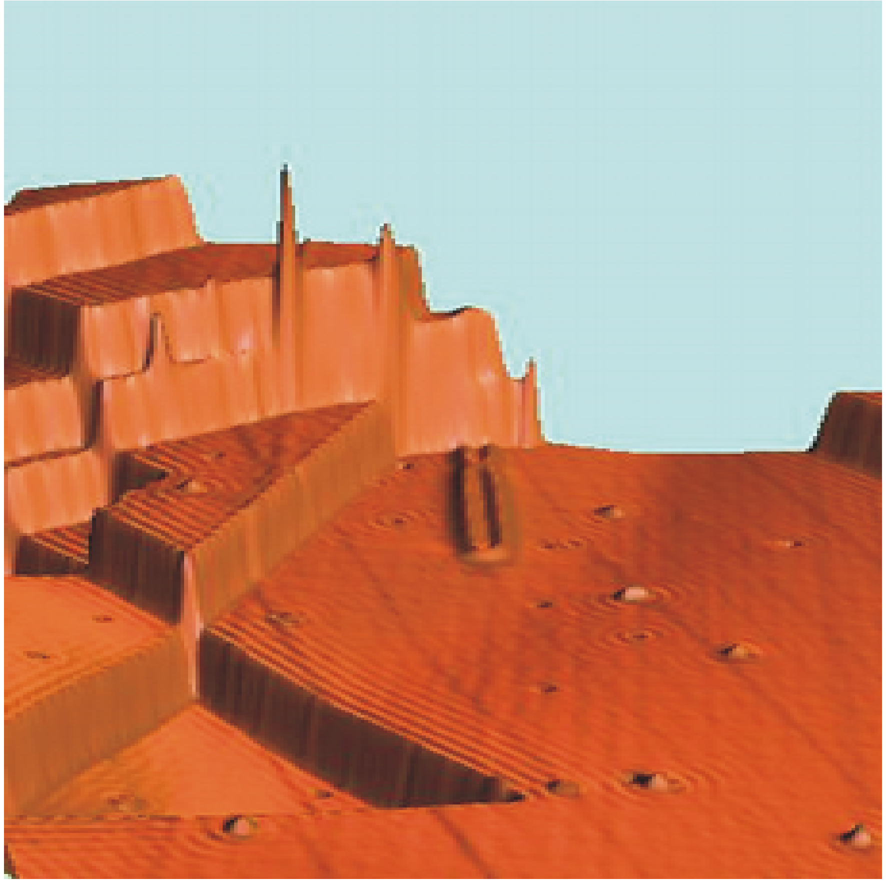

- Terraces
- Oscillations de Friedel :
  - Bord des marches
  - Impuretés
- Interférences d'électrons

M.F. Crommie , CP Lutz DM Eigler, Nature **363,** 524-527 (1993)

Doped GaAs 110 (semiconductor)

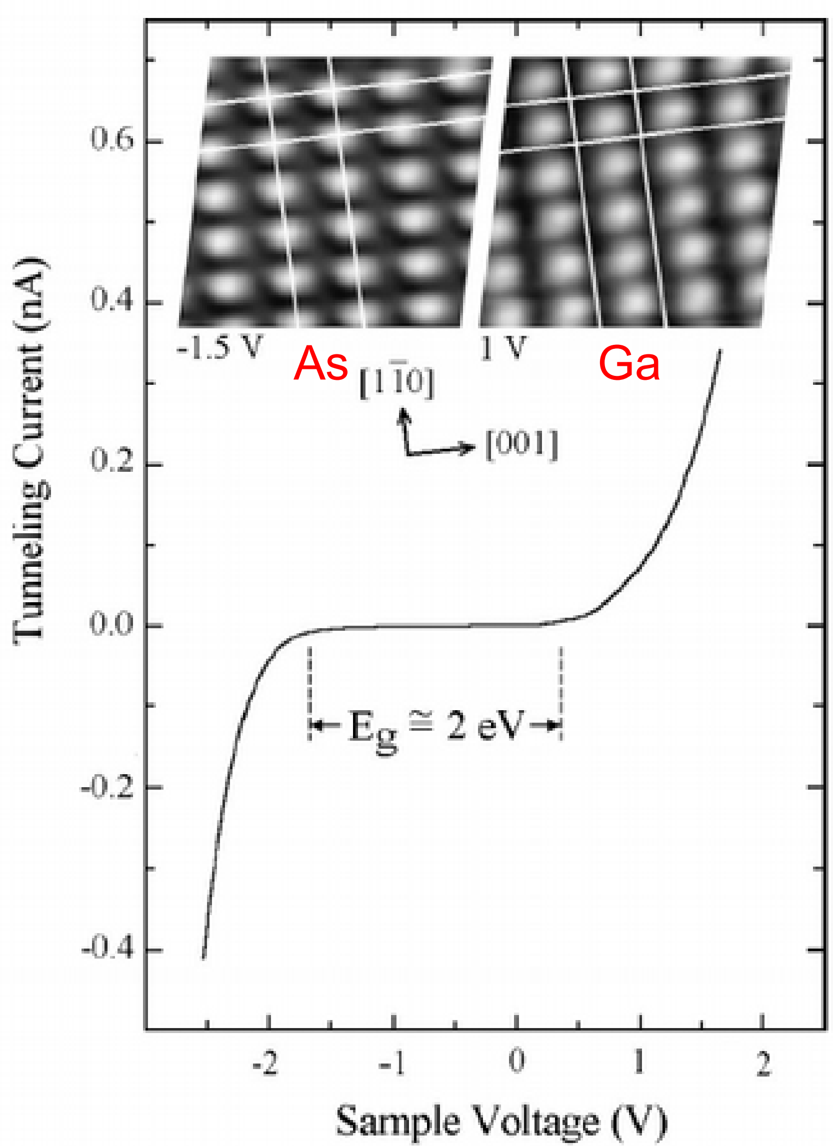

Large Voltages

- Tip effect, electric field ("band bending")
- Measurement NOT DOS

Ga and As atoms seen separately

A. Depuydt *et al.*, PRB **60**, 2619 (1999)

Atomic manipulations

Atomic manipulations
Building a quantum corral

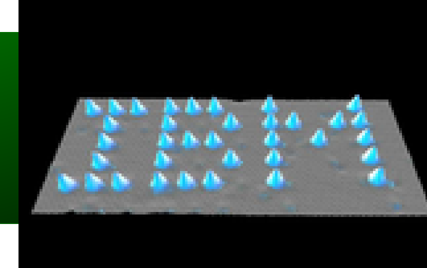

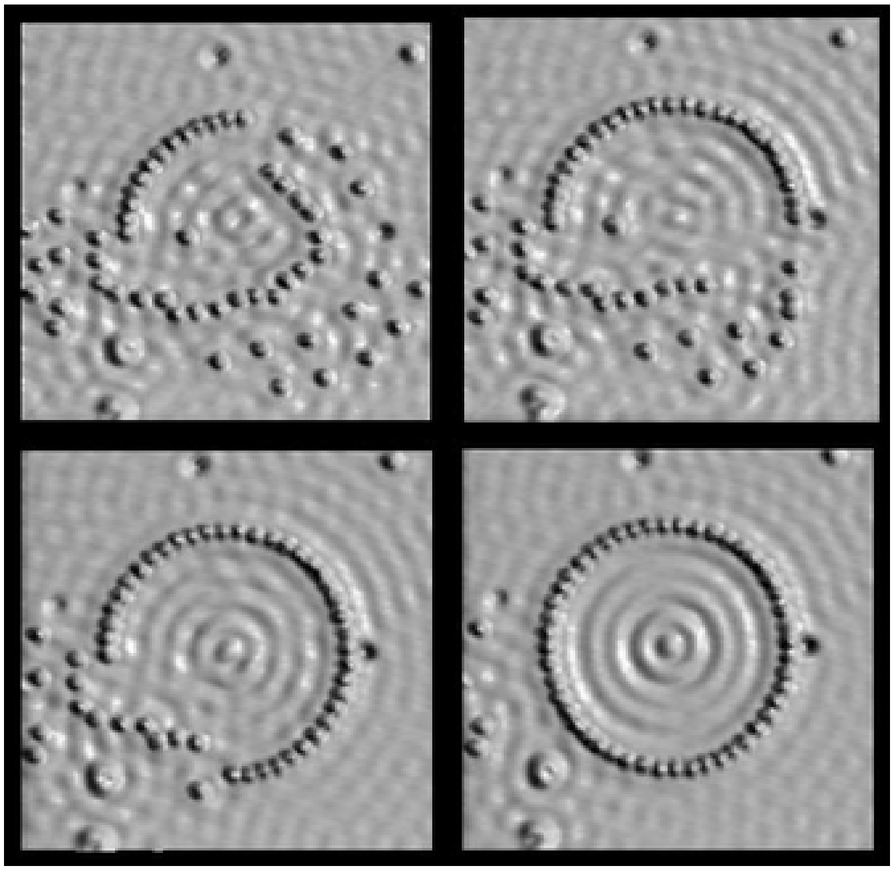

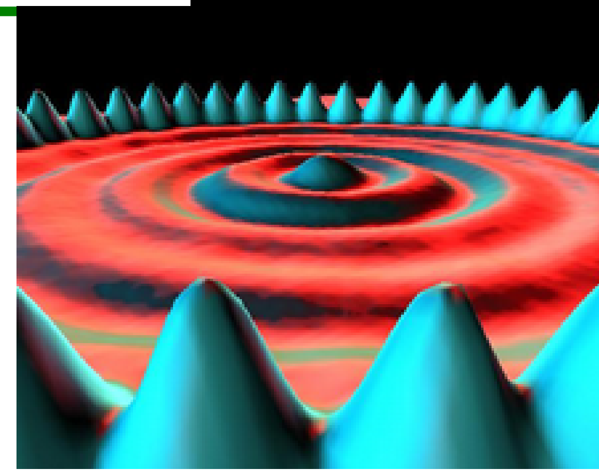

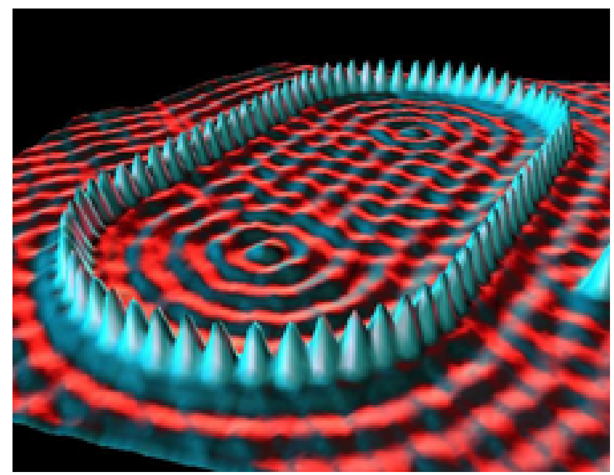

Fe on Cu(111)

M.F. Crommie, C.P. Lutz, D.M. Eigler

Confinement of electrons to quantum corrals on a metal surface.
Science 262, 218-220 (1993).

Atomic manipulations

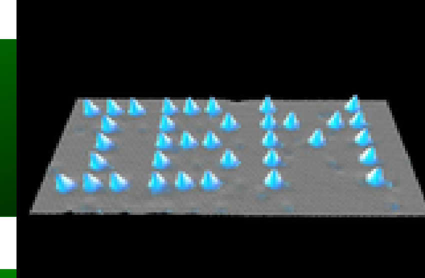

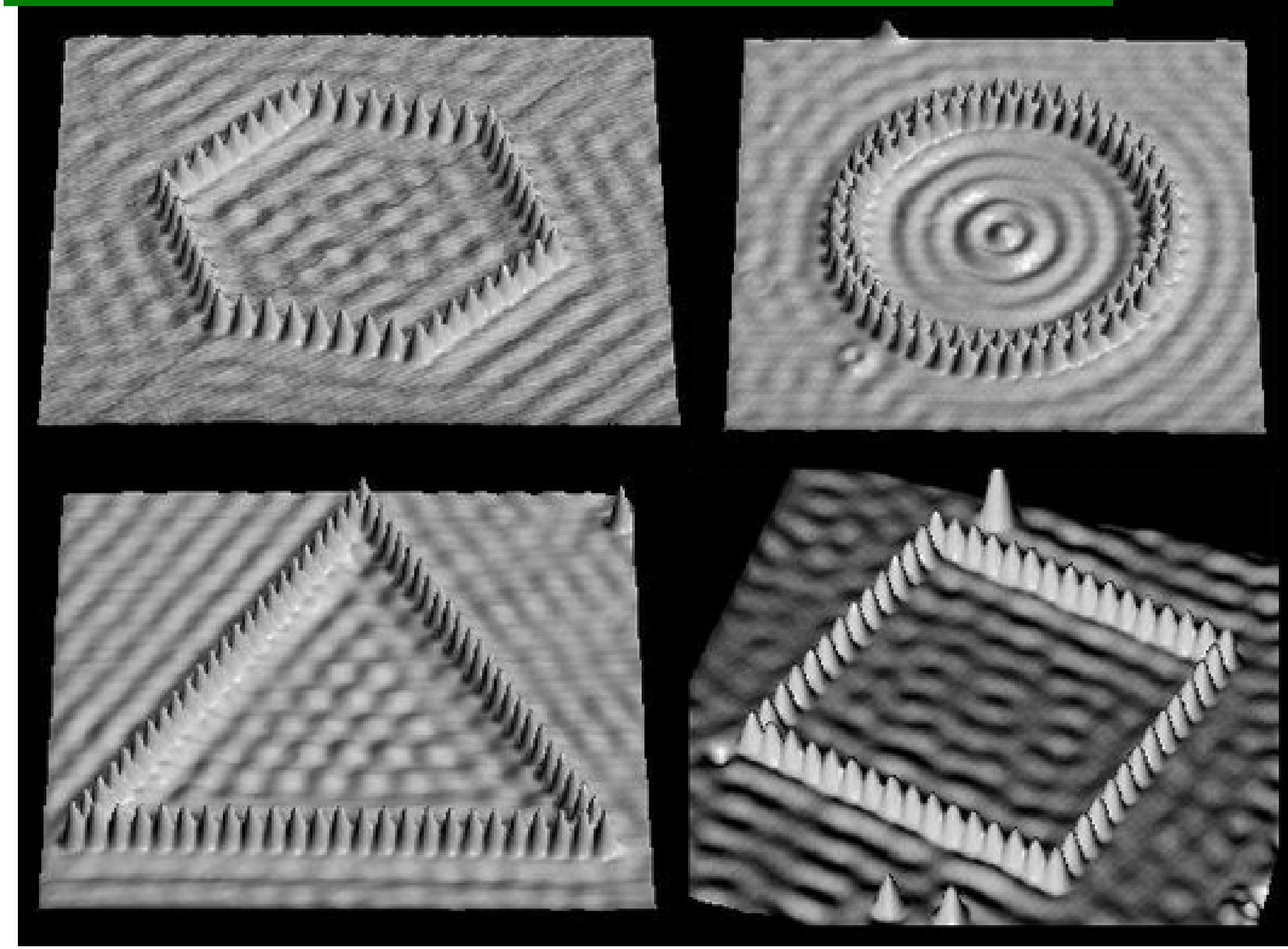

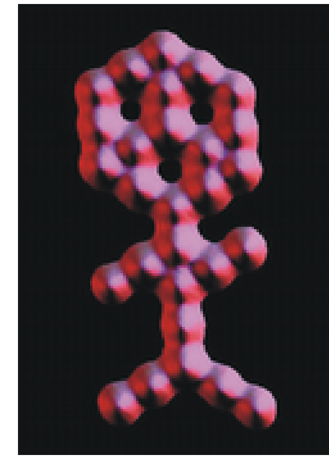

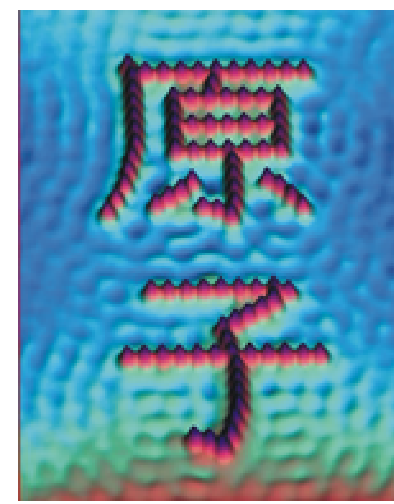

M.F. Crommie, C.P. Lutz, D.M. Eigler, E.J. Heller

Waves on a metal surface and quantum corrals.
Surface Review and Letters 2 (1), 127-137 (1995).

Other Manipulations / tip techniques

STM and molecular rotation

O_2 on Pt(111)

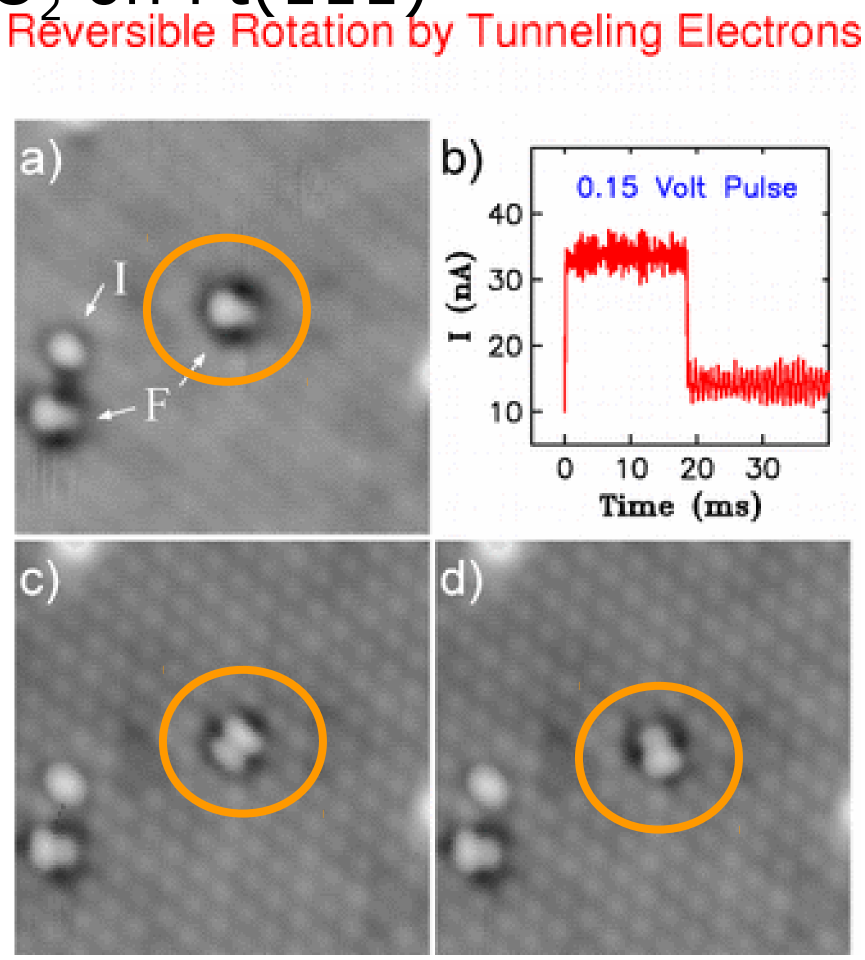

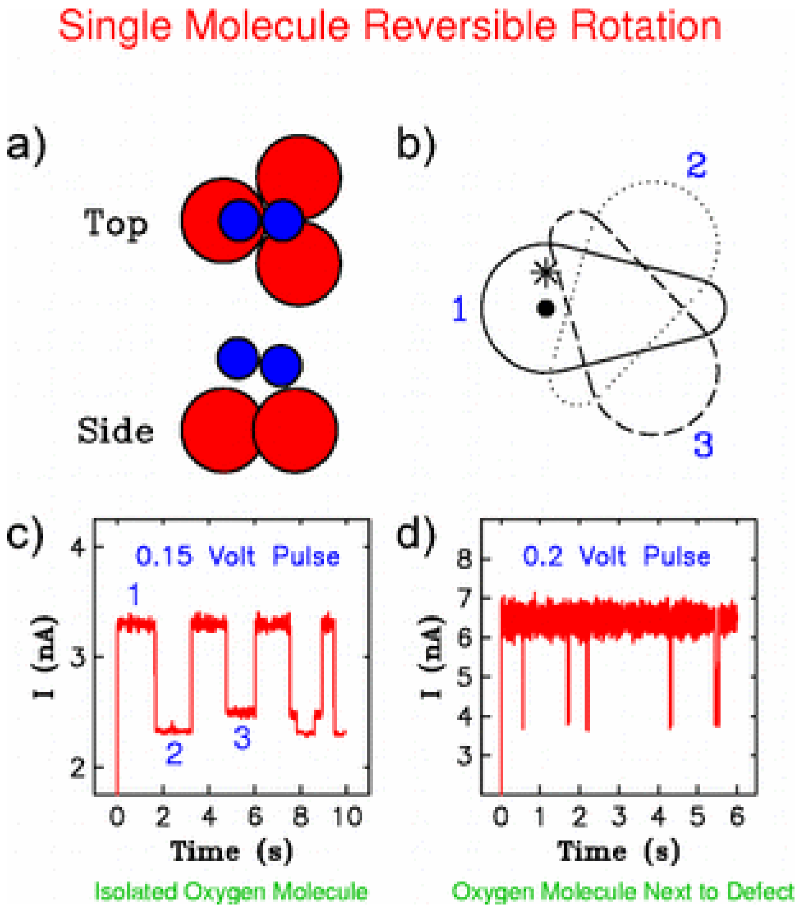

B. C. Stipe, M. A. Rezaei, W. Ho, Science **279**, 1907 (1998)

STM inélastique (IETS)

Mode de vibration de C2H2

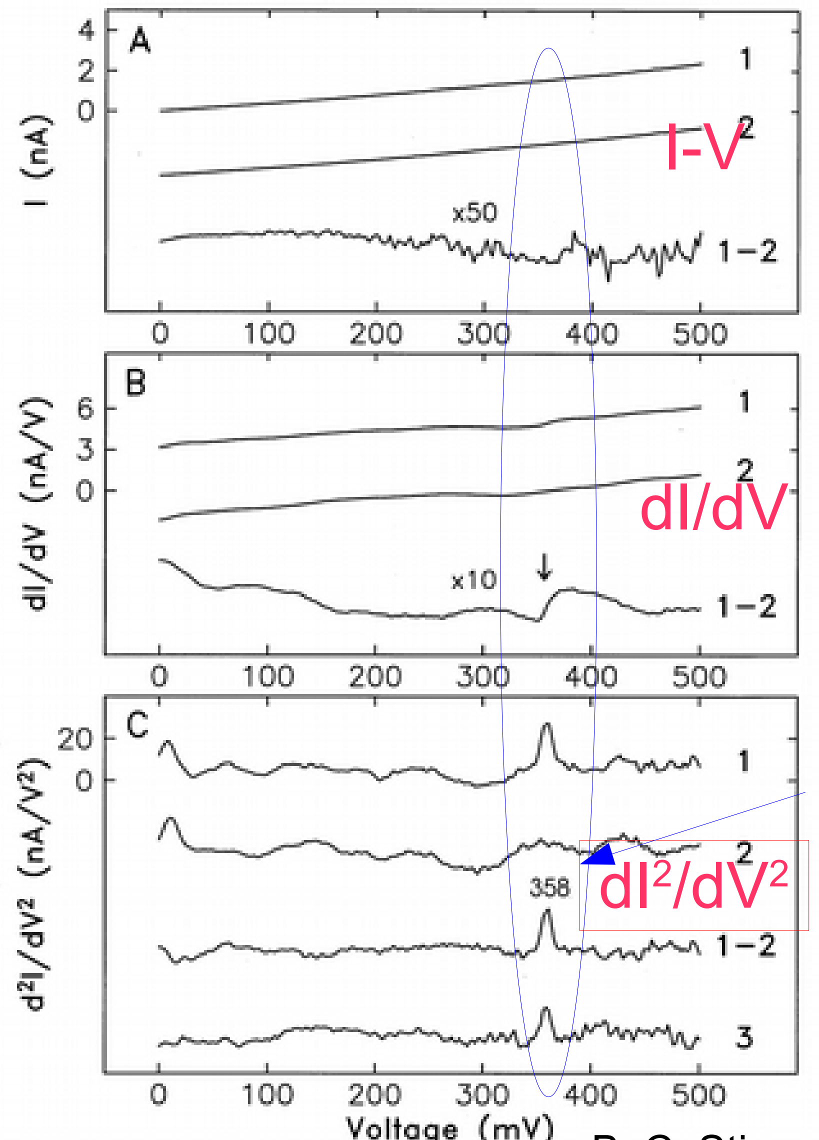

Excitation inélastique (mode de vibration, comme en Raman)

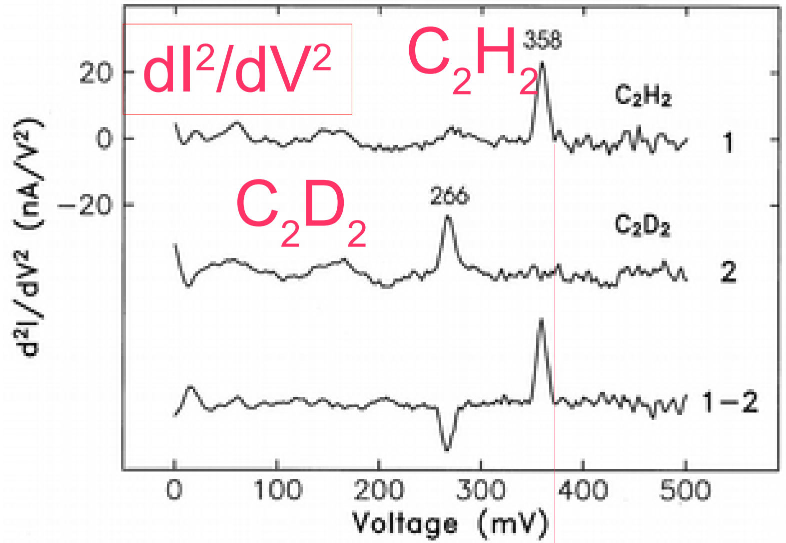

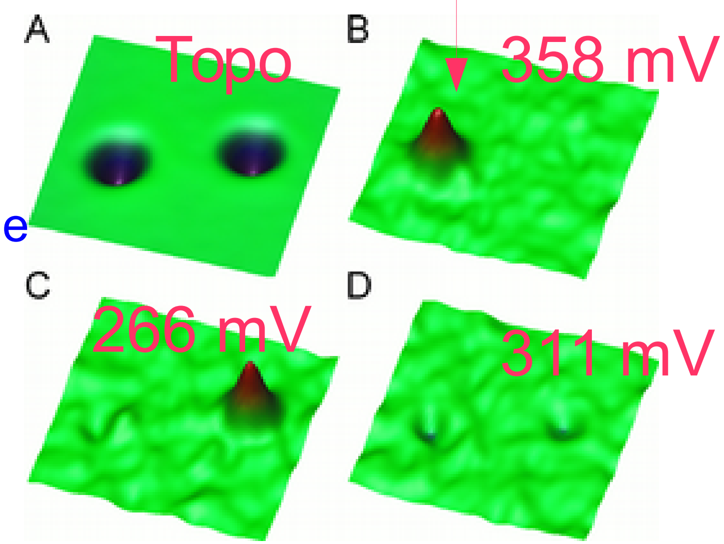

B. C. Stipe, M. A. Rezaei and W. Ho, Science **280**, 1732 (1998)

Magnetic imaging

STM polarized STM (Mn on W)

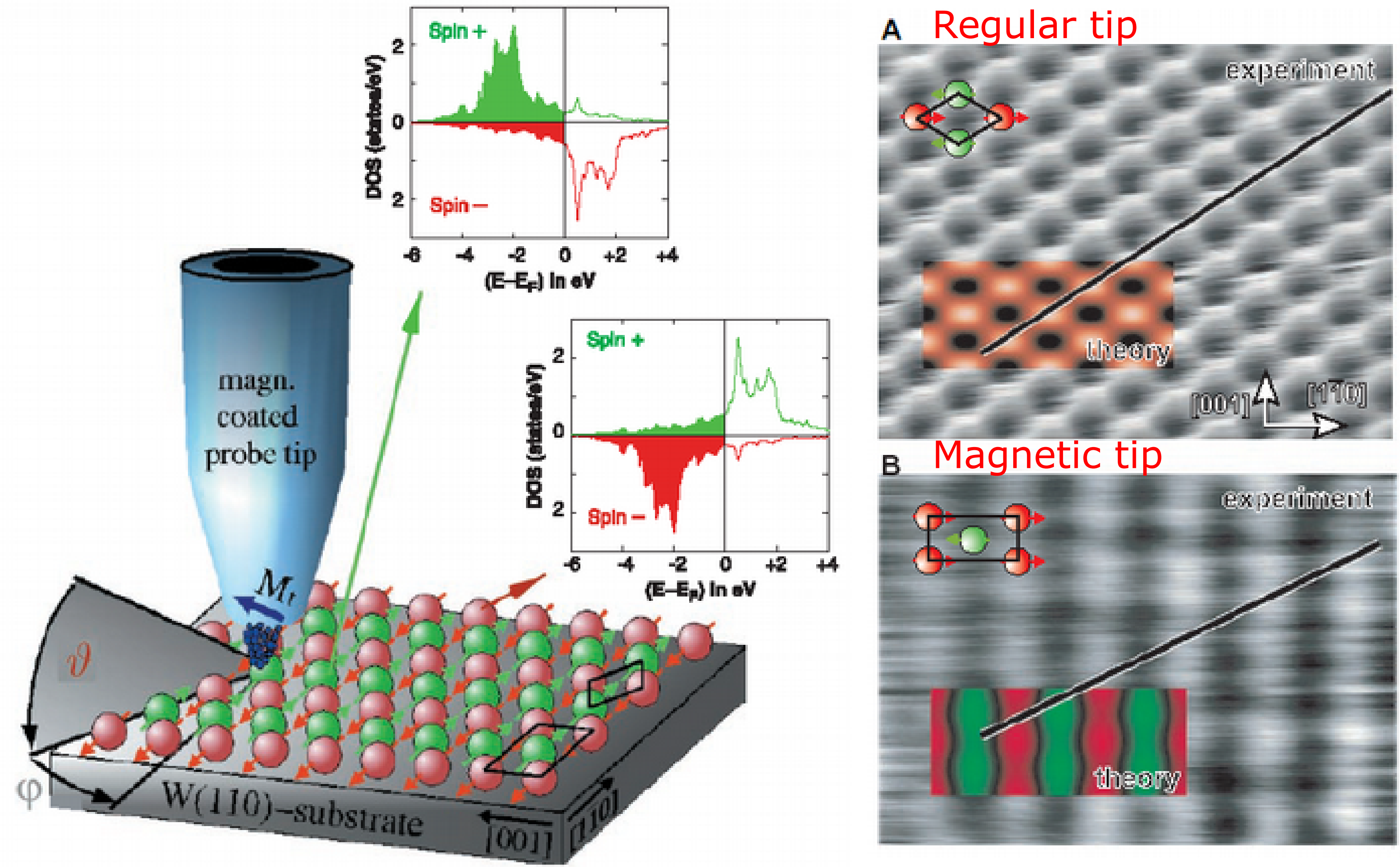

S. Heinze *et al.*, science **288**, 1805 (2000)

Conductance maps

Surface waves (Ge 111 surface states)

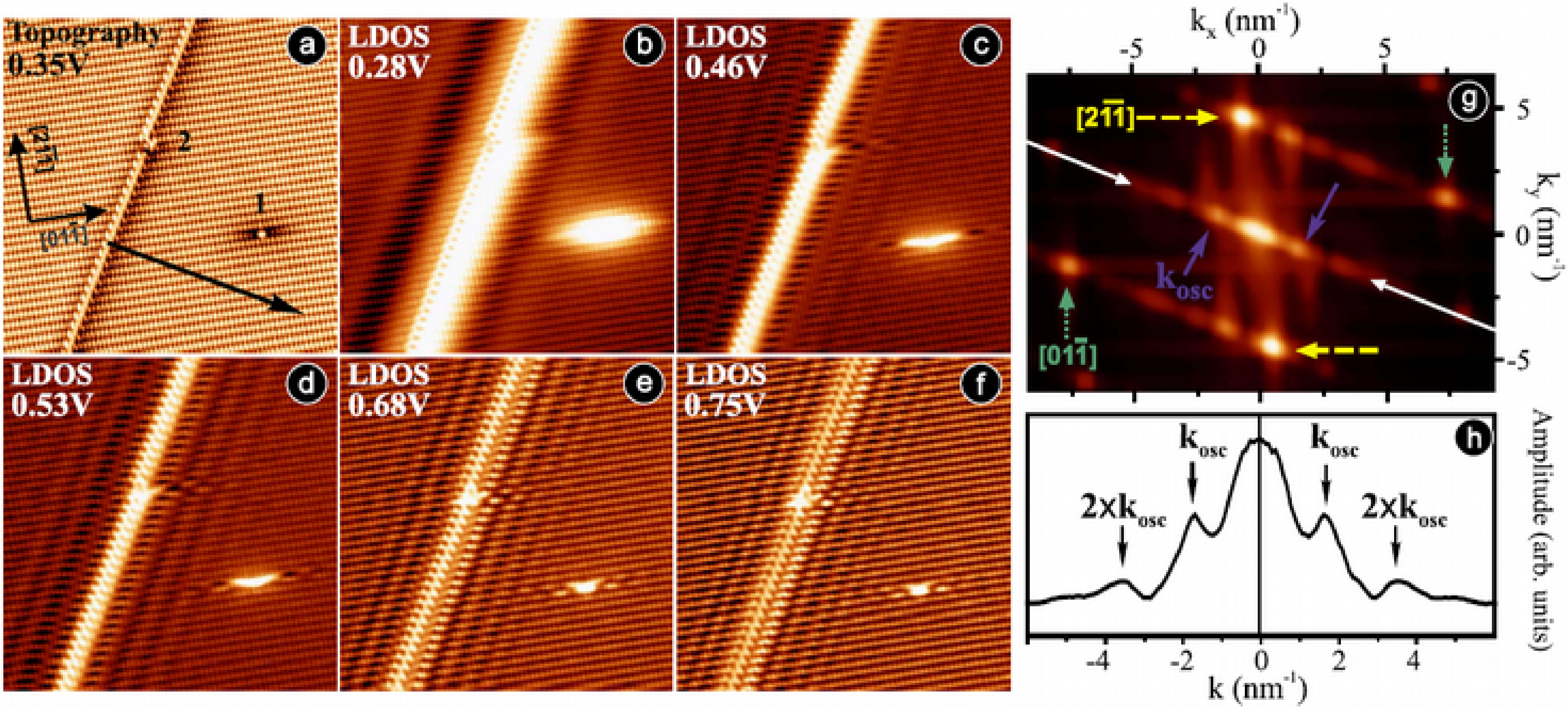

DOS wave caused by domain boundary (crystal defect)

Muzychenko, PRB 81, 035313 (2010)

Quantum Mirage:
combining atomic control and dI/dV maps

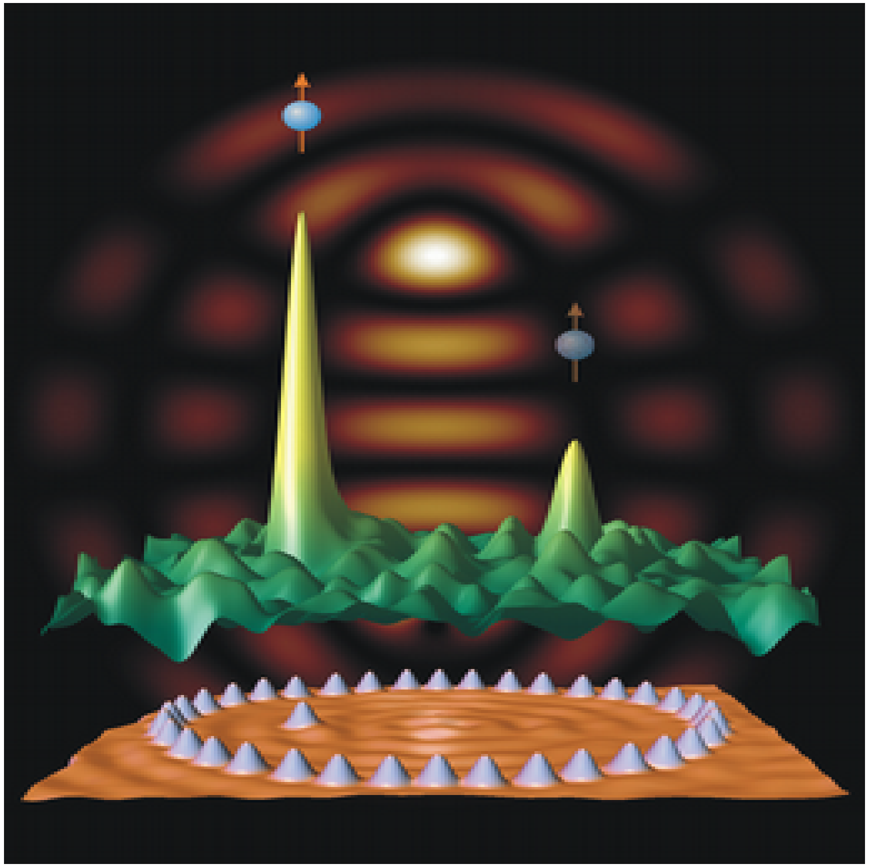

H. C. Manoharan, C. P. Lutz & D. M. Eigler, Nature 403, 512 (2000).

Mirage Quantique

Cu(111)/Co

Topo

Co : kondo state

Mirage

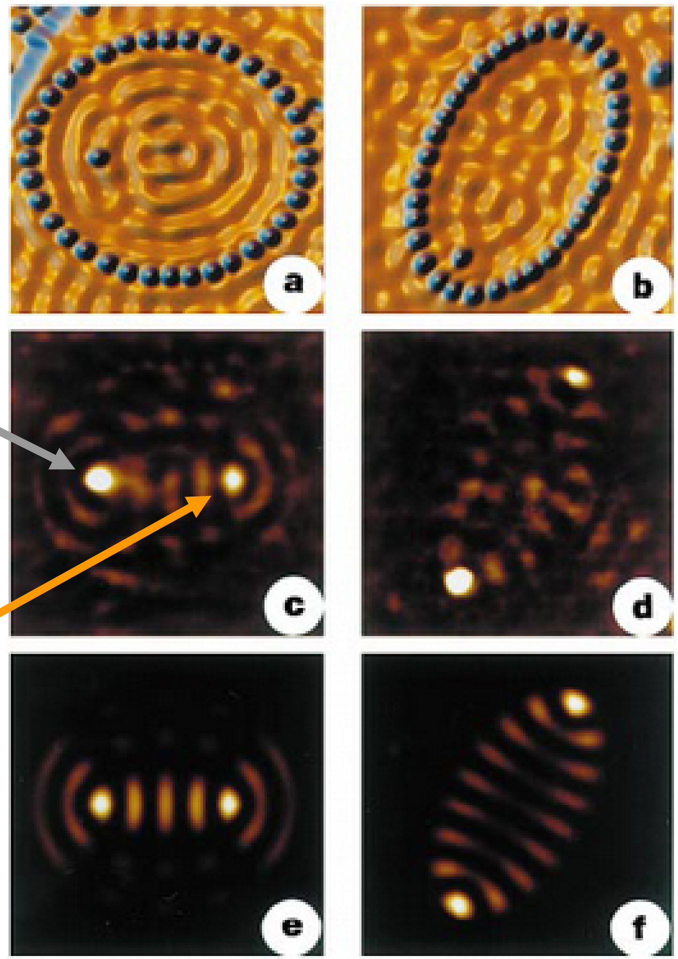

dI/dV maps

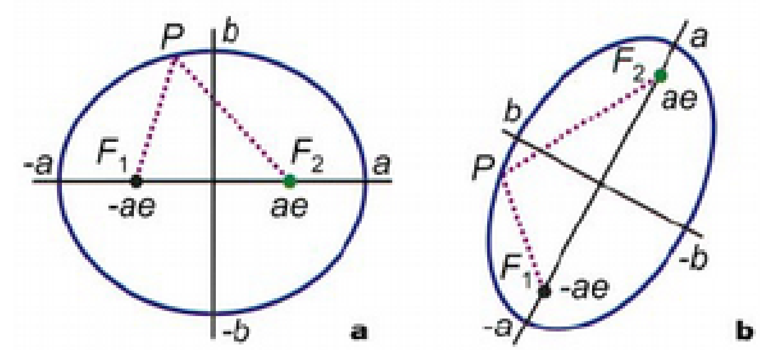

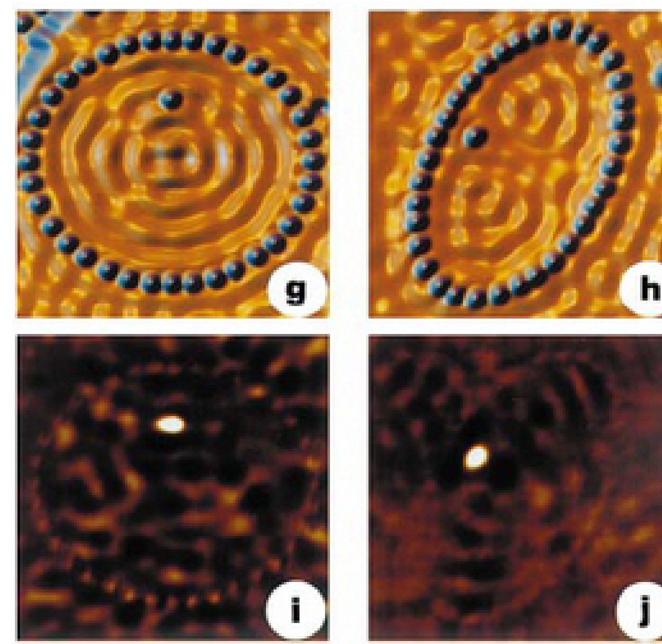

H. C. Manoharan, C. P. Lutz & D. M. Eigler, Nature 403, 512 (2000).

$Bi_2Sr_2CaCu_2O_{8+\delta}$

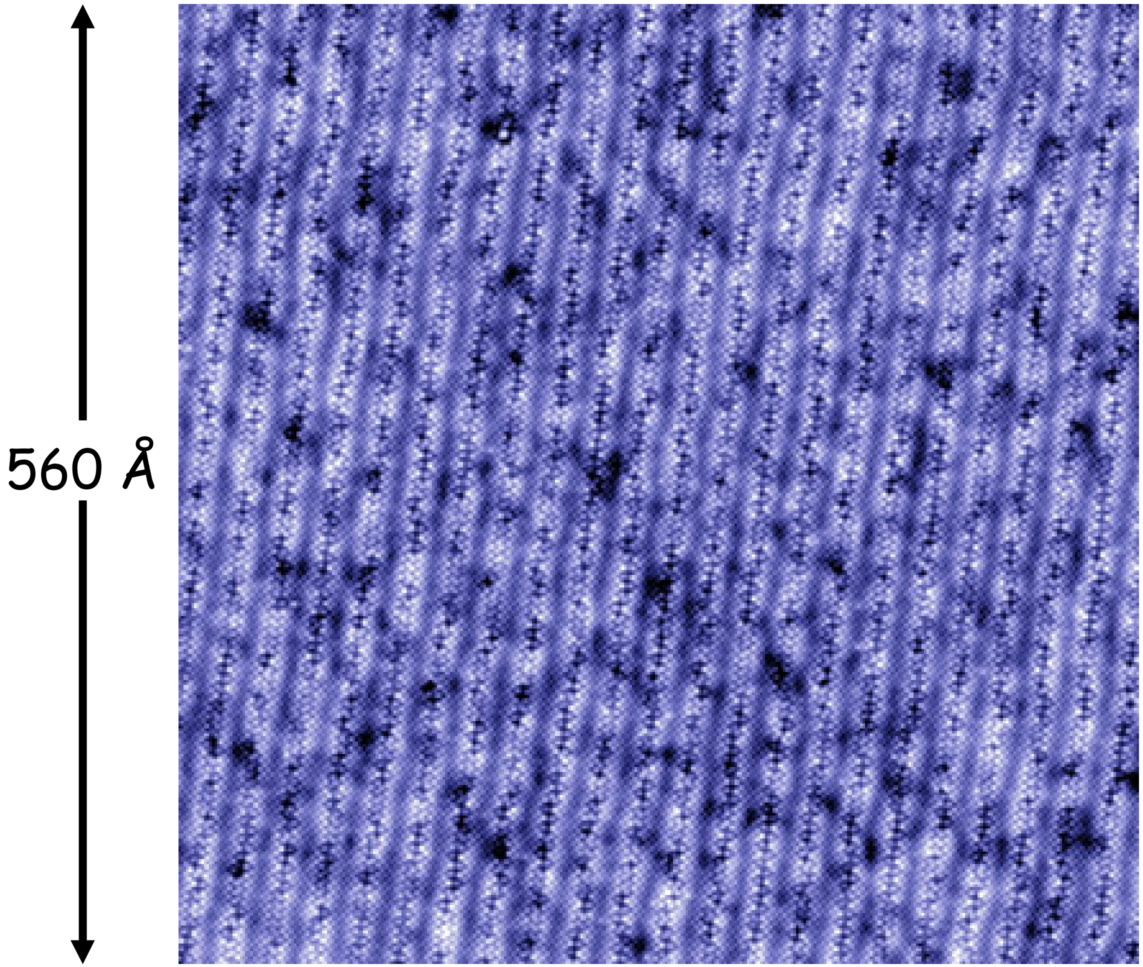

T= 4.2K, B = 0T
100pA, -100mV

$Bi_2Sr_2CaCu_2O_{8+\delta}$

Each bright spot is a Bi atom.

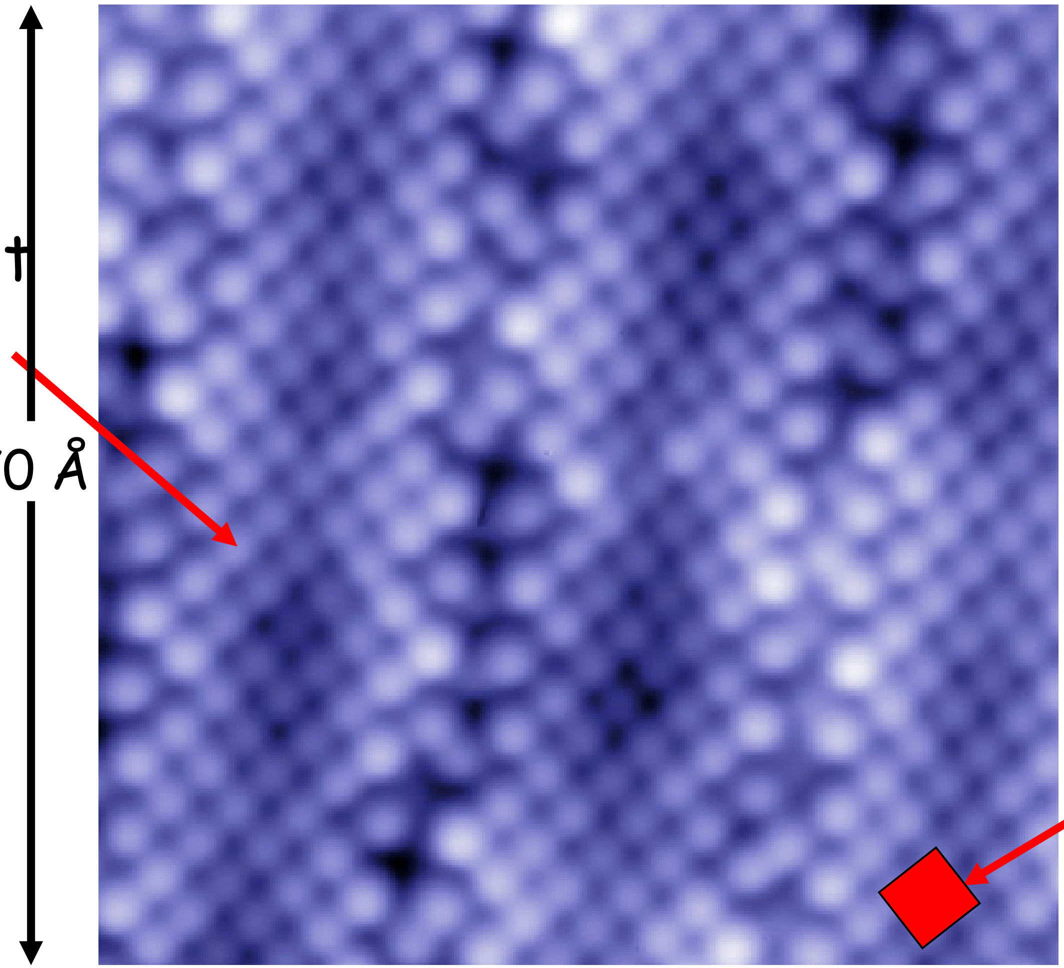

Size & orientation of CuO_2 unit cell (~ 5Å below surface).

T= 4.2K, B = 0T
100pA, -100mV

$Bi_2Sr_2Ca(Cu_{1-x}Zn_x)_2O_{8-\delta}$: $x \approx 0.6\%$

Can you find the defects (Zn)?

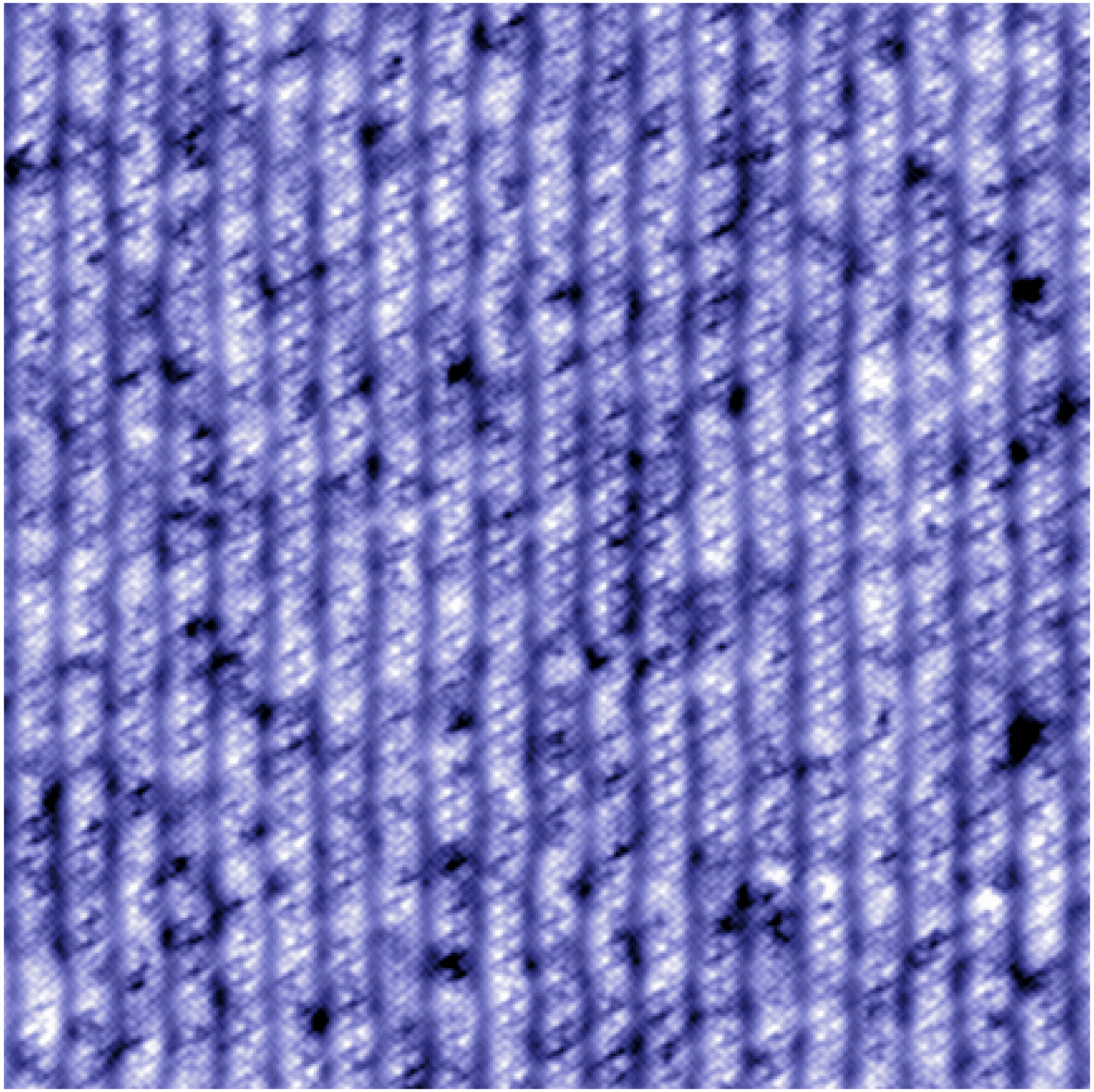

500 Å, 4.2 K
200 pA, -200 mV

Sample: H. Eisaki, S. Uchida

$Bi_2Sr_2Ca(Cu_{1-x}Zn_x)_2O_{8-\delta}$: $x \approx 0.6\%$

LDOS Map at
–1.5 meV

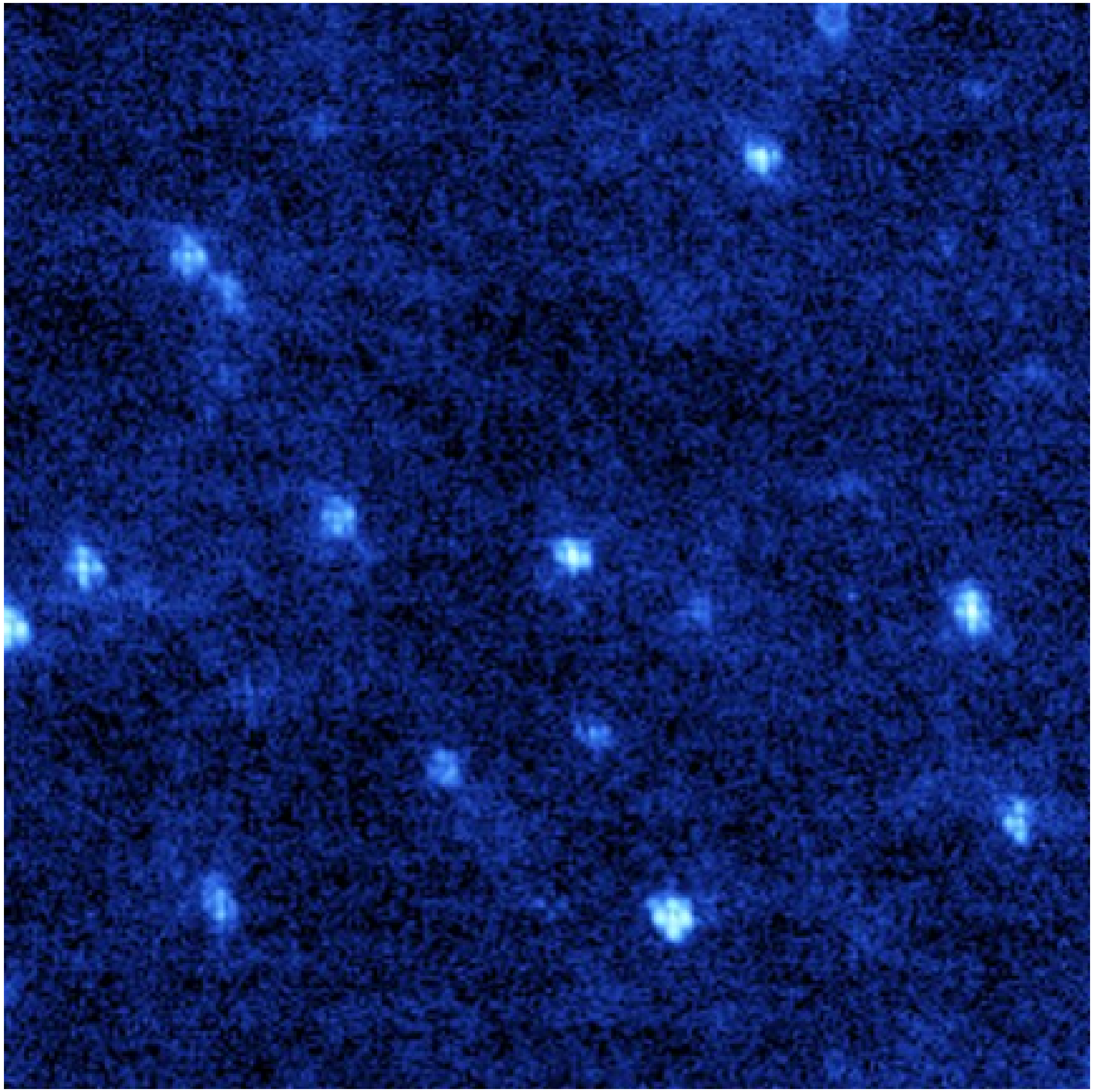

500 Å, 4.2 K
200 pA, -200 mV

S.H. Pan, *et al.* *Nature* **403,** 746 (2000).

$Bi_2Sr_2Ca(Cu_{1-x}Zn_x)_2O_{8-\delta}$ spectra

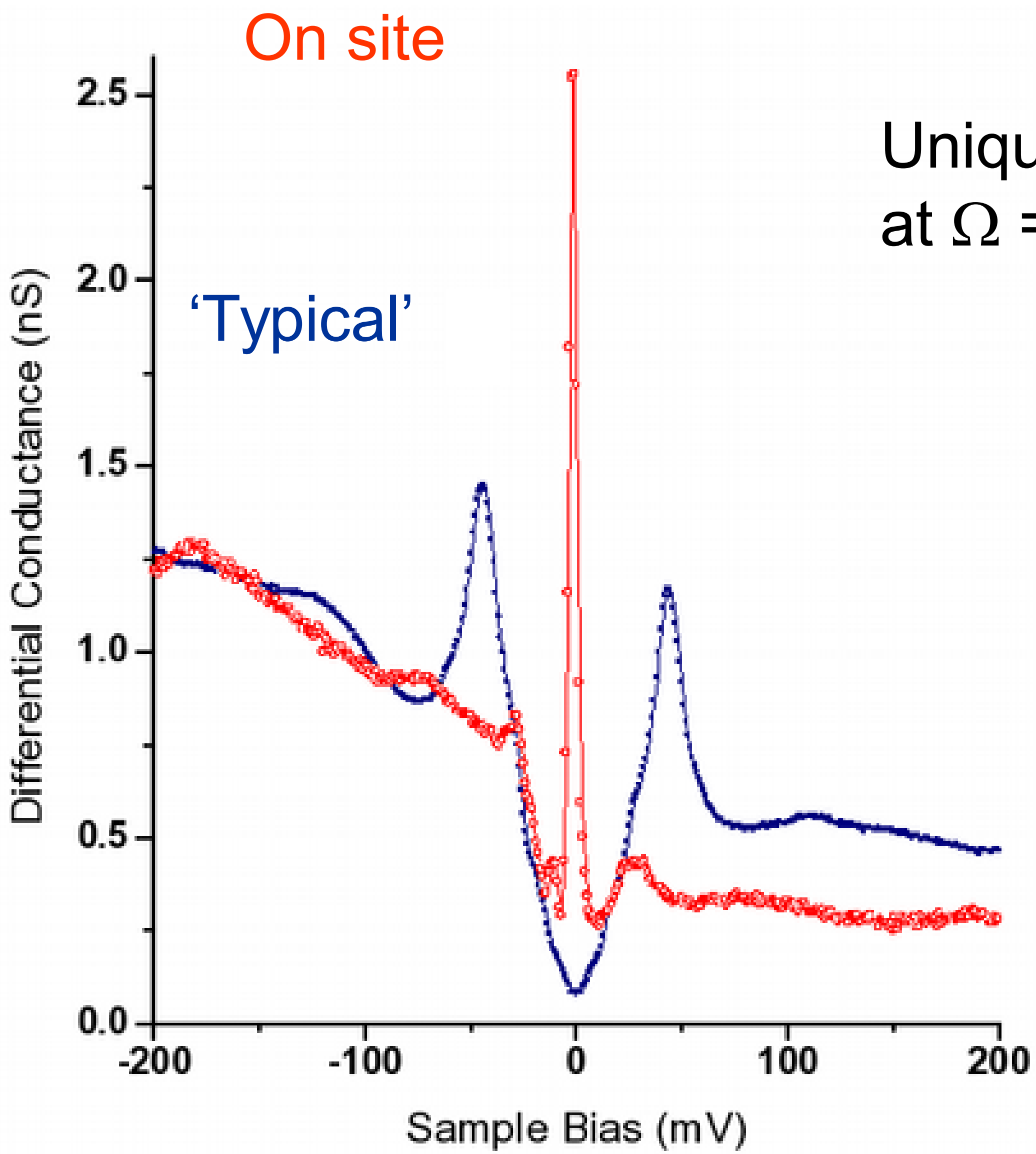

Unique resonance at Ω = -1.5 meV

Nature **403,** 746 (2000).

Zn Impurity State Location and Orientation

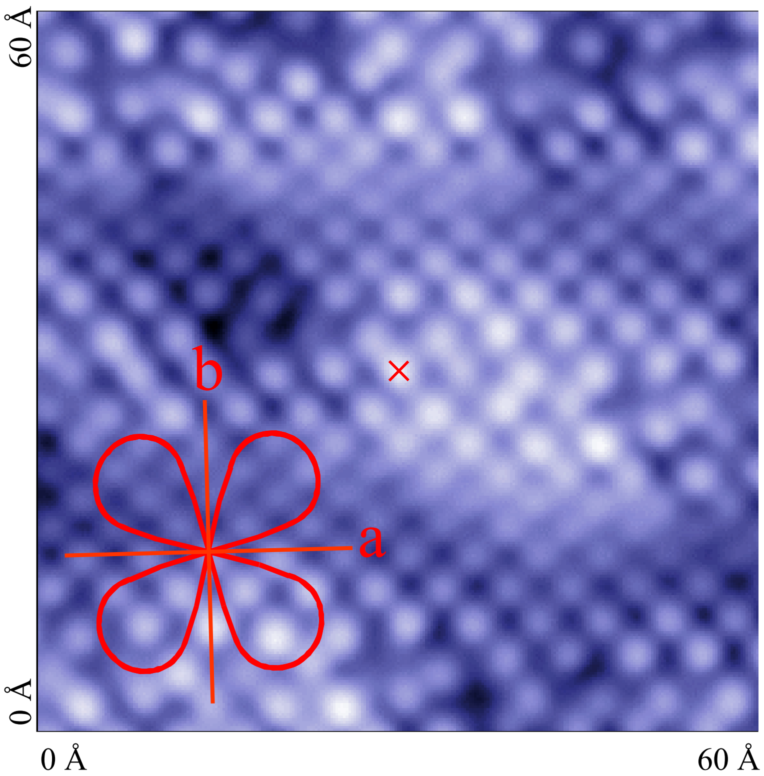

Topography (BiO Plane)

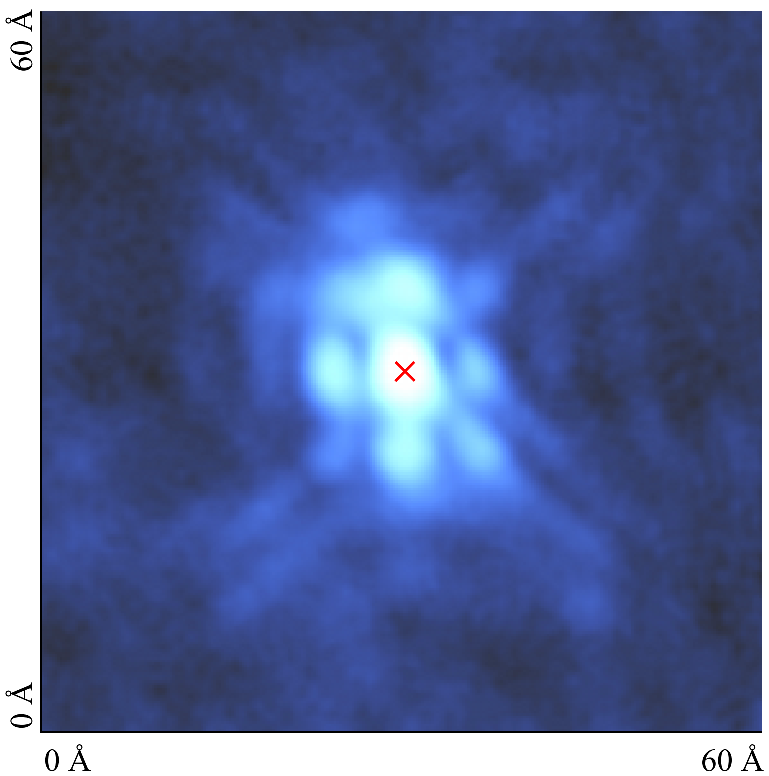

LDOS Map, V = -1 mV

Nature **403,** 746 (2000).

60 Å, 4.2 K
200 pA, -200 mV

$Bi_2Sr_2Ca(Cu_{1-x}Ni_x)_2O_{8+\delta}$ Topo, $x \approx 0.5\%$

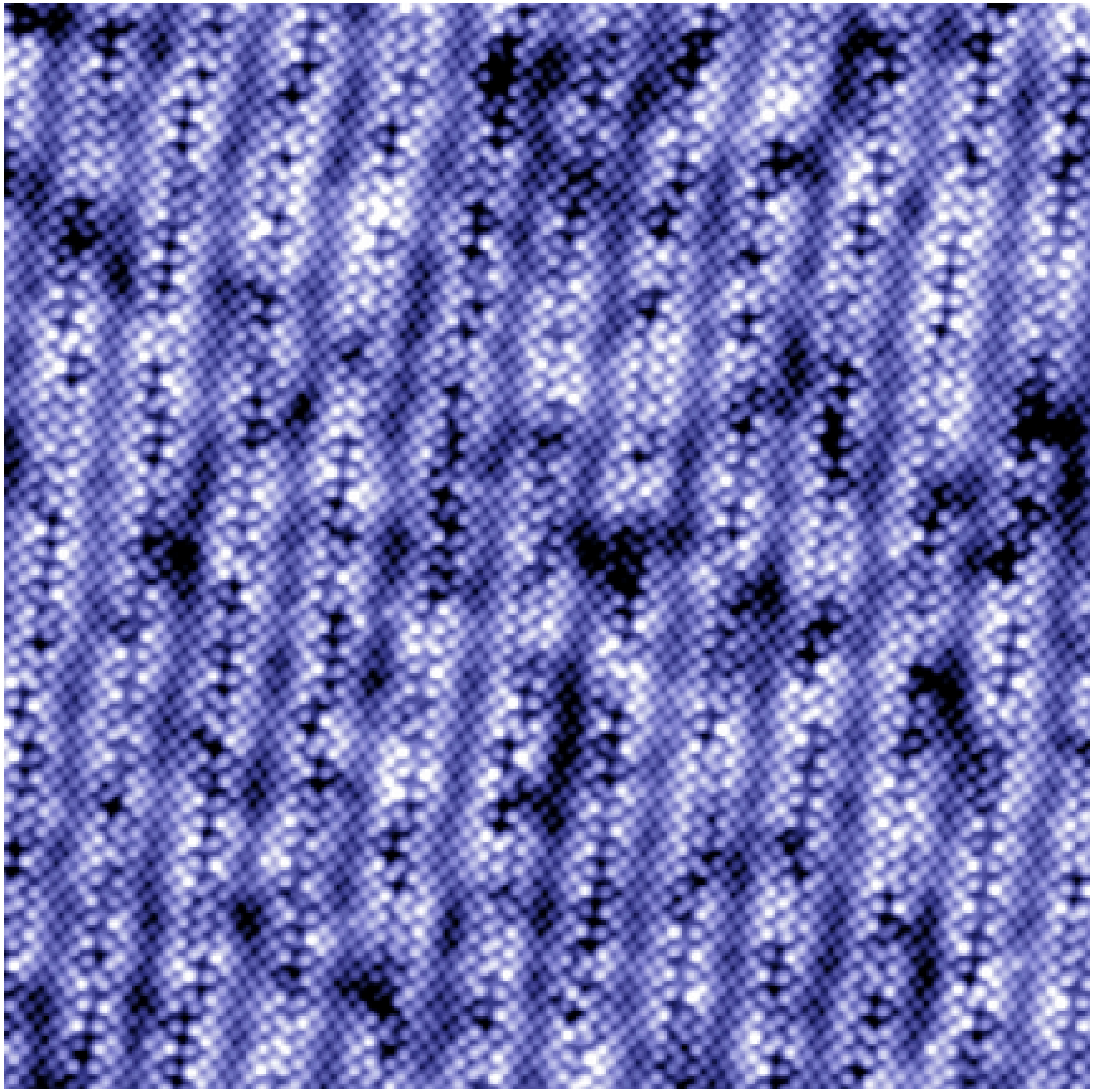

256 Å, 4.2 K
100 pA, -100 mV

Sample: H. Eisaki, S. Uchida

$Bi_2Sr_2Ca(Cu_{1-x}Ni_x)_2O_{8+\delta}$, $x \approx 0.5\%$ conductance map at +10 meV

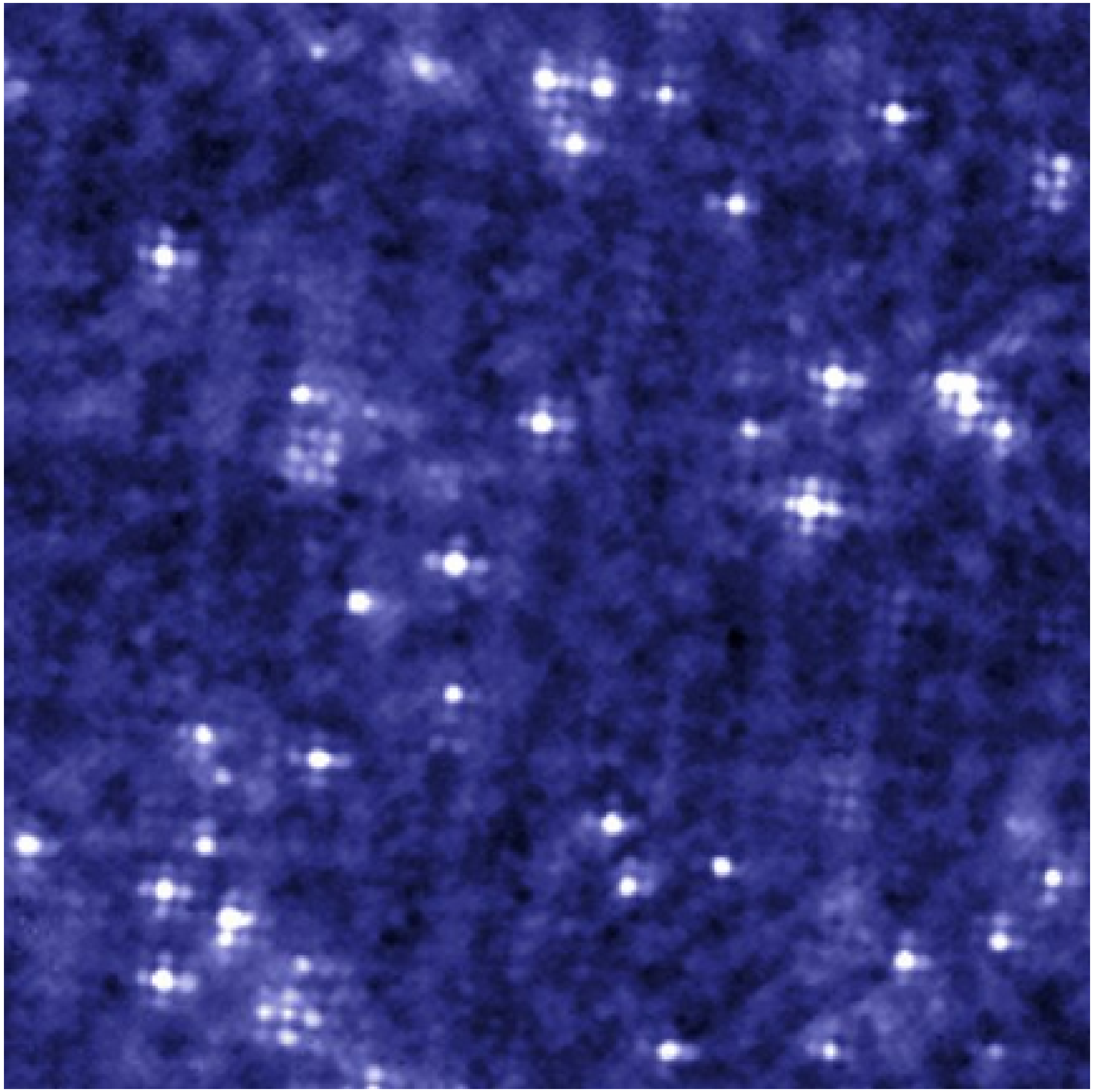

256 Å, 4.2 K
100 pA, -100 mV

E.W. Hudson. *et al.*, *Nature* **411**, 920 (2001).

$Bi_2Sr_2Ca(Cu_{1-x}Ni_x)_2O_{8+\delta}$ Spectra

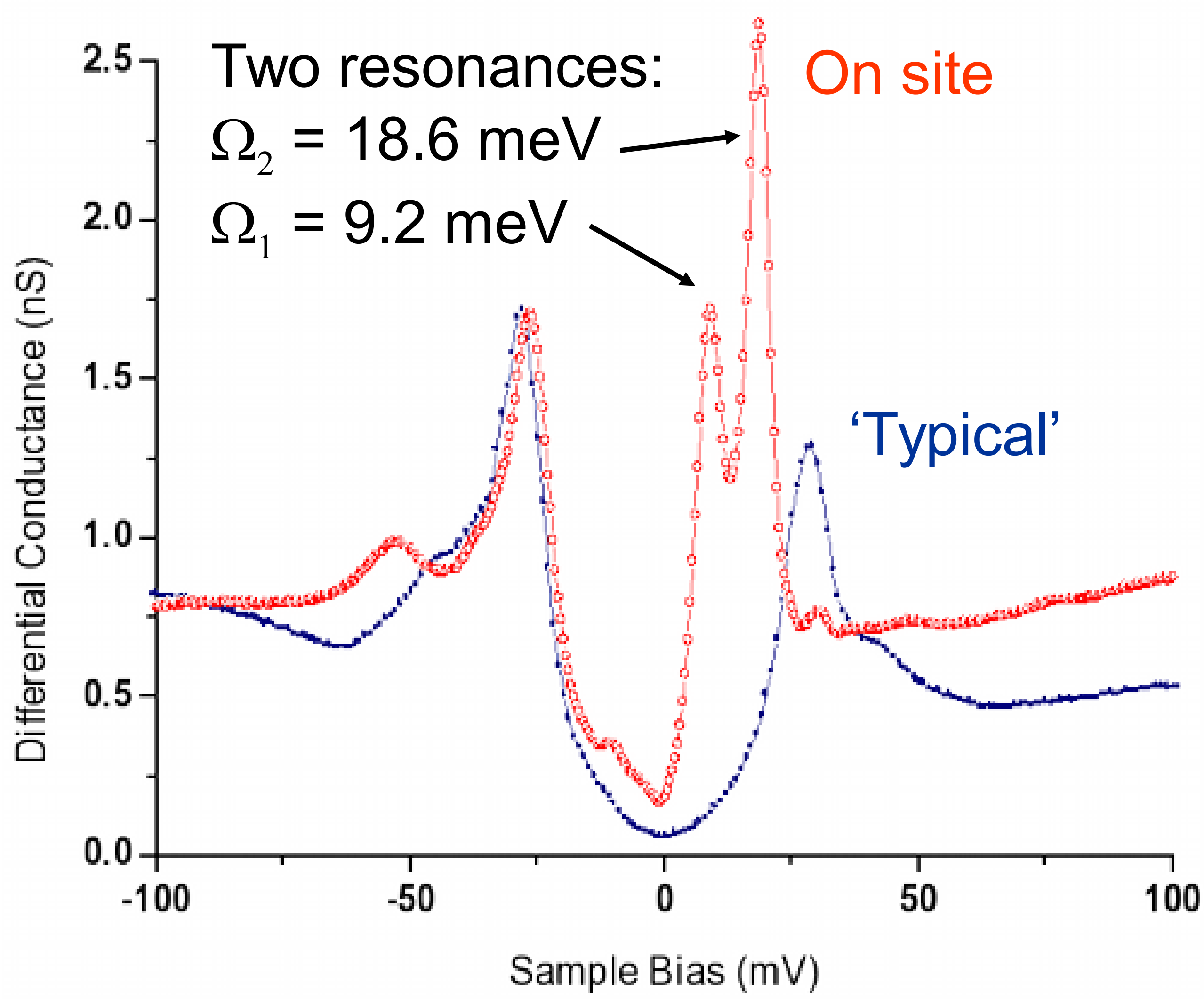

Superconducting Gap maps

Gap map as a function of location:

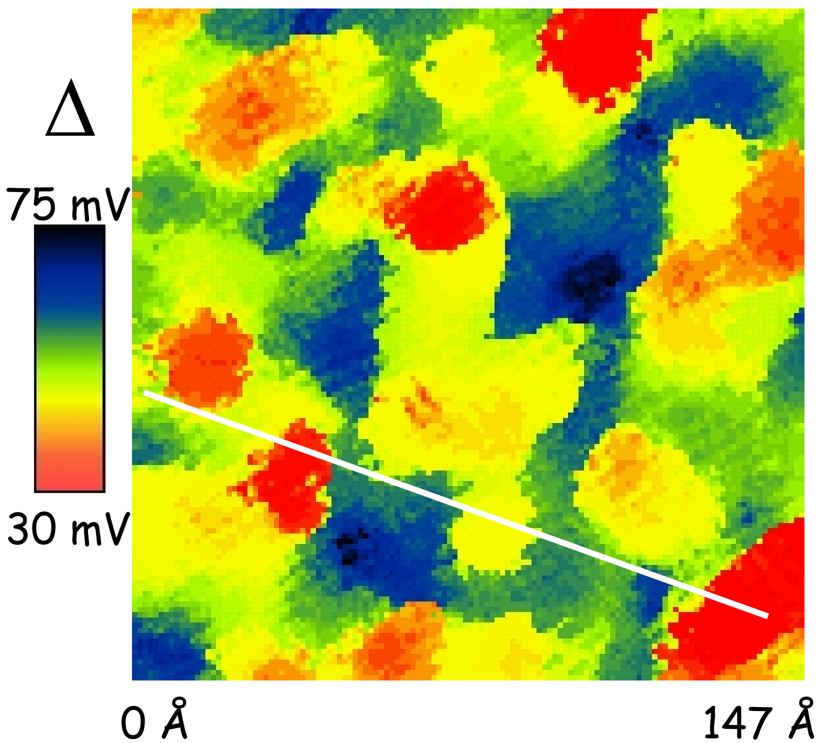

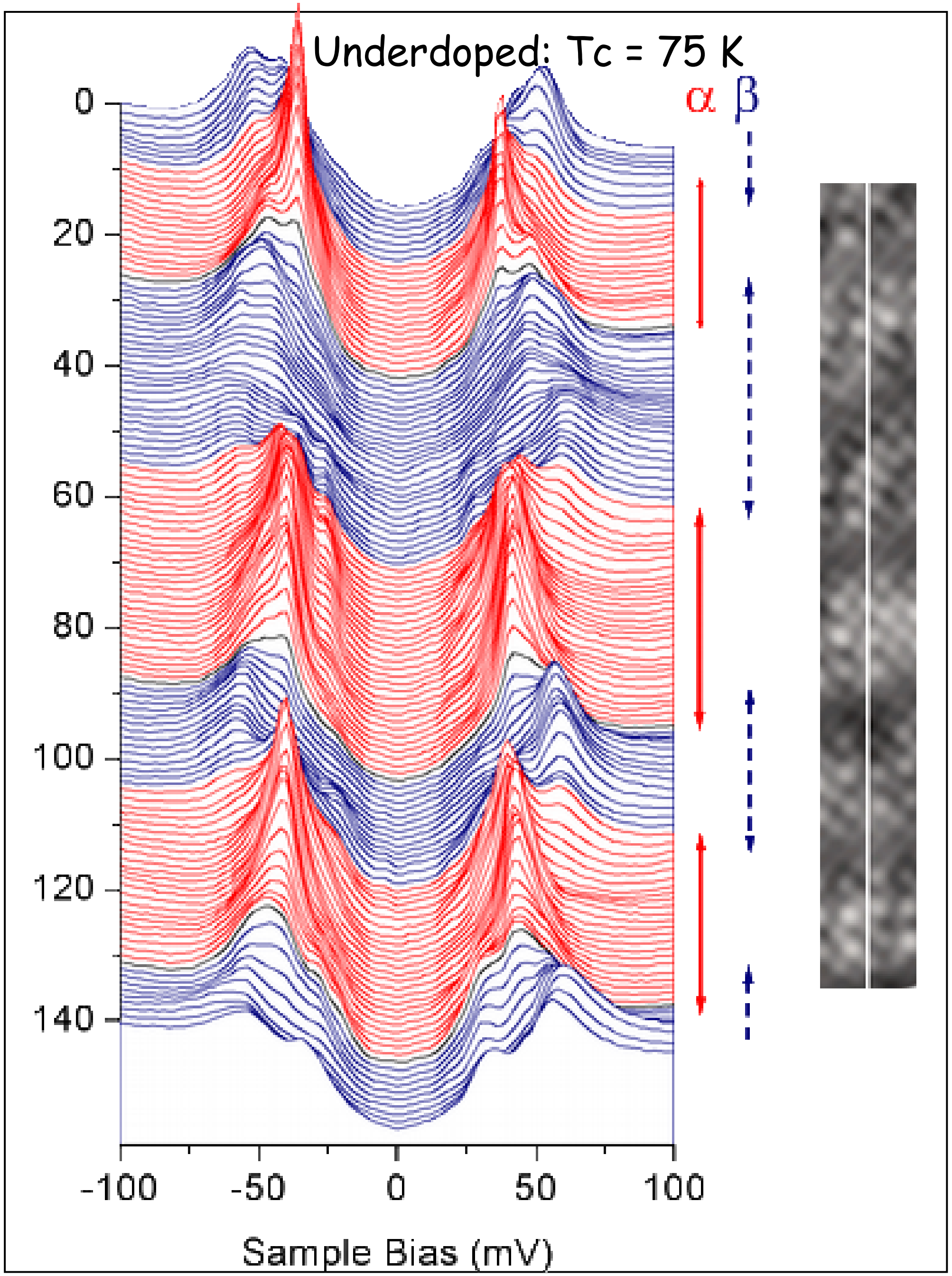

Gap size is heterogeneous

Average size ~3 nm

Nature 415, 412 (2002)

New spectral type appears and eventually dominates at low p

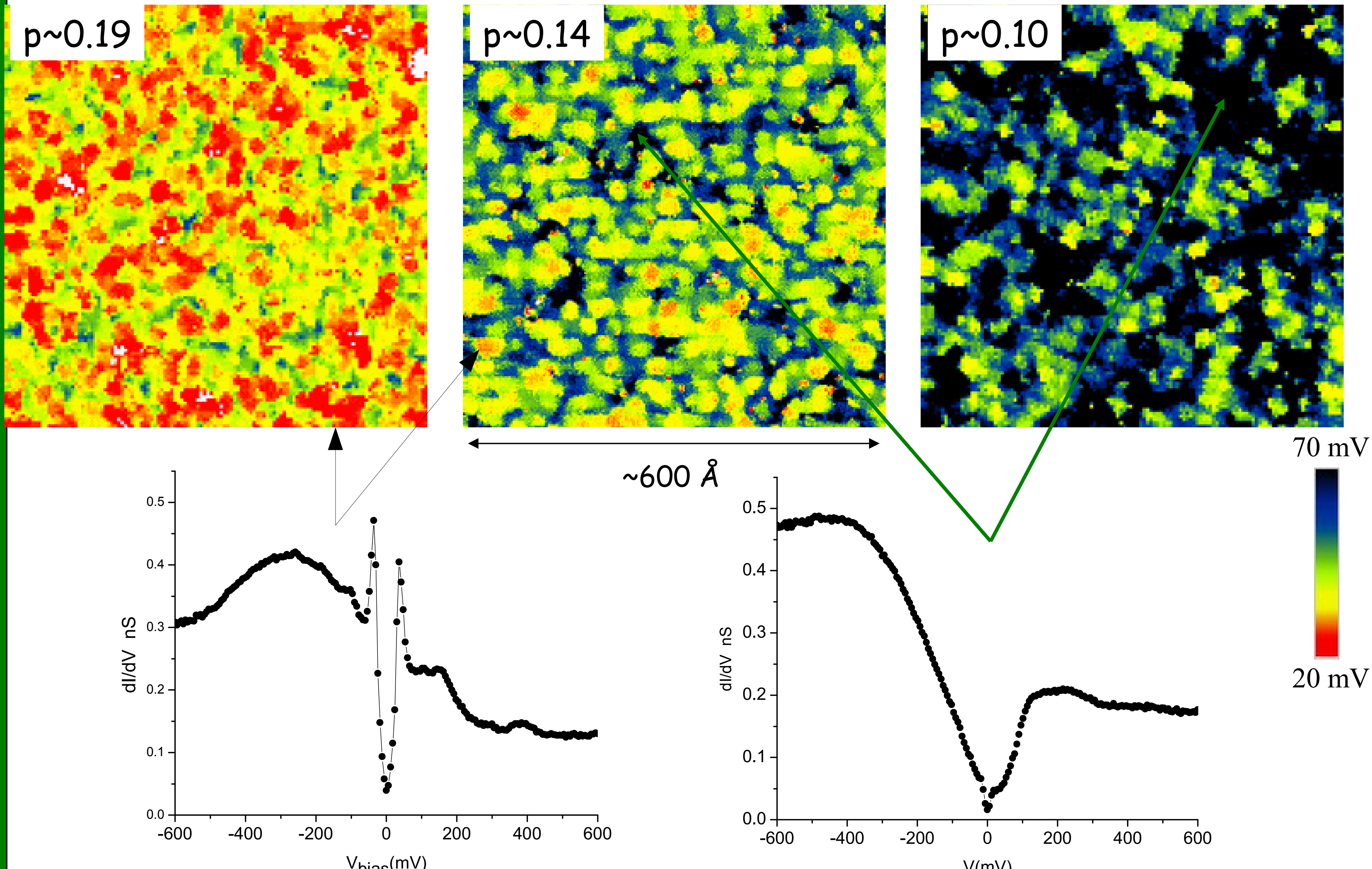

d-SC Spectrum

ZTPG Spectrum

McElroy *et al* PRL **94**, 197005 (2005)

UNIVERSITÉ DE SHERBROOKE

DOS structure

Topo image of CaCl plane of $Ca_{1.9}Na_{0.1}CuO_2Cl_2$

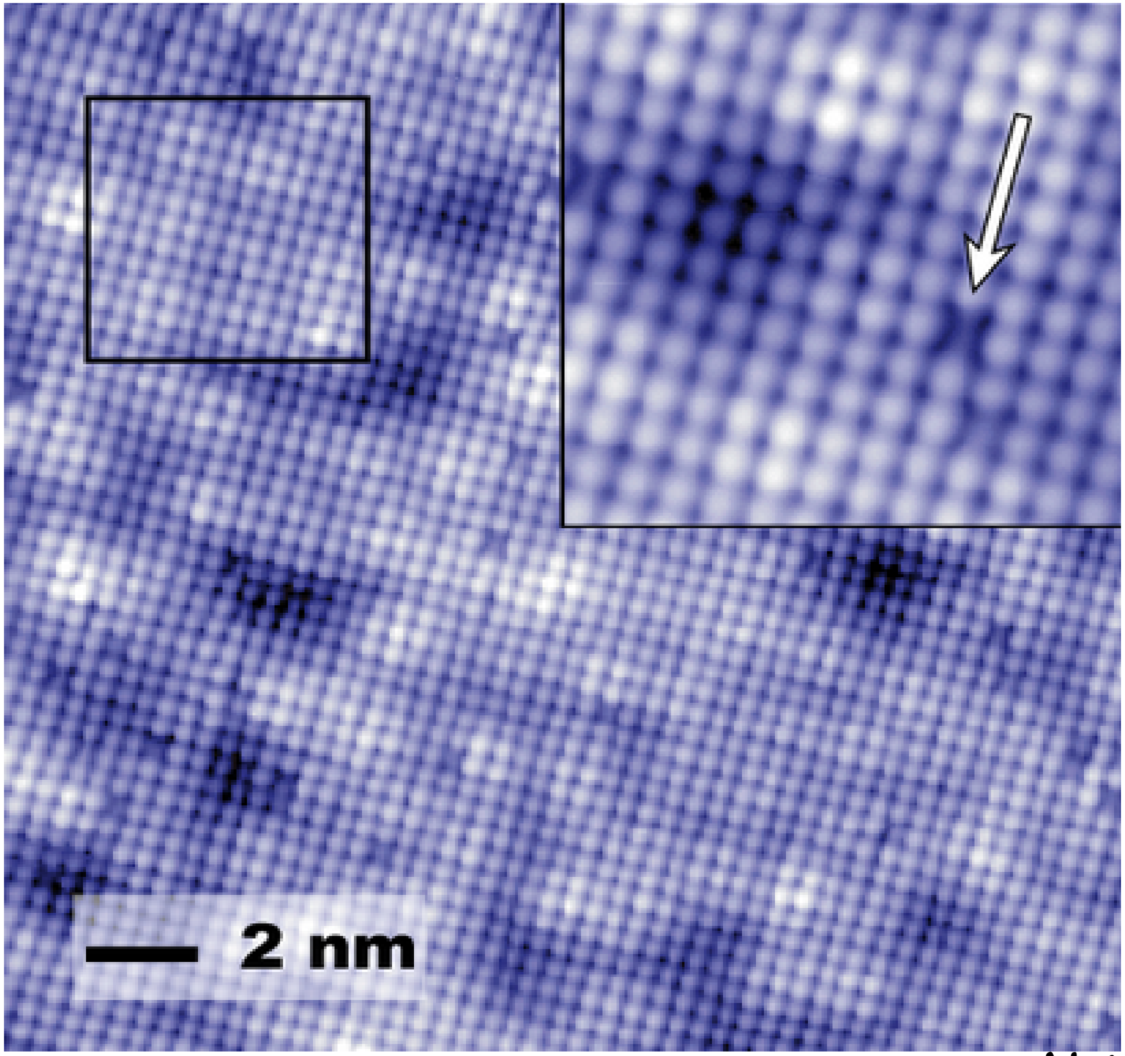

200 mV / 50 pA

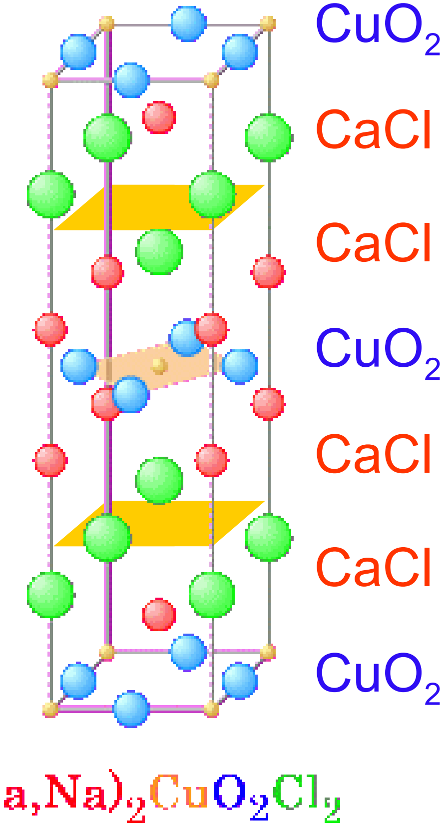

Nature 430, 1001 (Aug. 26 2004)

Spectroscopic imaging within pseudogap

Topograph

T < 250 mK

V_{sample} = 200 m

I_t = 50 pA

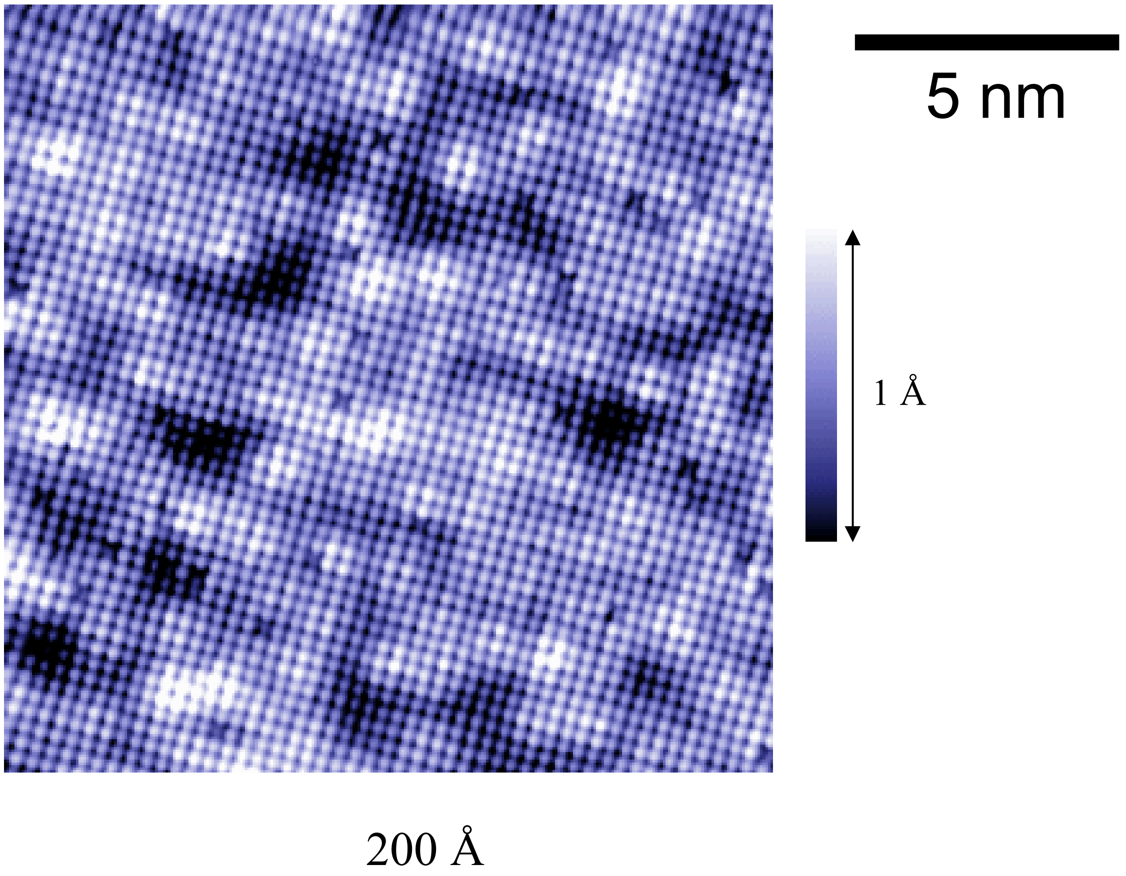

Nature 430, 1001 (Aug. 26 2004)

Spectroscopic imaging within pseudogap

$dI/dV|_{+24mV}$

T < 250 mK

V_{sample} = 200 mV

I_t = 100 pA

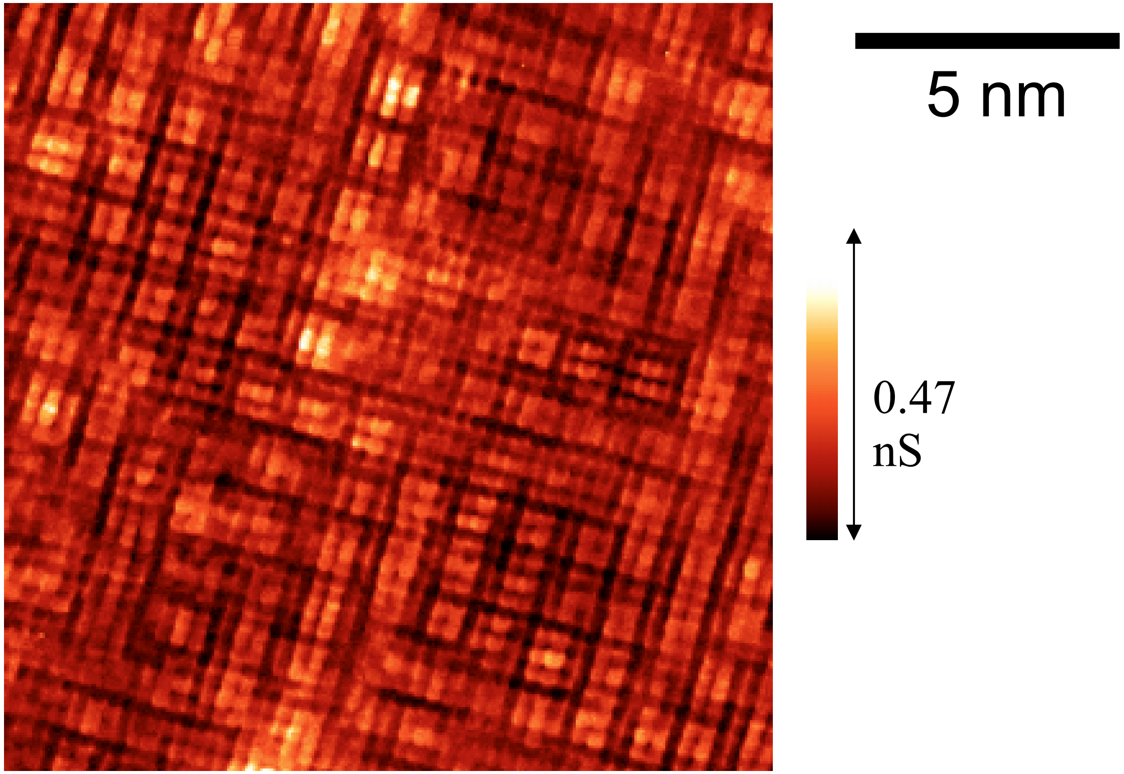

200 Å

Nature 430, 1001 (Aug. 26 2004)

Maps 10% doping

-150 mV

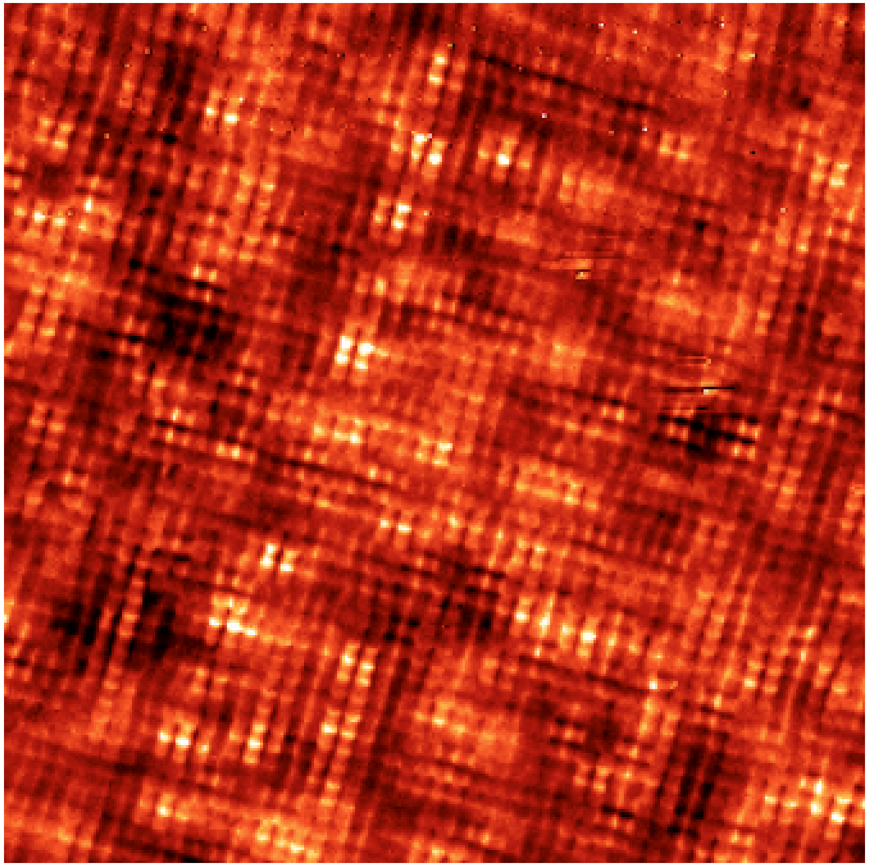

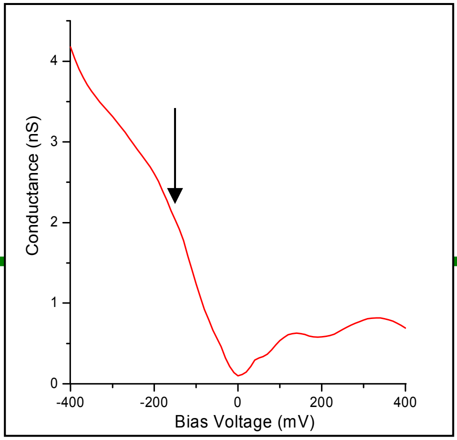

Examine spatial structure directly at the atomic scale

Topograph

T < 250 mK

V_{sample} = 200 mV

I_t = 50 pA

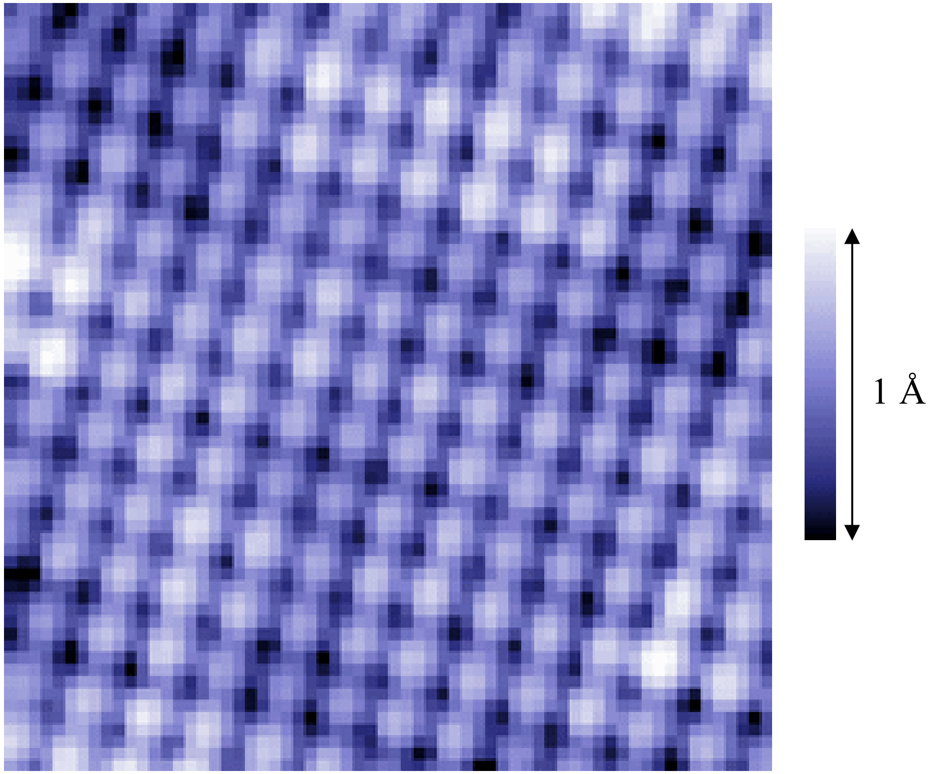

Nature **430, 1001 (Aug. 26 2004)**

Examine spatial structure directly at the atomic scale

$dI/dV|_{+25mV}$

T < 250 mK

V_{sample} = 200 mV

I_t = 100 pA

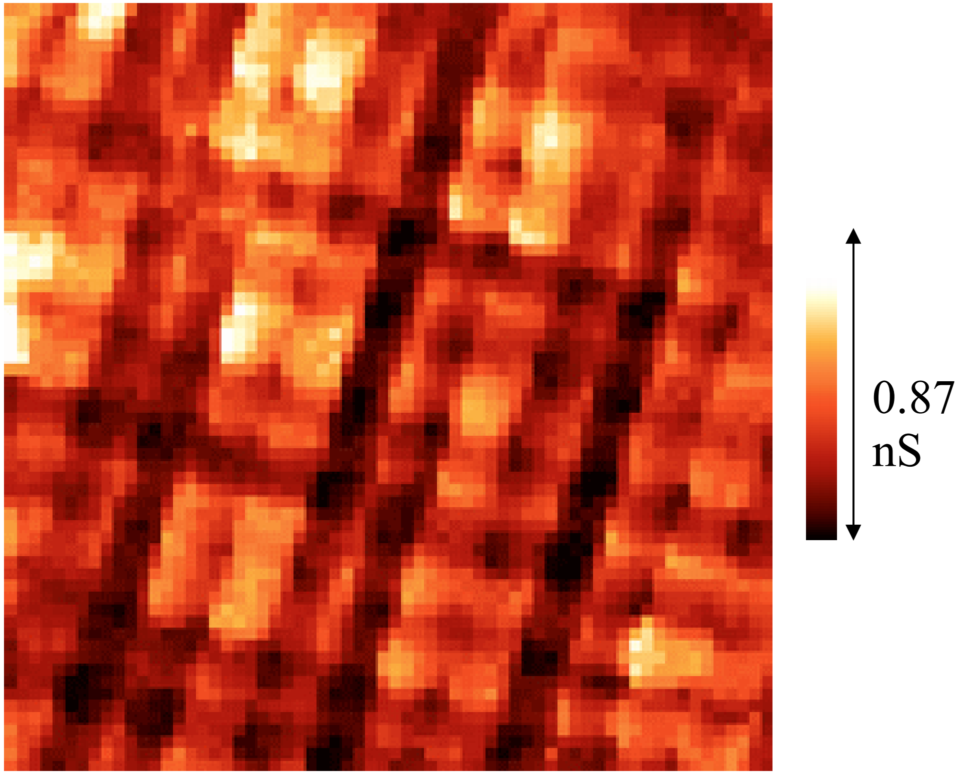

Nature **430, 1001 (Aug. 26 2004)**

Doping dependence

- Similar patterns for different samples/dopings
- Coexistence with SC order (as in underdoped Bi-2212)

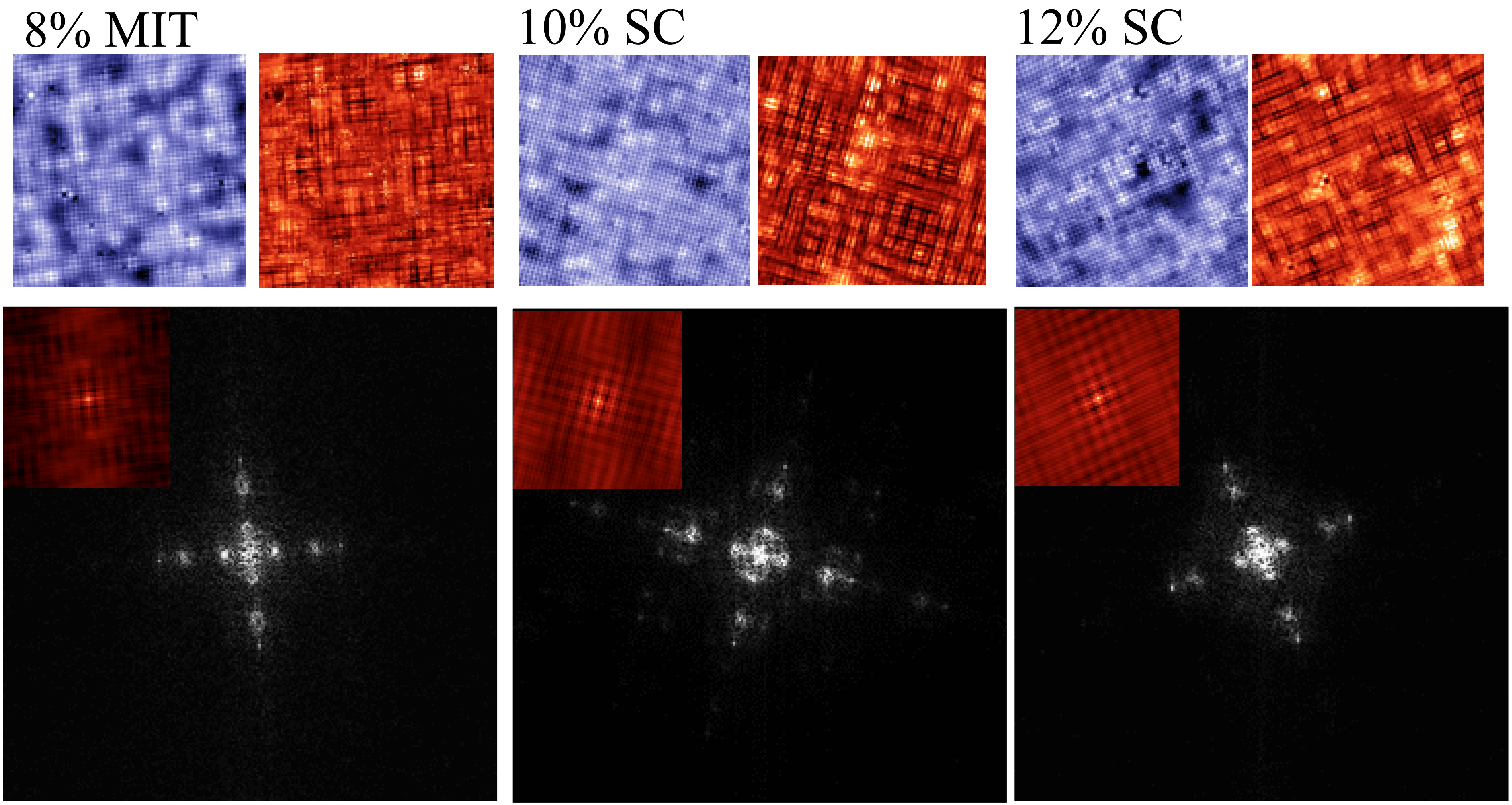

QPI

Quasi-Particle Interference (QPI)

First Normal metal
Fermi Surface

Add superconductivity
Gap with nodes

Banana like dispersion

Points with the largest
Density produce the most
Scattering (q vectors)

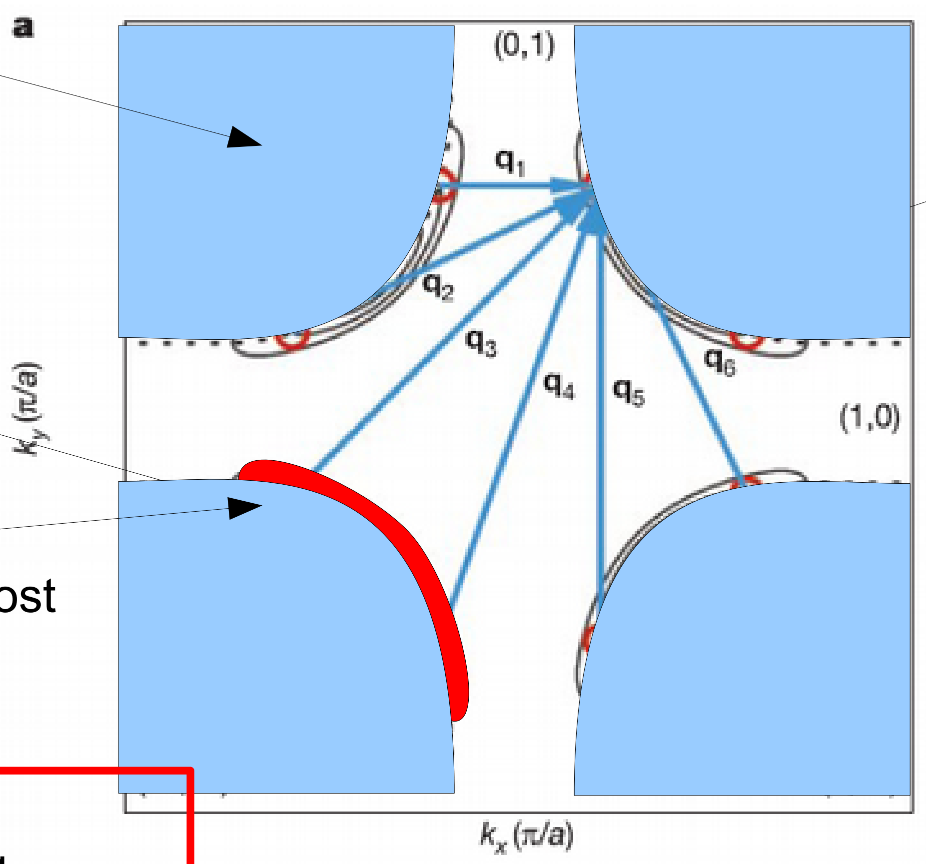

Node

Needed:
•Source of scattering
•Large joint density of states

K. McElroy *et al.*, Nature **422**, 592 (2003)

ARPES: Normal State Fermi Surface & Band Structure

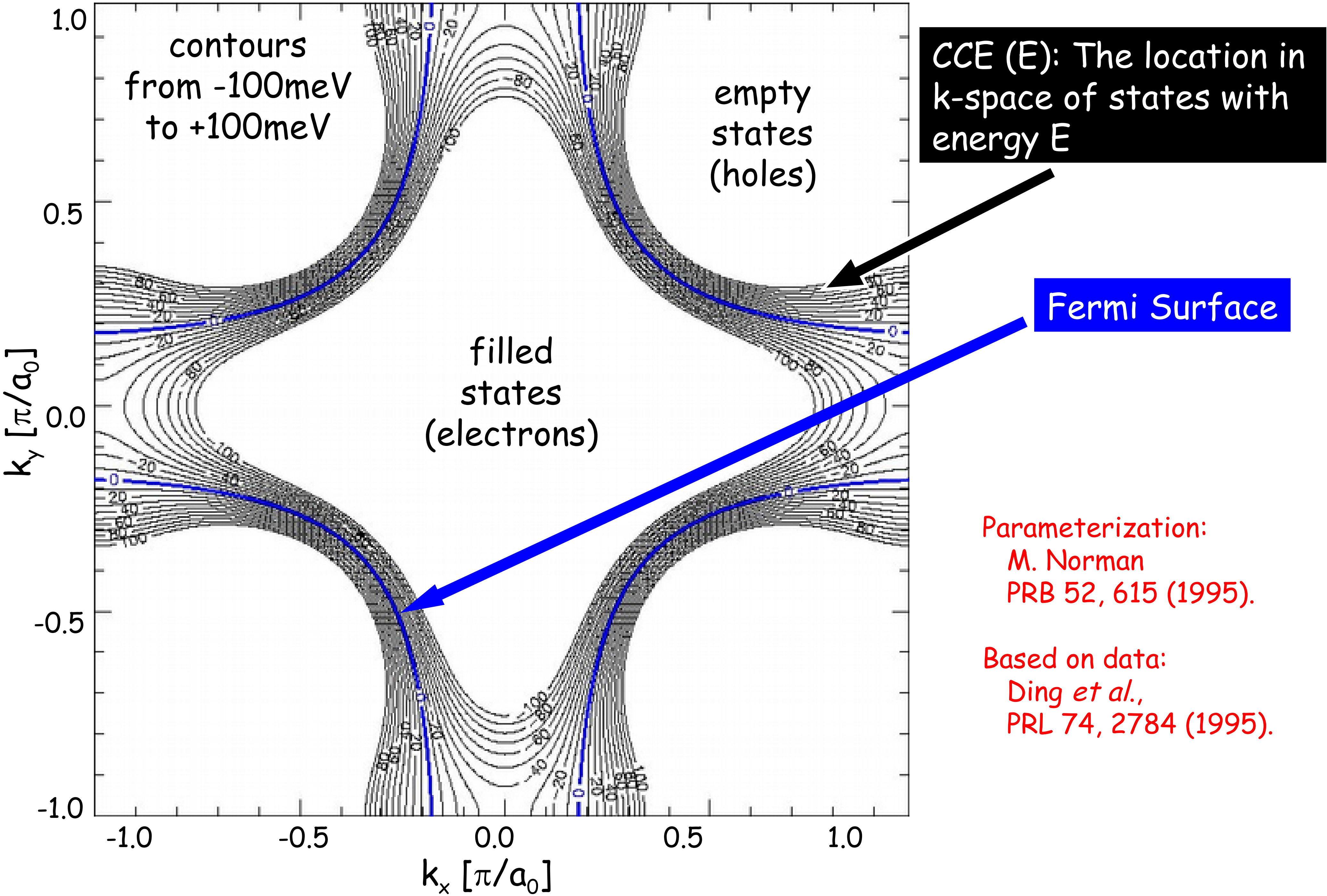

Parameterization:
M. Norman
PRB 52, 615 (1995).

Based on data:
Ding *et al.*,
PRL 74, 2784 (1995).

ARPES: Superconducting anisotropic gap $\Delta(k)$

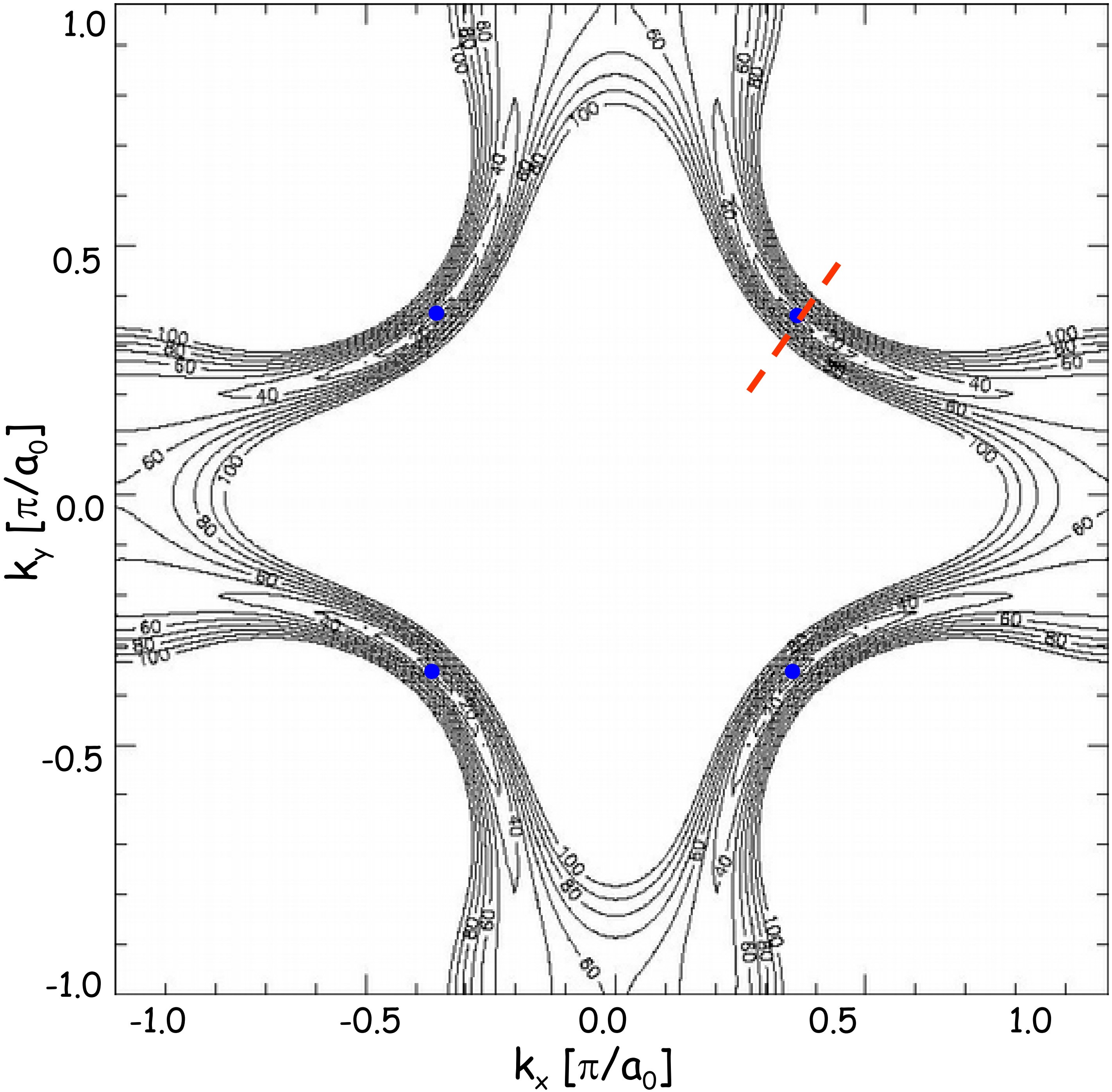

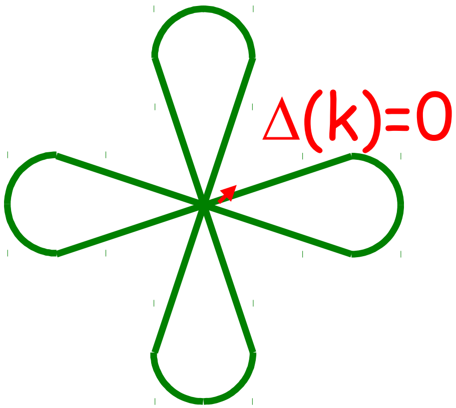

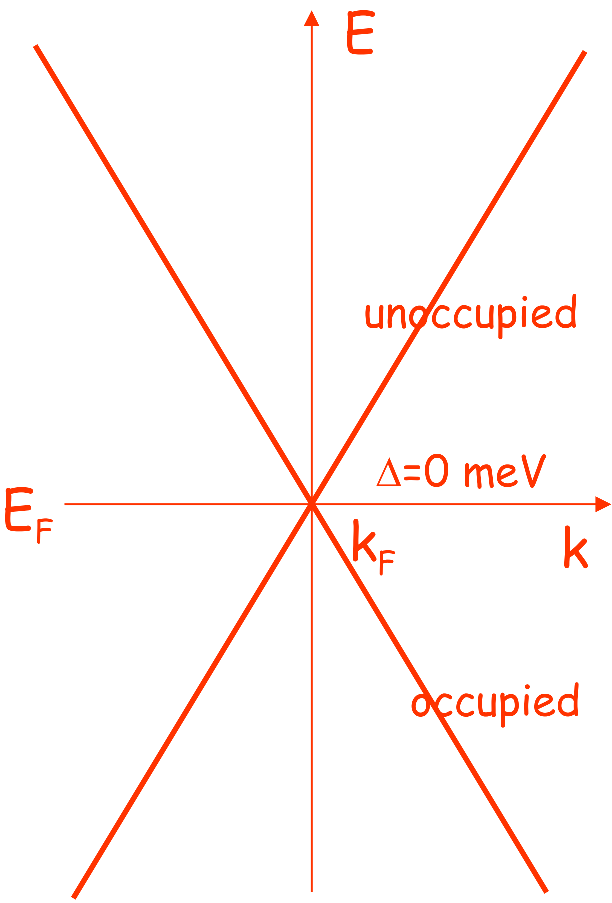

SHERBROOKE

ARPES: Superconducting anisotropic gap $\Delta(k)$

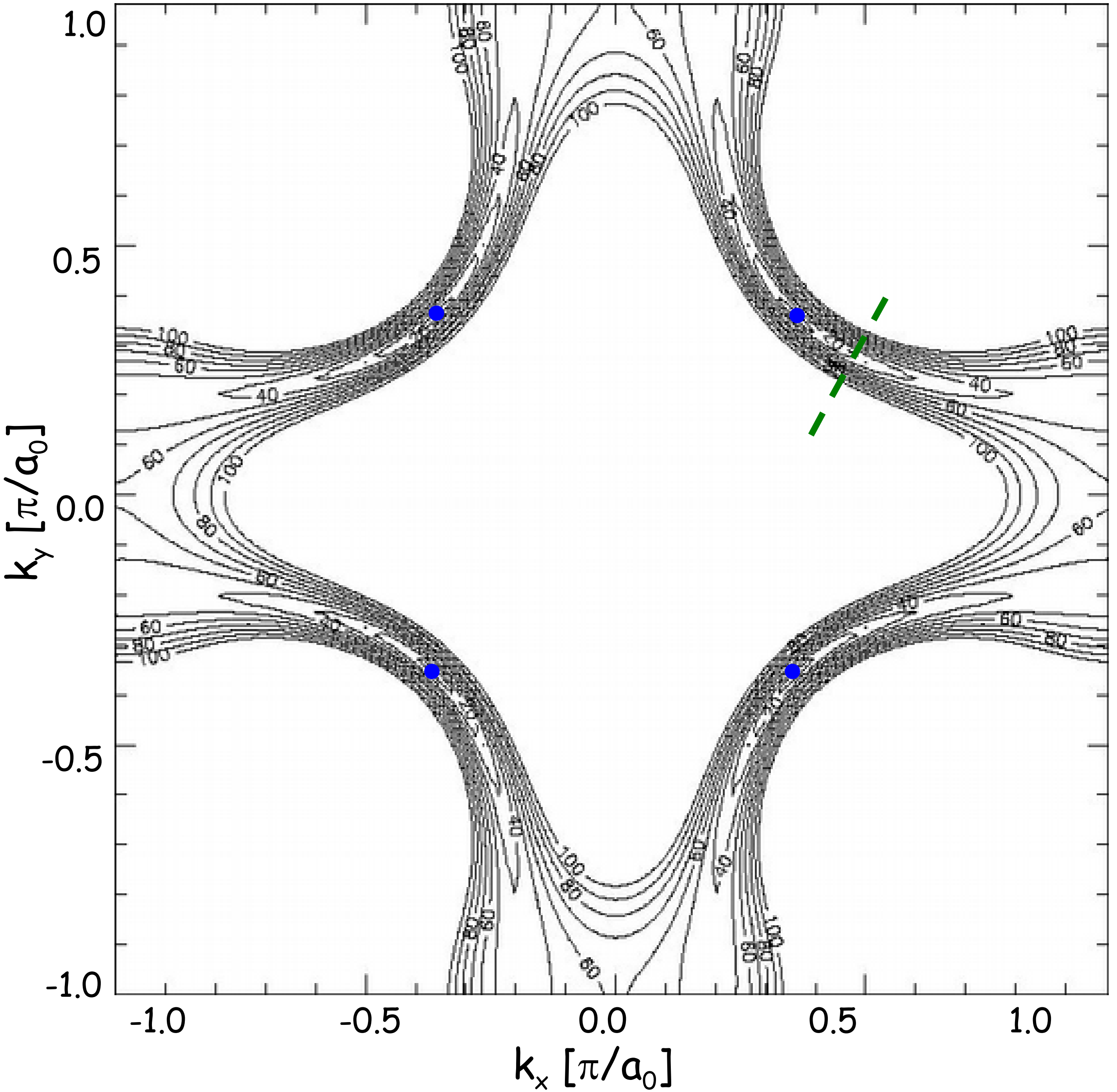

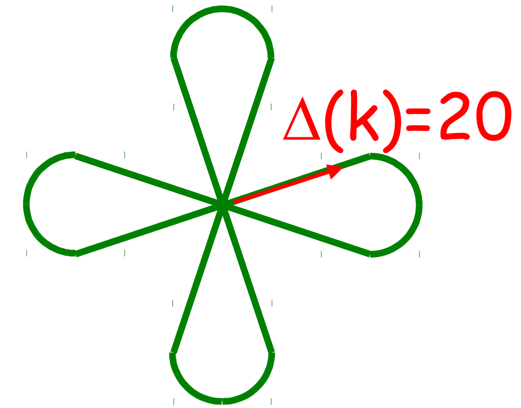

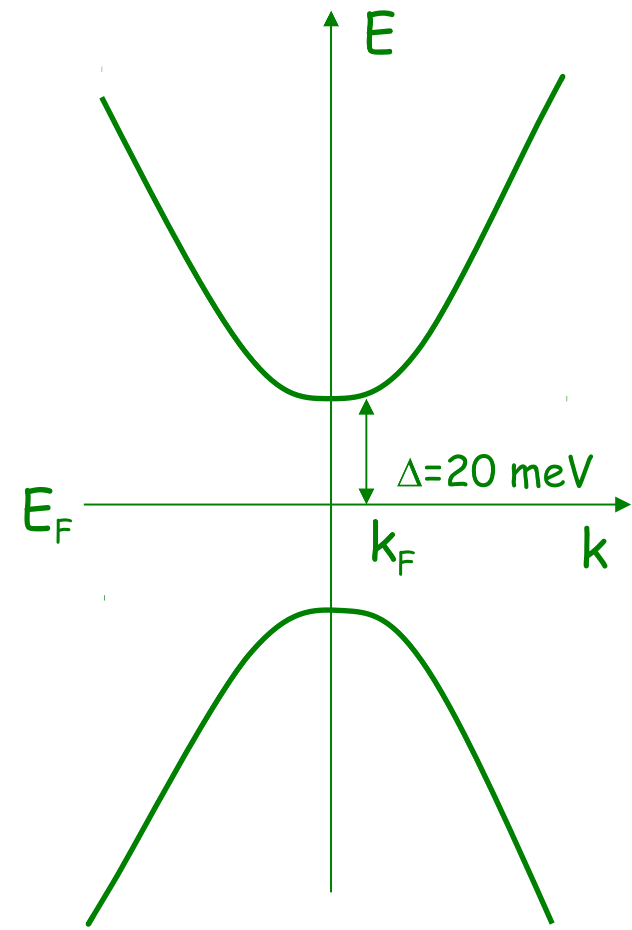

ARPES: Superconducting anisotropic gap $\Delta(k)$

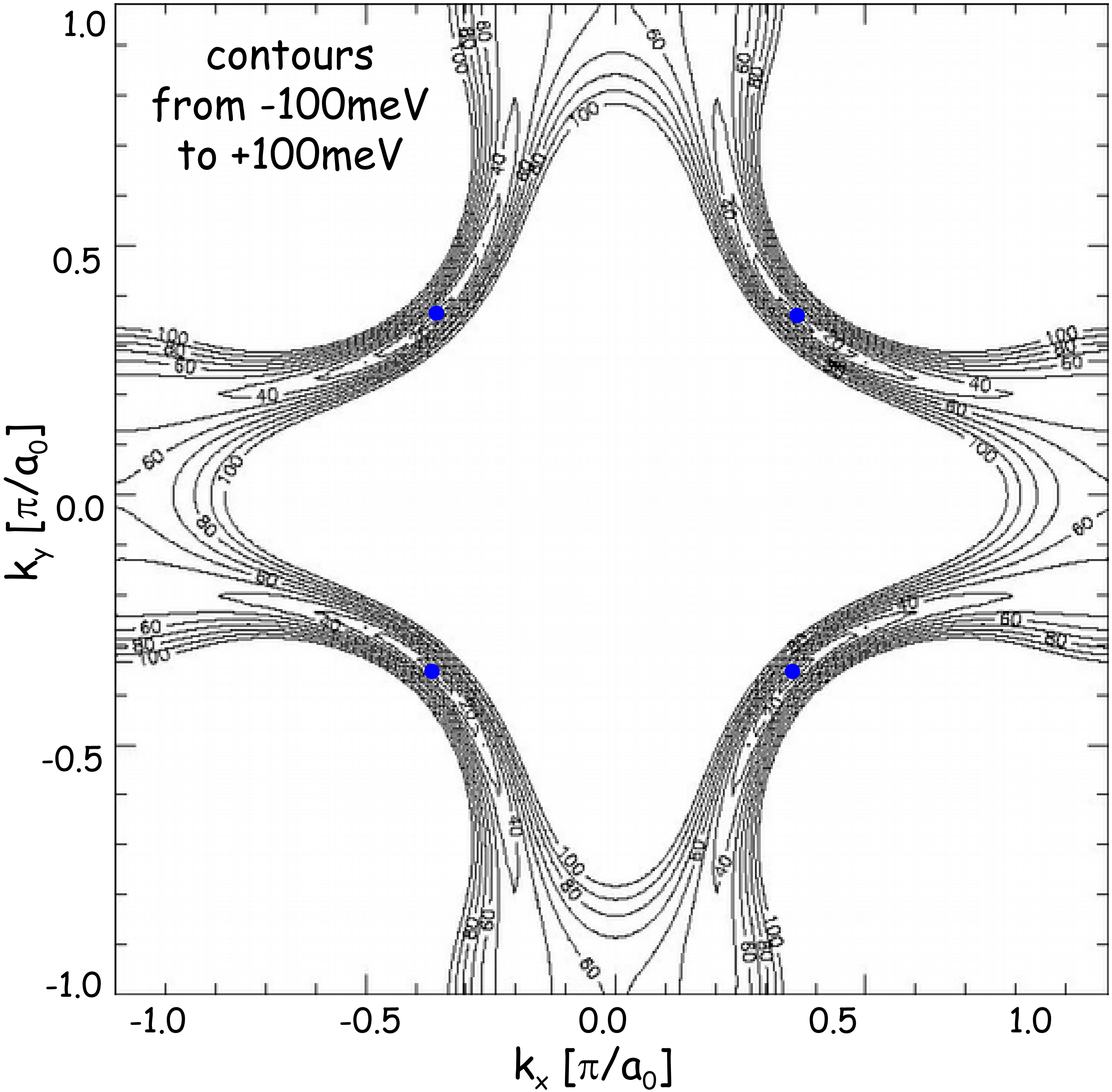

Ding *et al.*, PRLB 54, 9678 (1996)

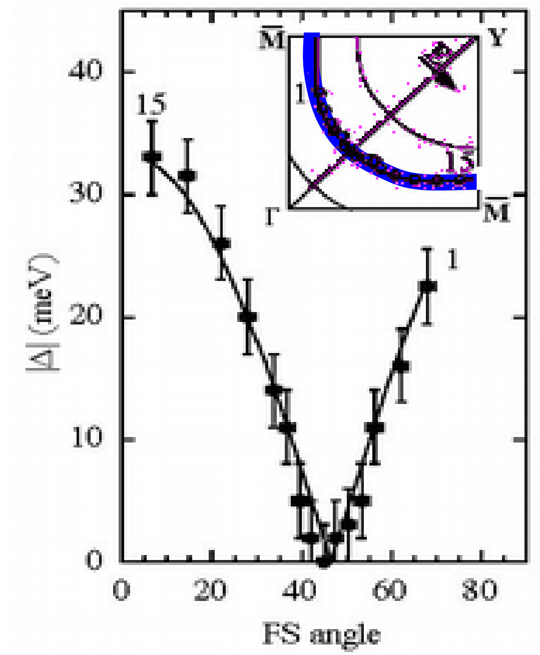

Shen *et al*, PRL **70** 1553 (1993)
Ding *et al*, PRB **54** 9678 (1996)
Mesot *et al*, PRL **83** 840 (1999)

The scattering vectors of QI model

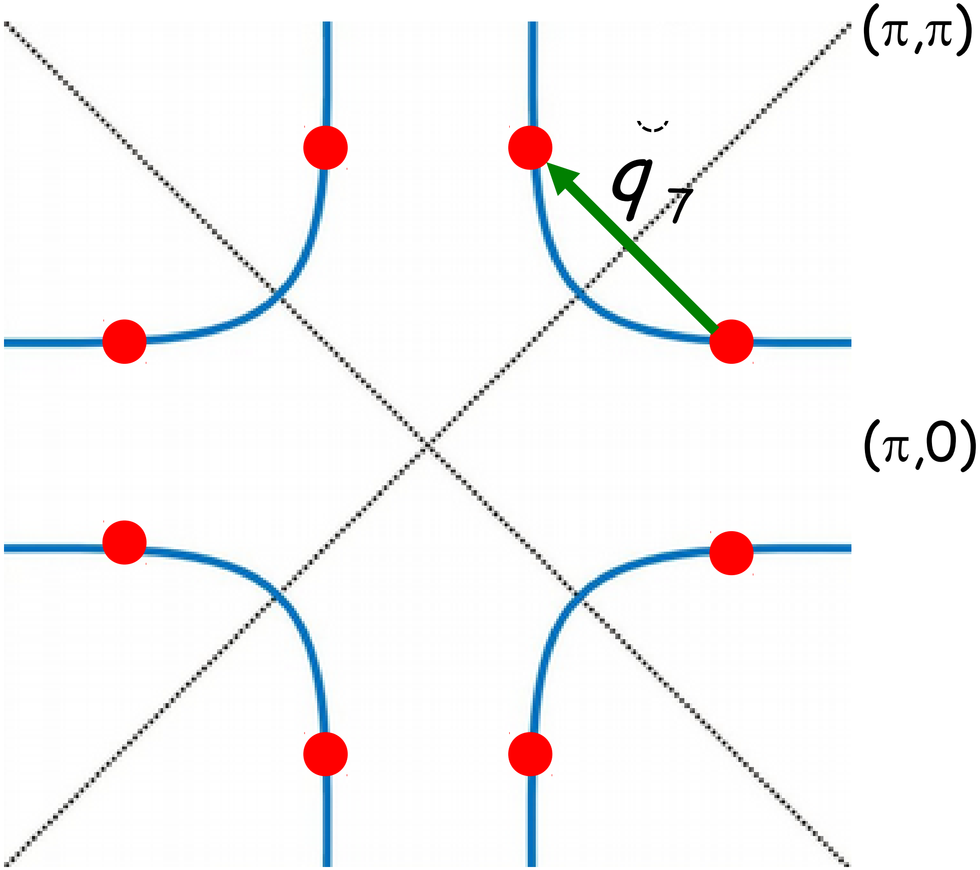

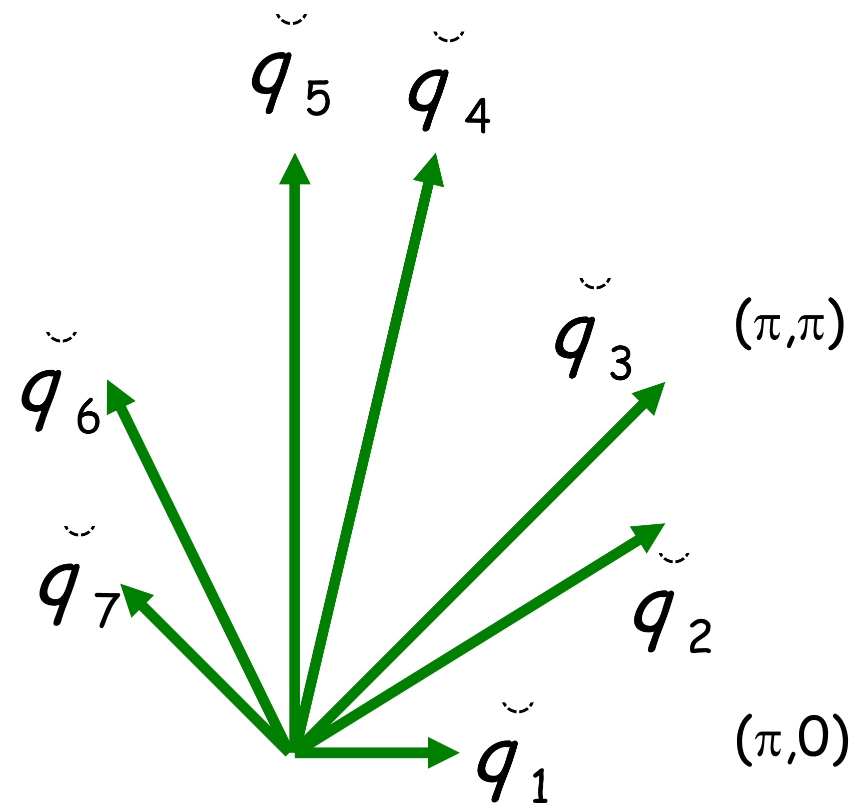

Total sets of $\boldsymbol{q}_i$ (7X8) : 56
Inequivalent sets of $\boldsymbol{q}_i$: 32
Distinguishable via FT-STS : 16

k-space:
- unperturbed eigenstates
- not directly accessible to STM
- measured by ARPES

q-space:
- Scattering → standing waves $q = 2\pi/\lambda$
- Measure q from FT of LDOS image

Expected structure of FFT of LDOS(r,E) (for a fixed E)

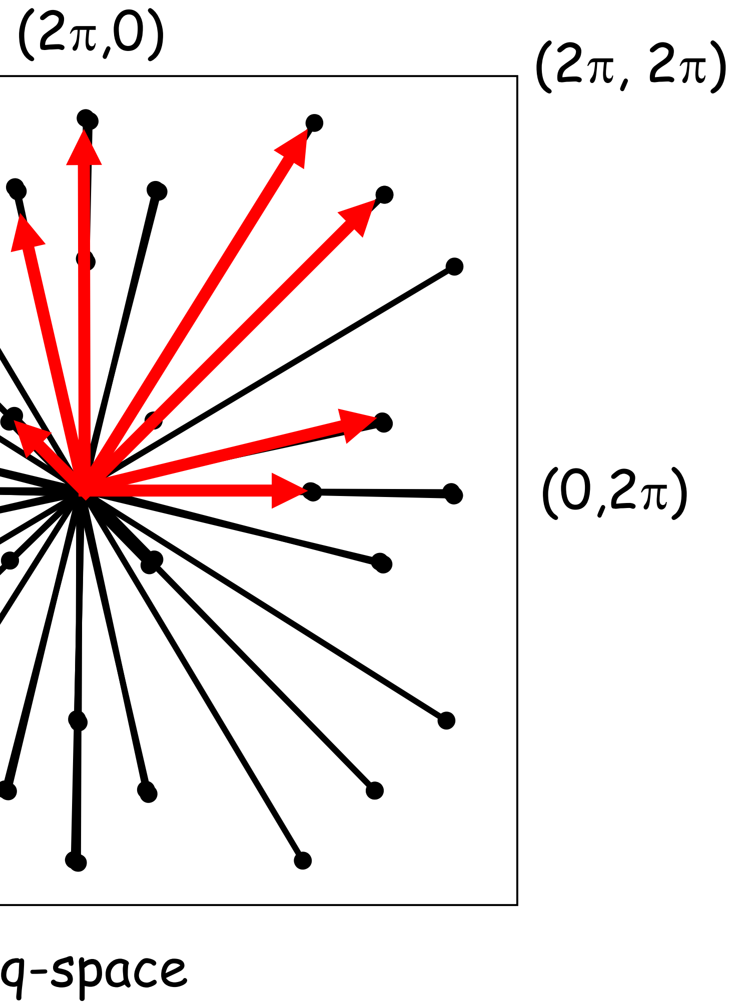

Finally, some data...

topograph

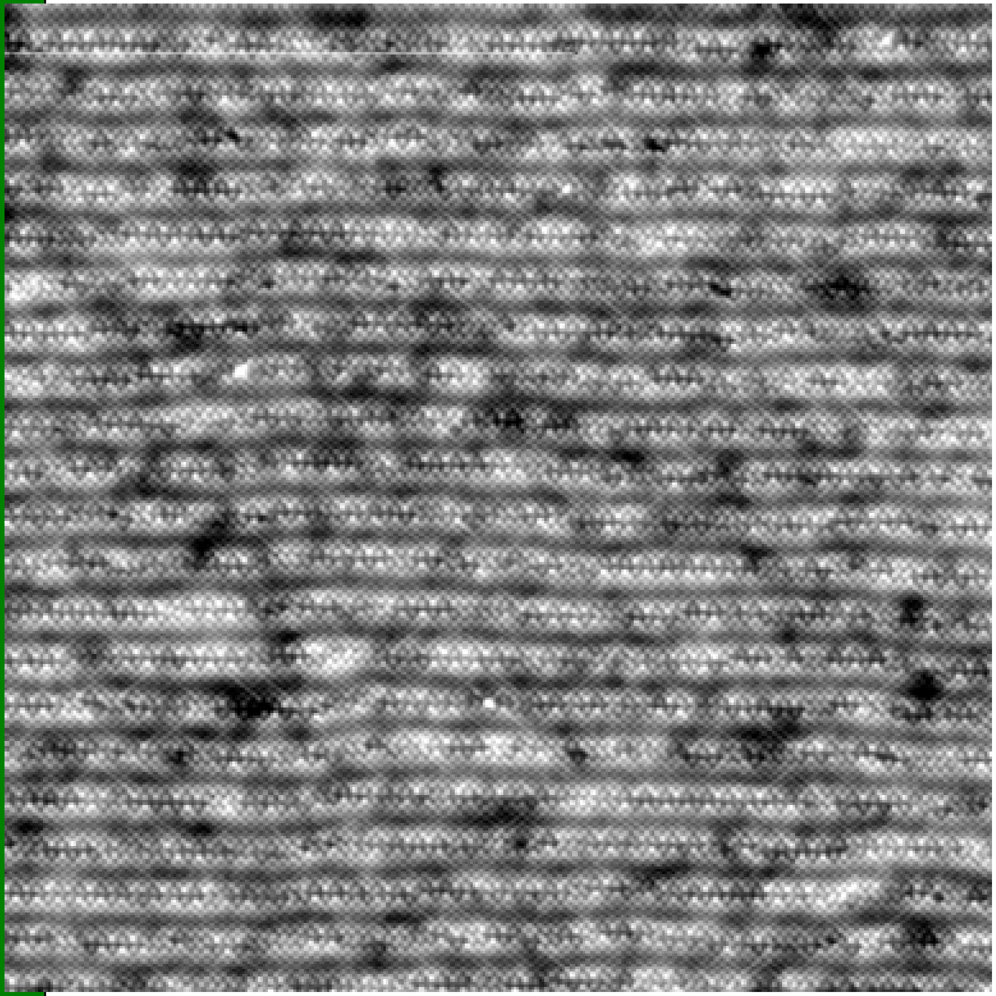

545 Å

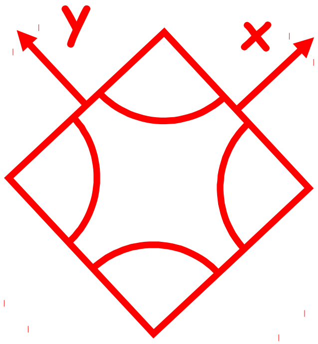

Bi-2212
T_c=76 K
Δ~51meV

energy (meV)

Imaging quasiparticle wavefunctions

$g(\vec{r},E)$

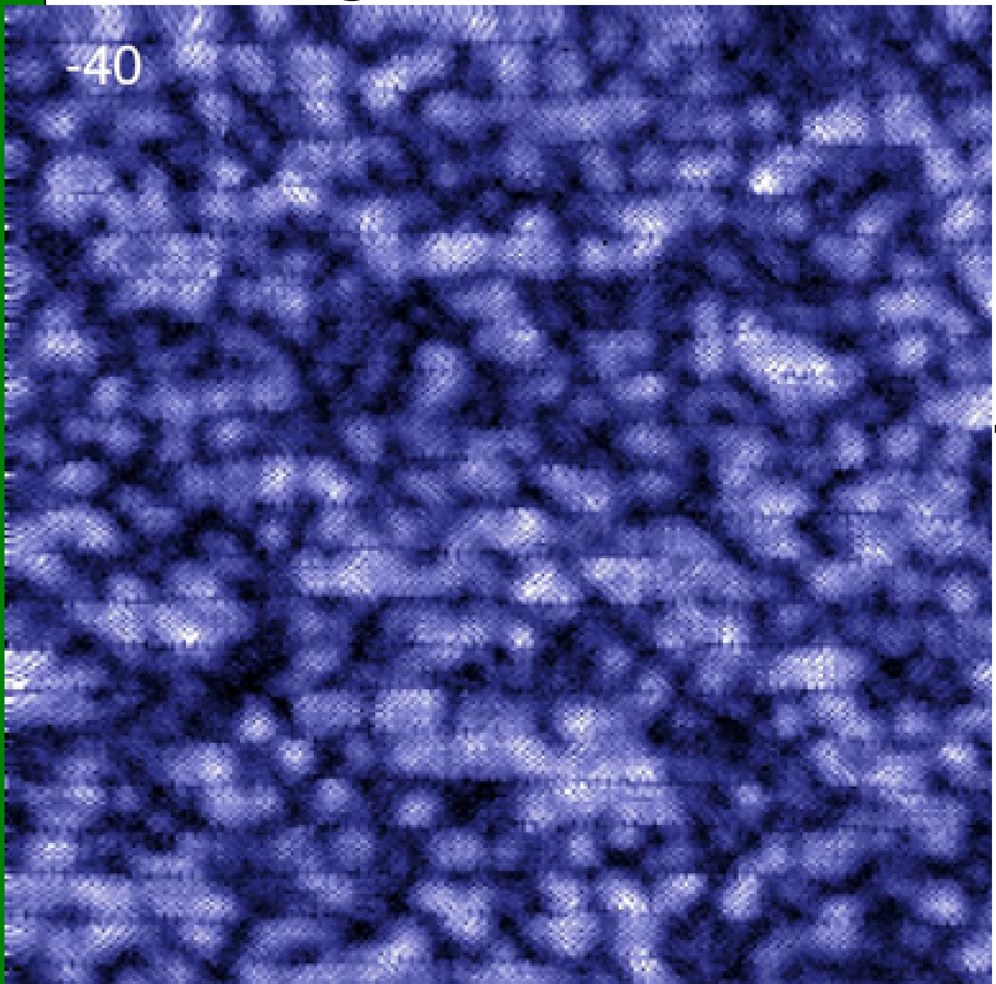

545 Å

FFT

$g(\vec{q},E)=\sqrt{P(\vec{q},E)}$

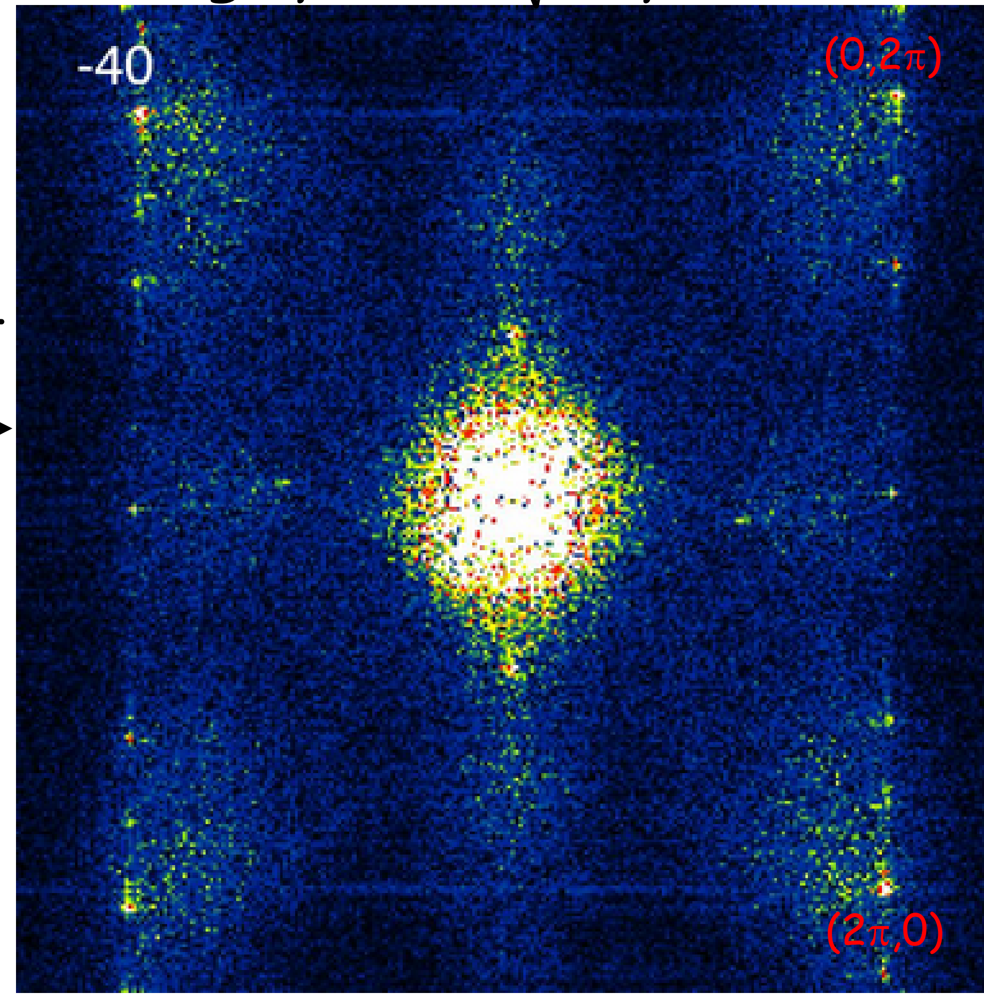

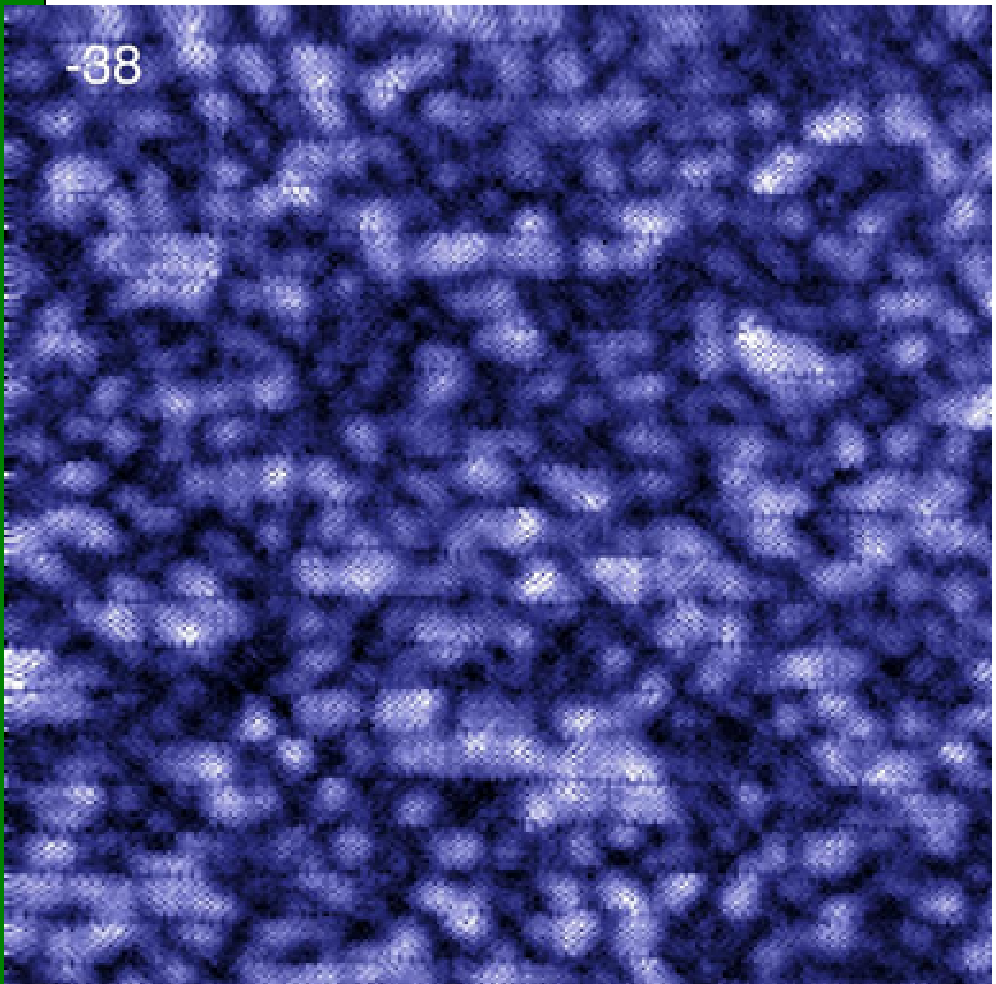

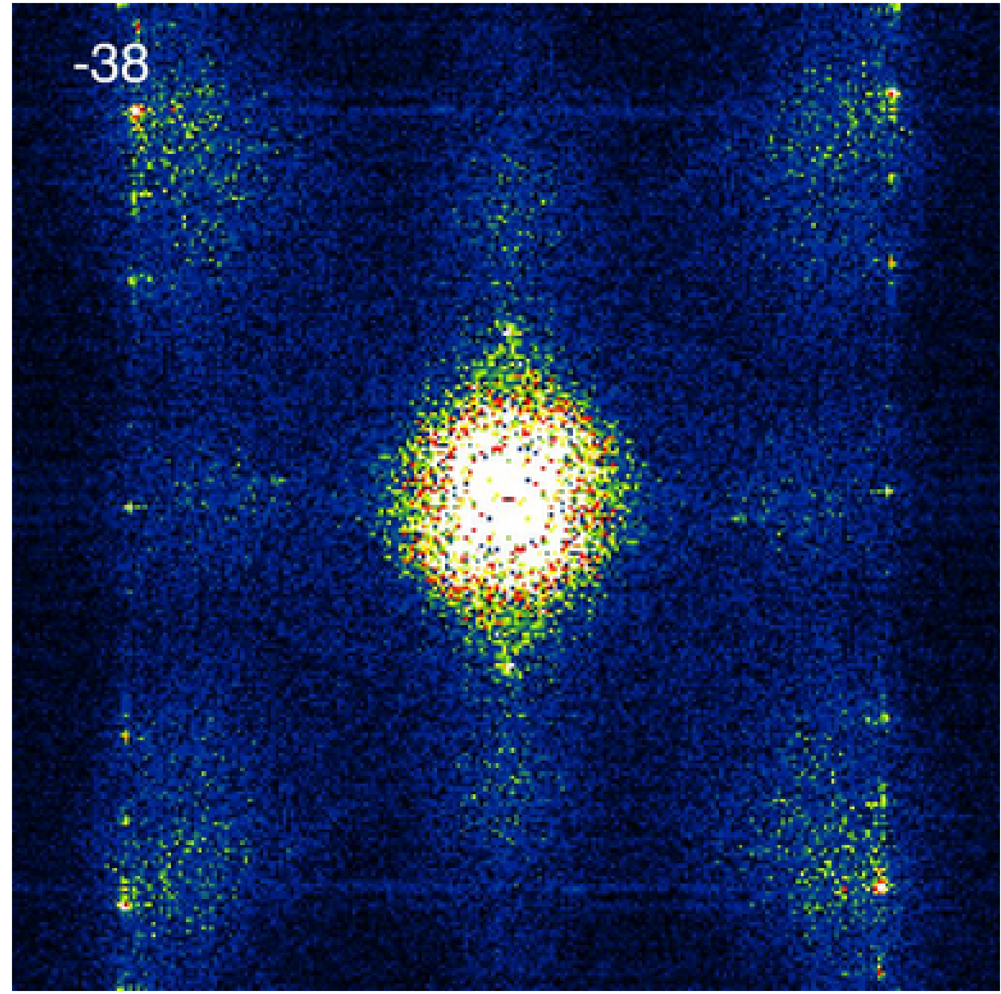

UNIVERSITÉ DE SHERBROOKE

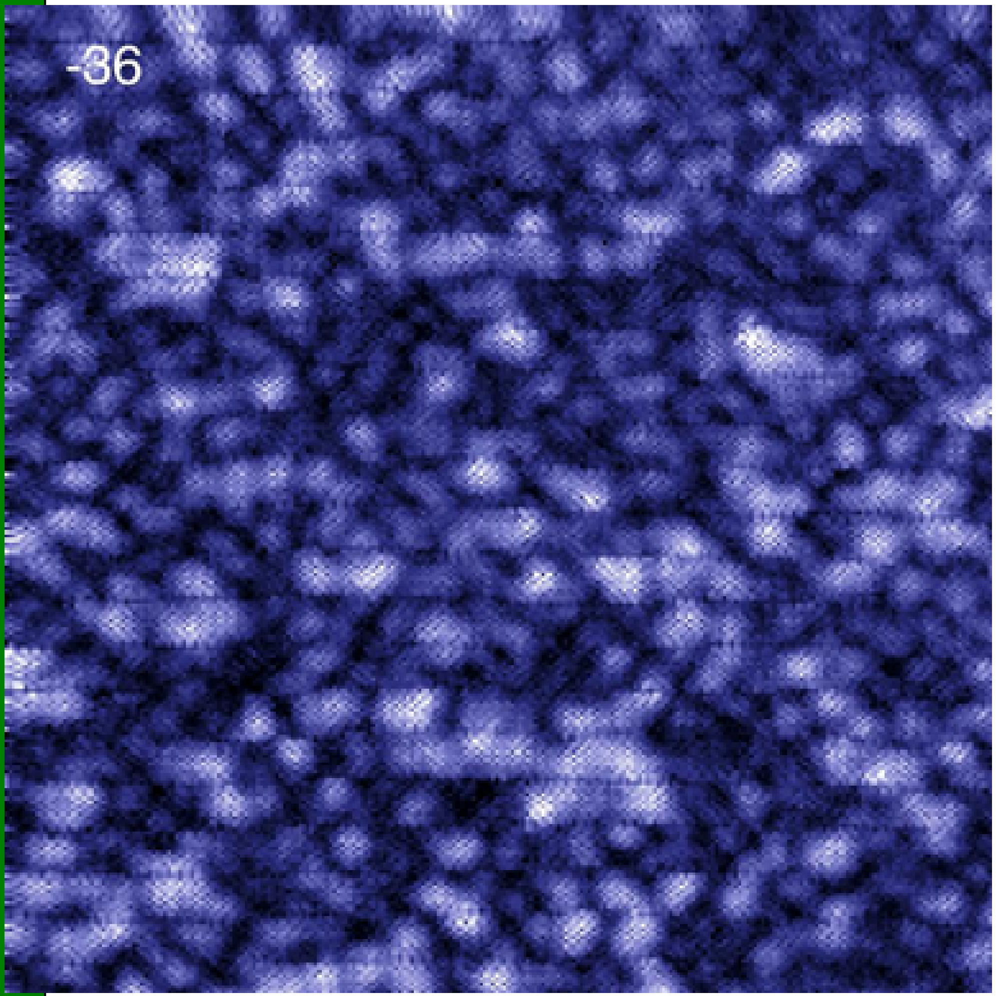
-36

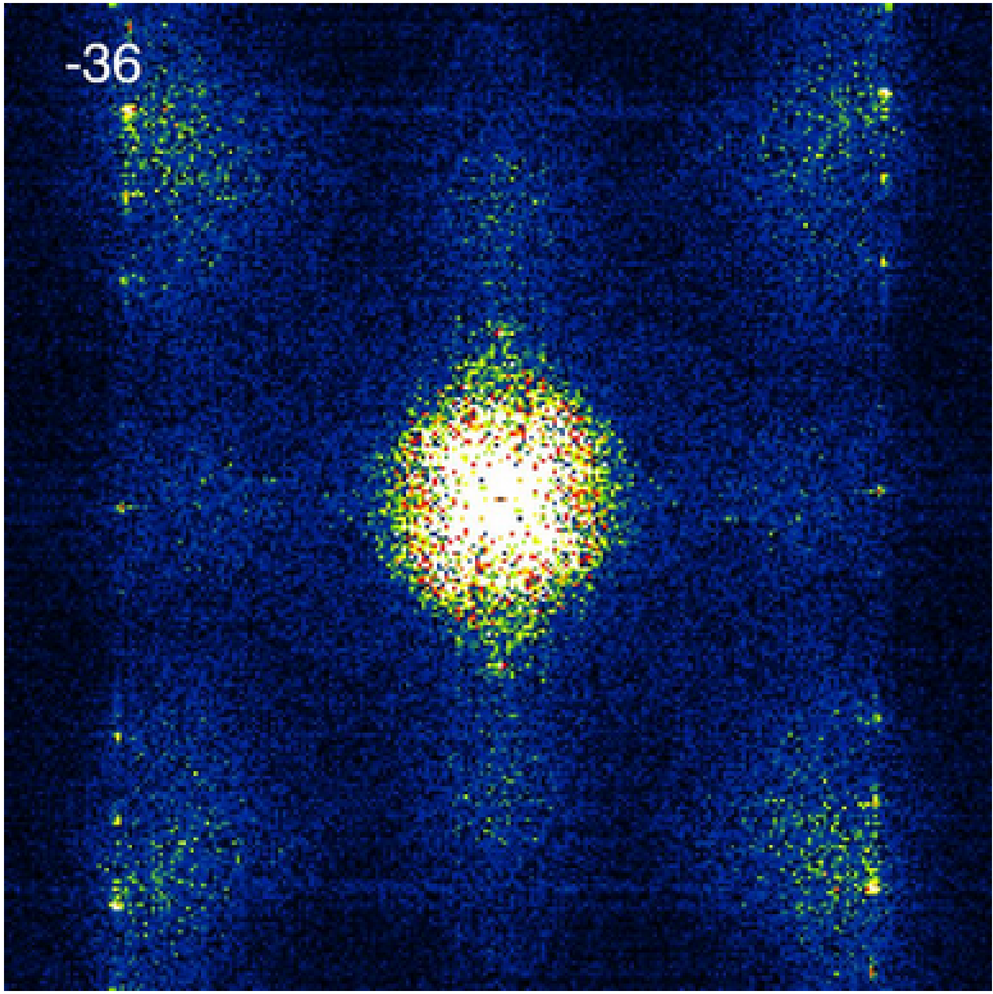
-36

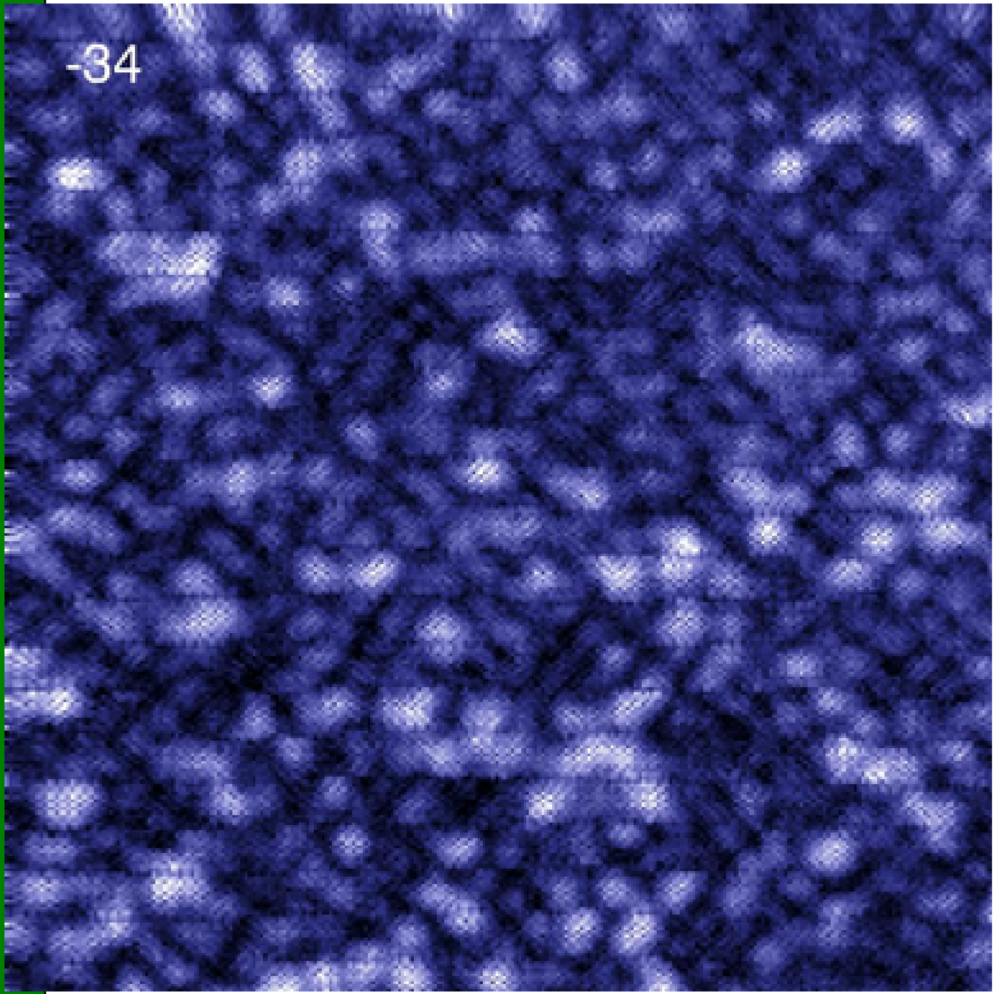
-34

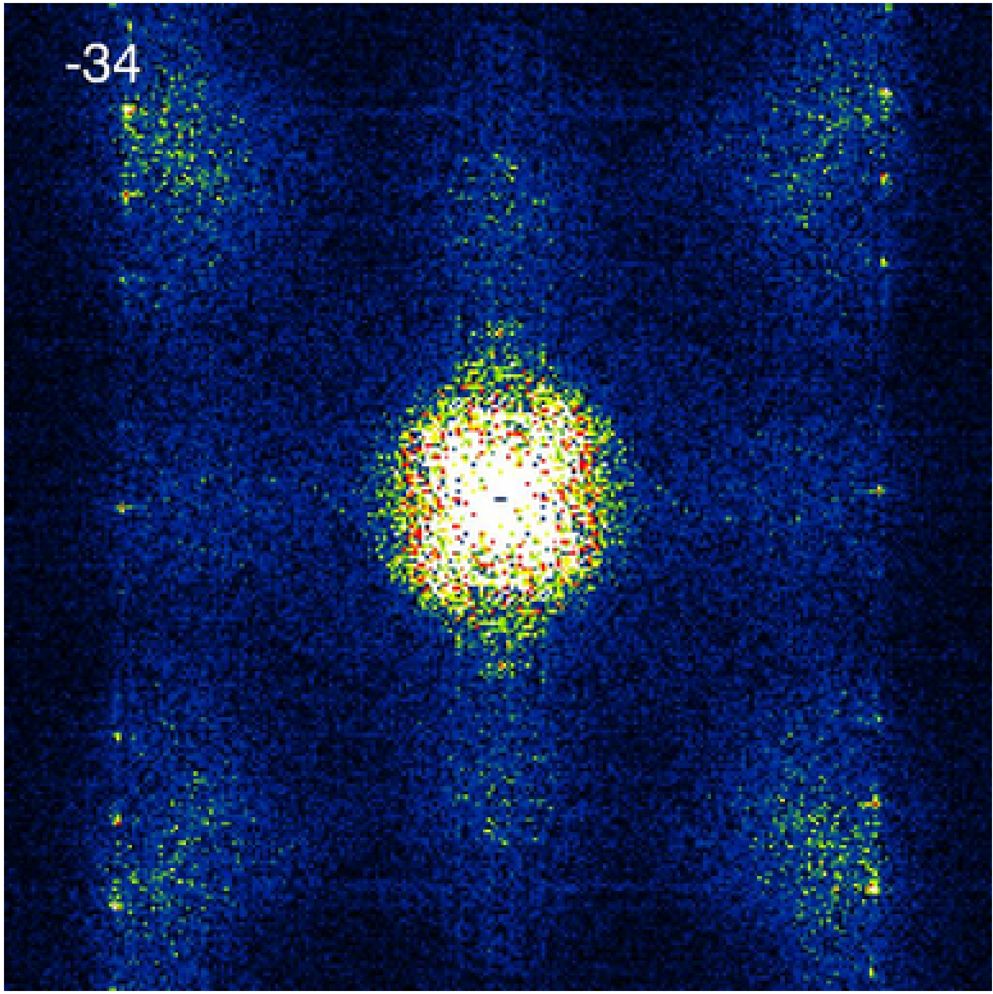
-34

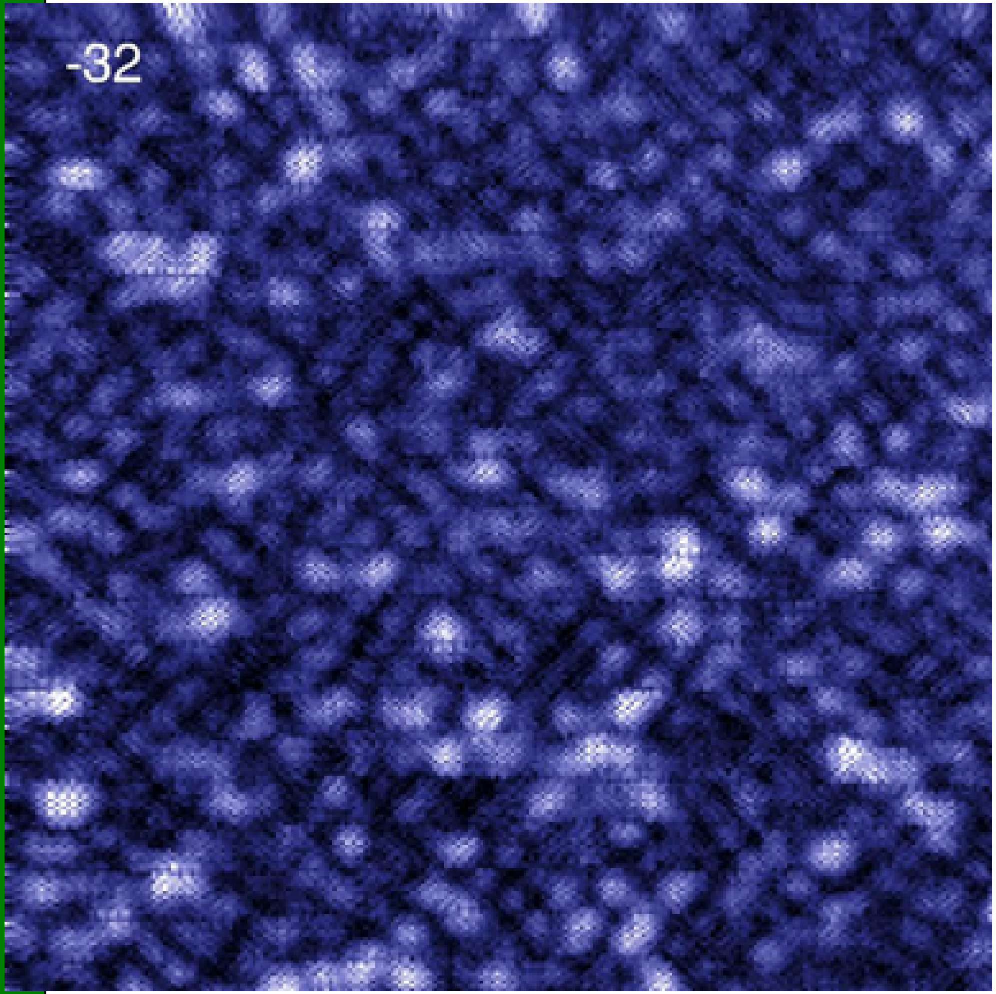

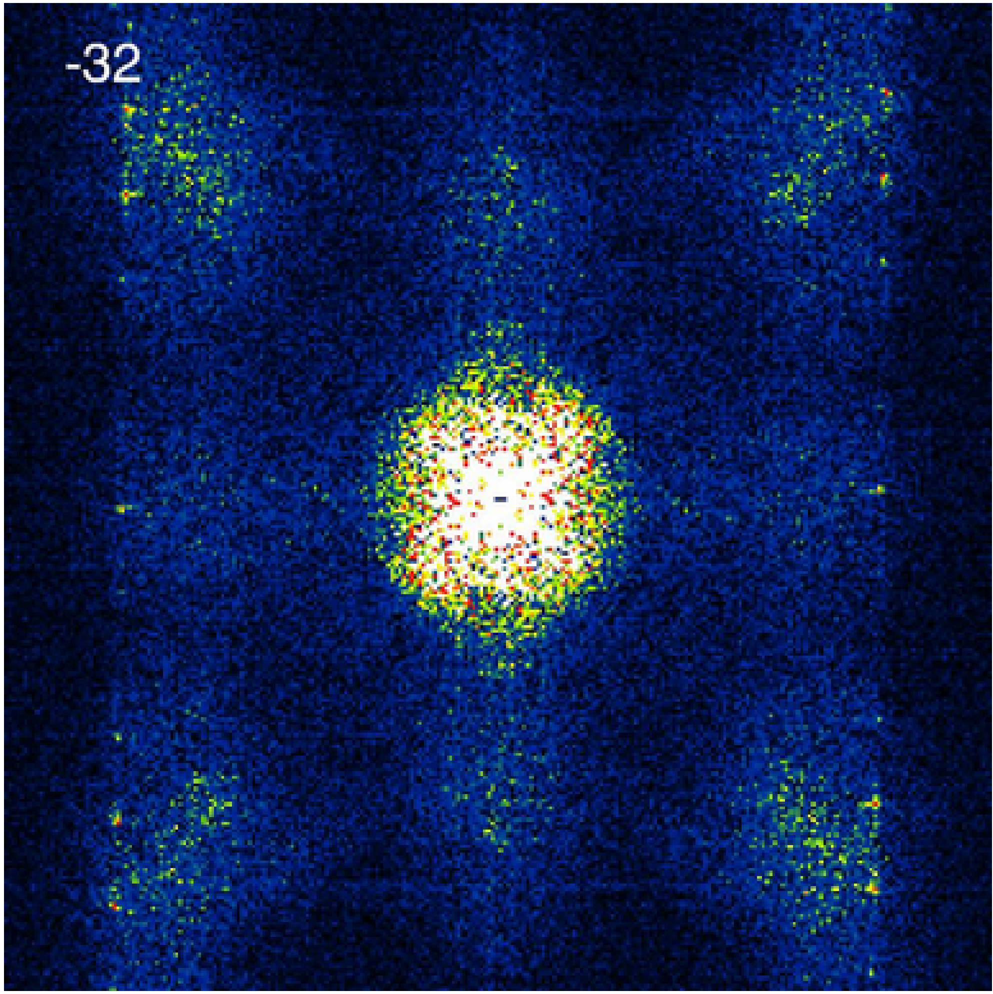

UNIVERSITÉ DE SHERBROOKE

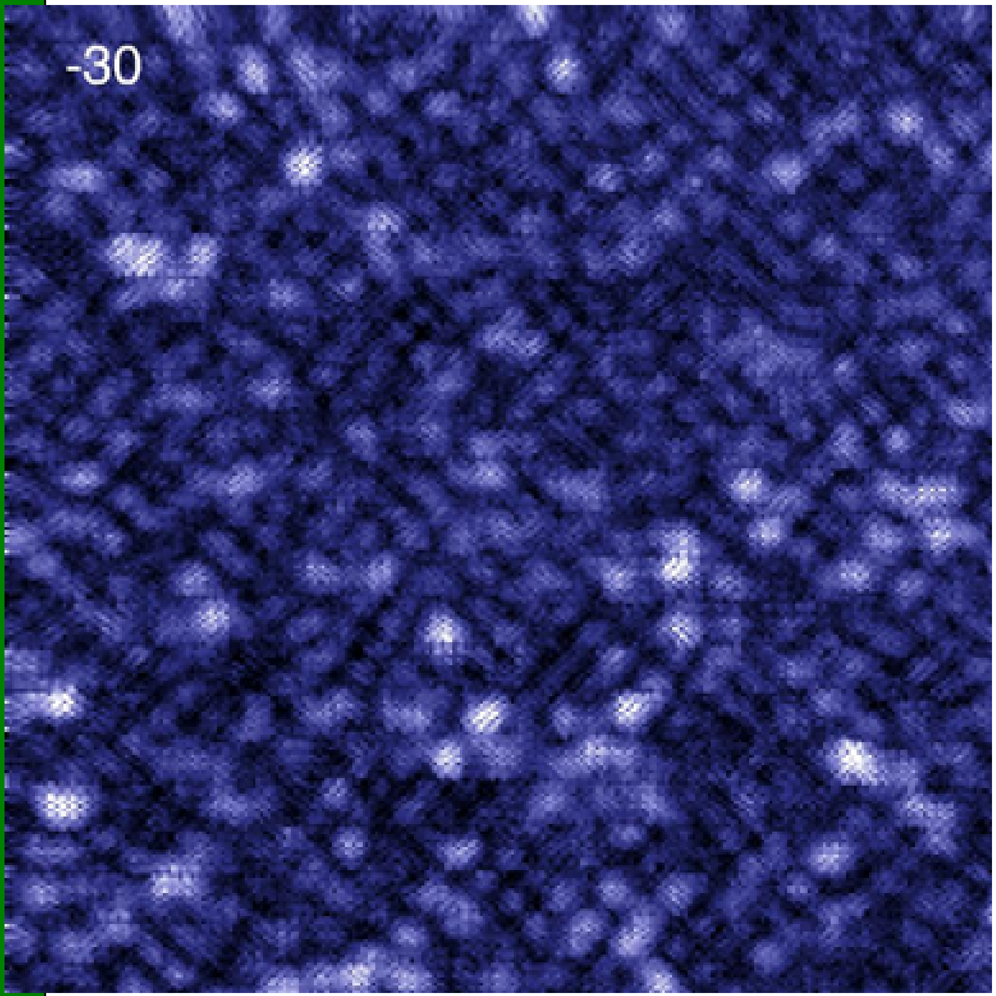
-30

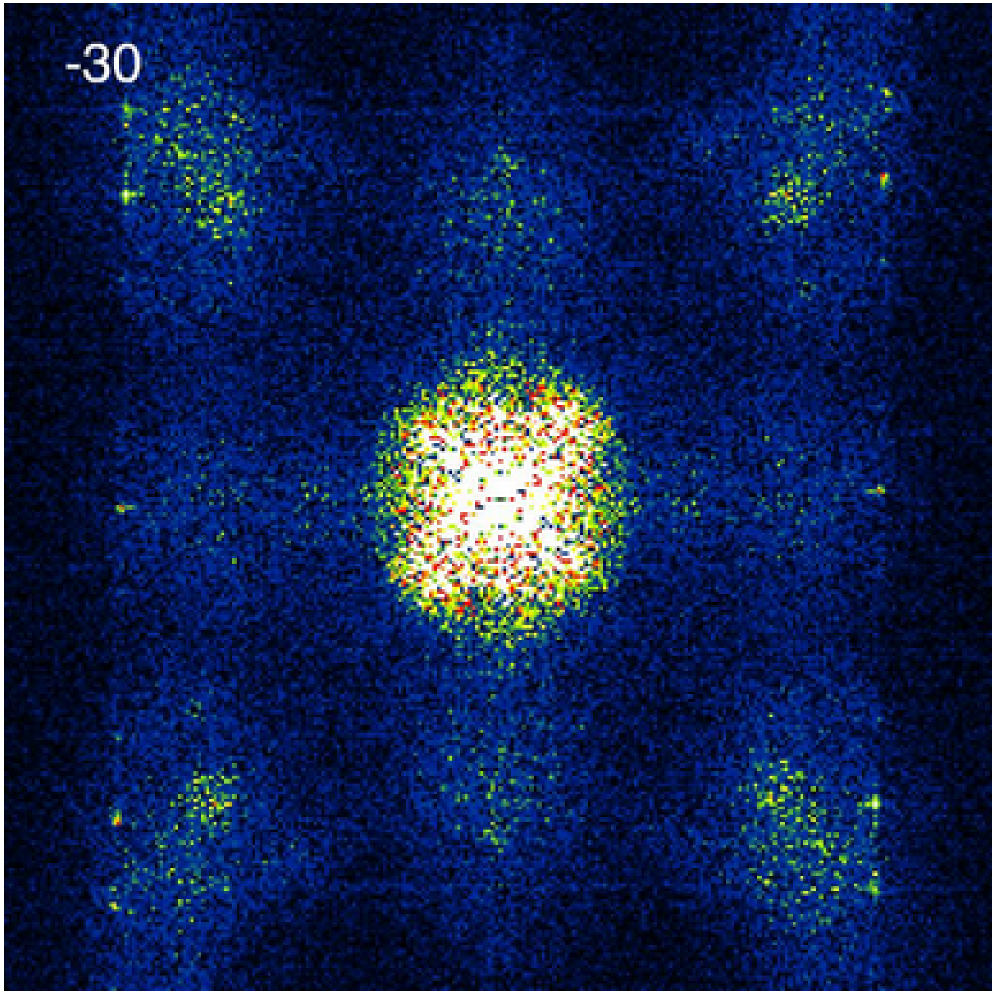
-30

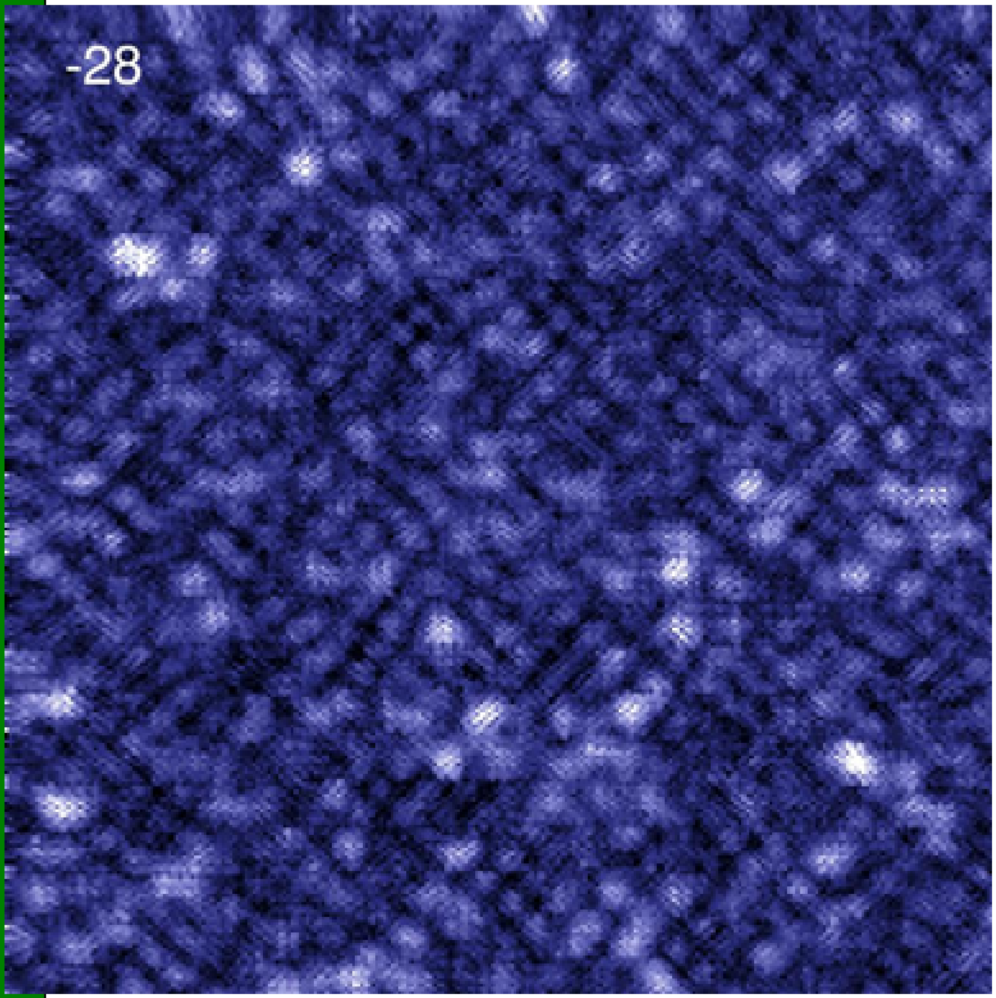
-28

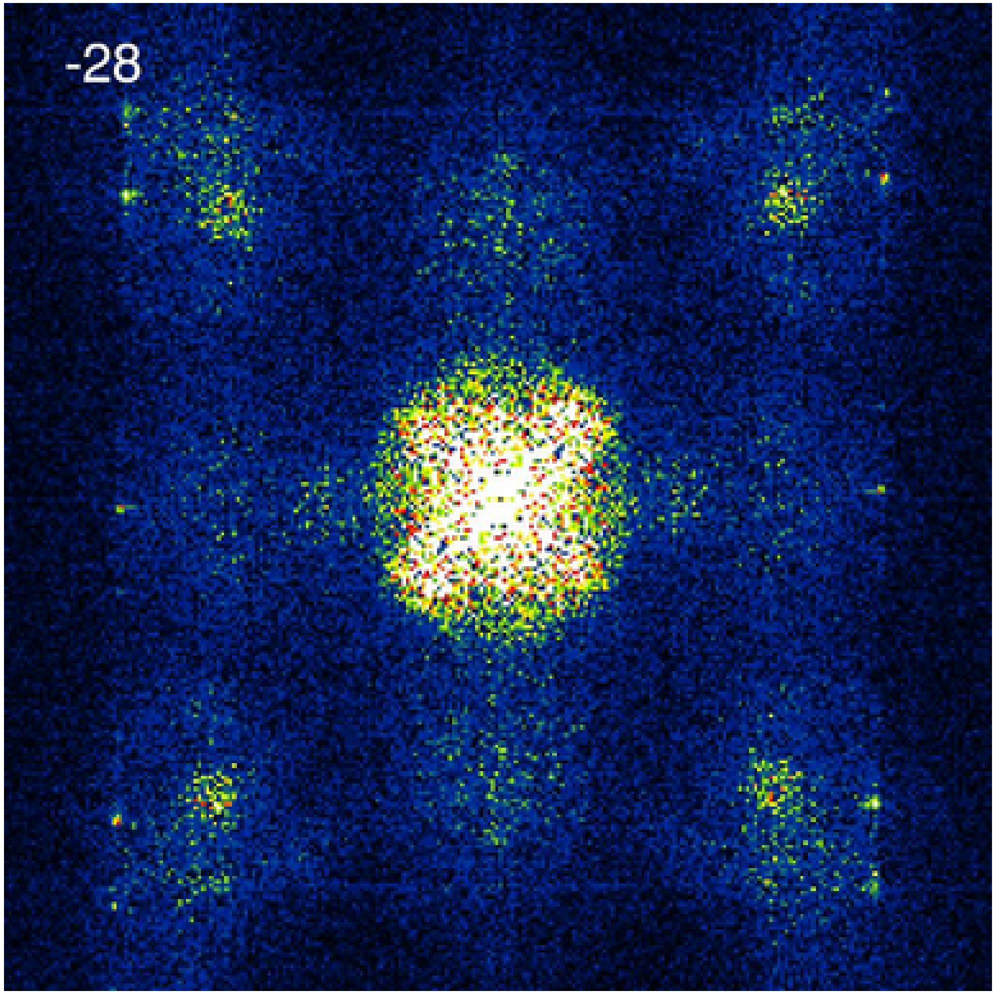
-28

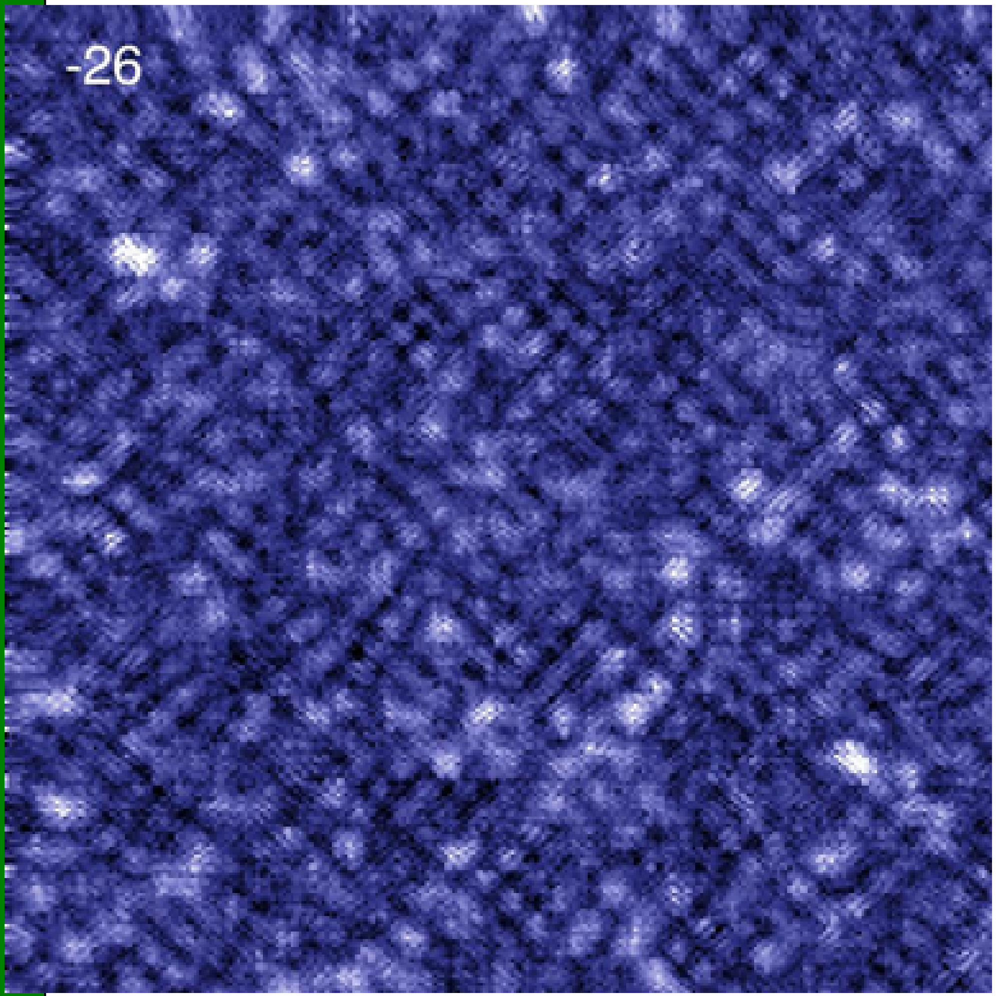
-26

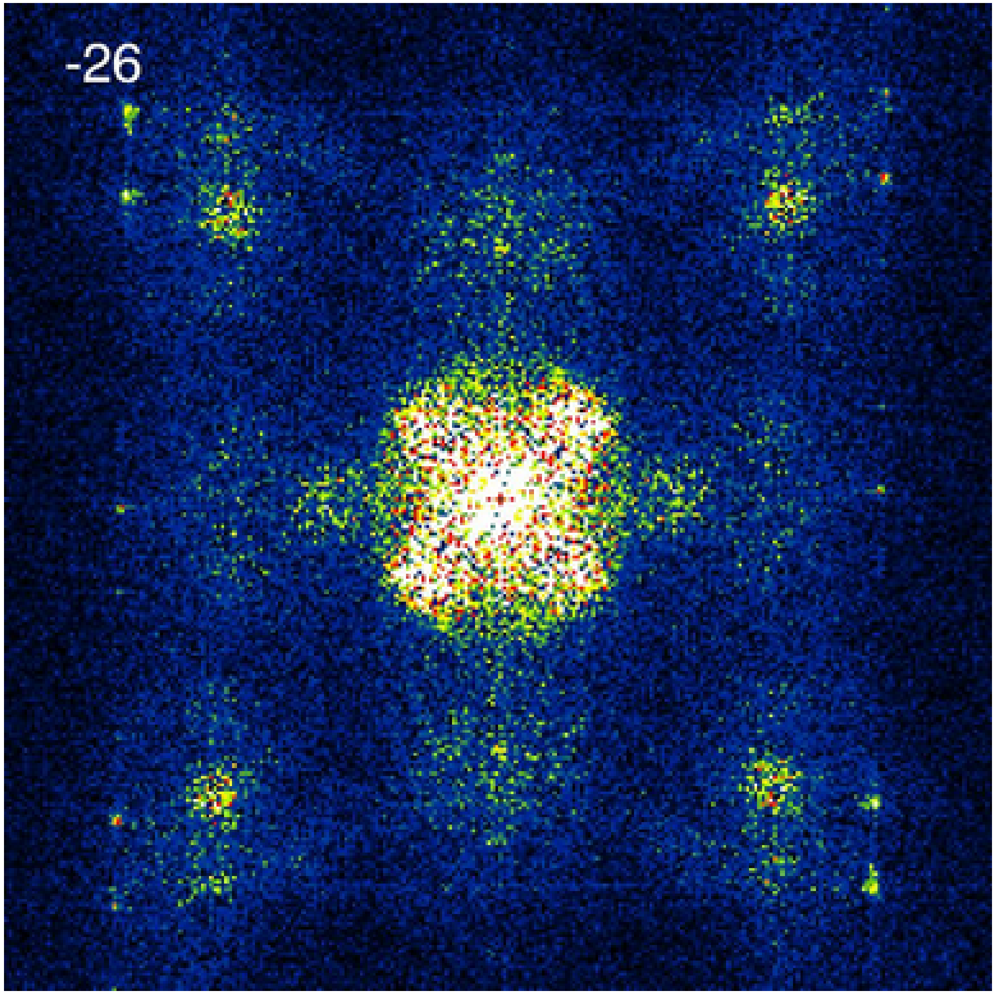
-26

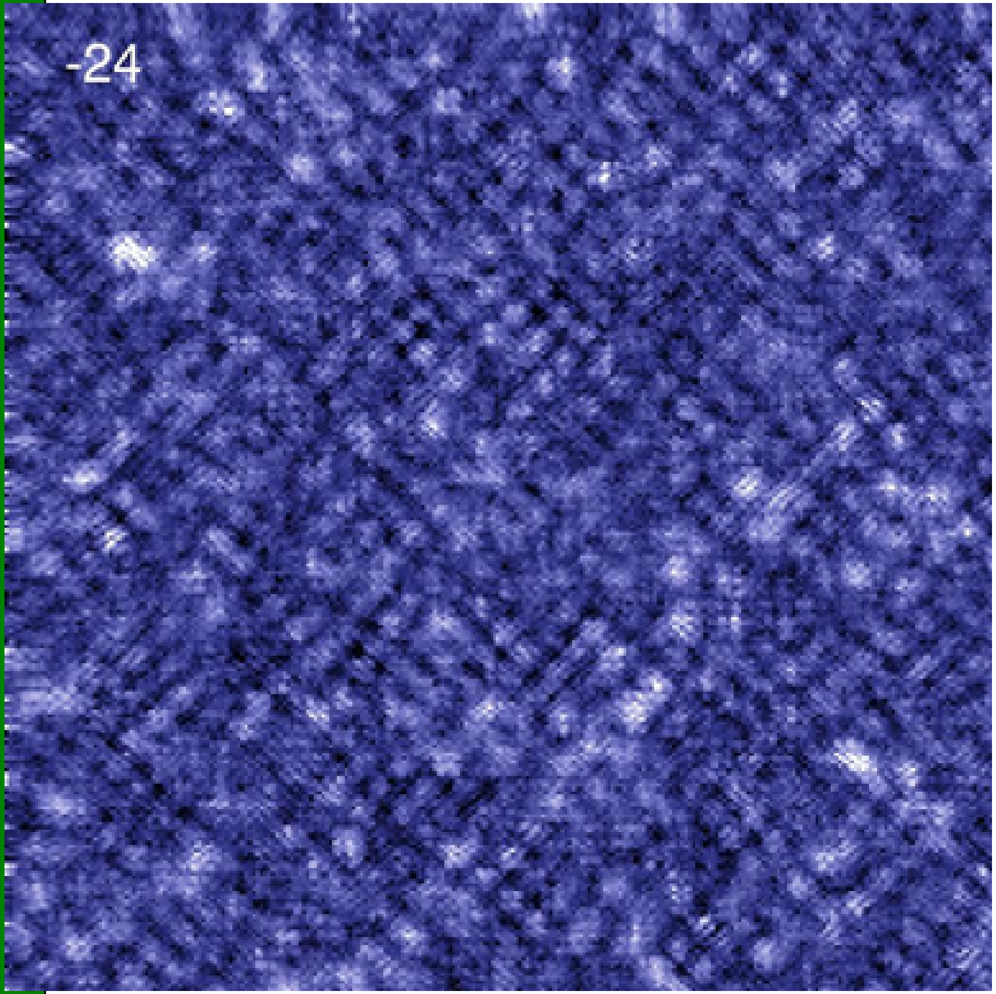
-24

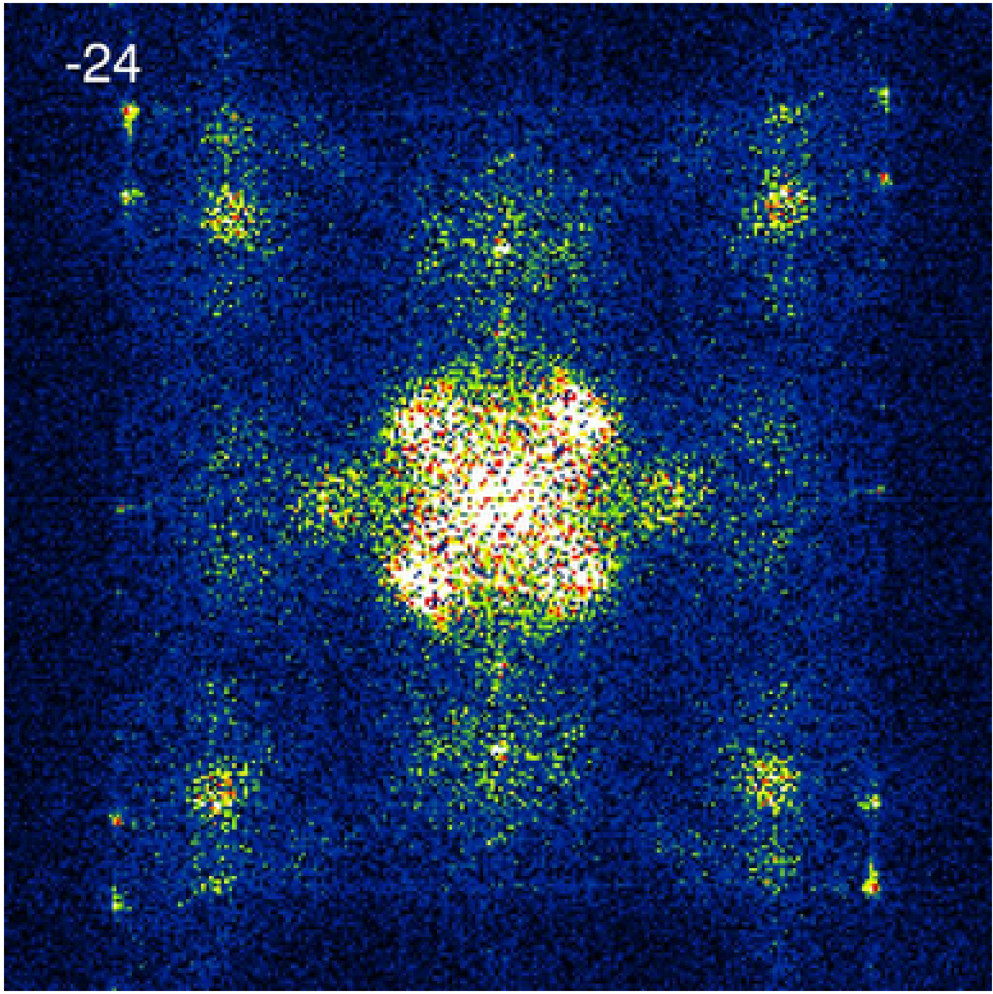
-24

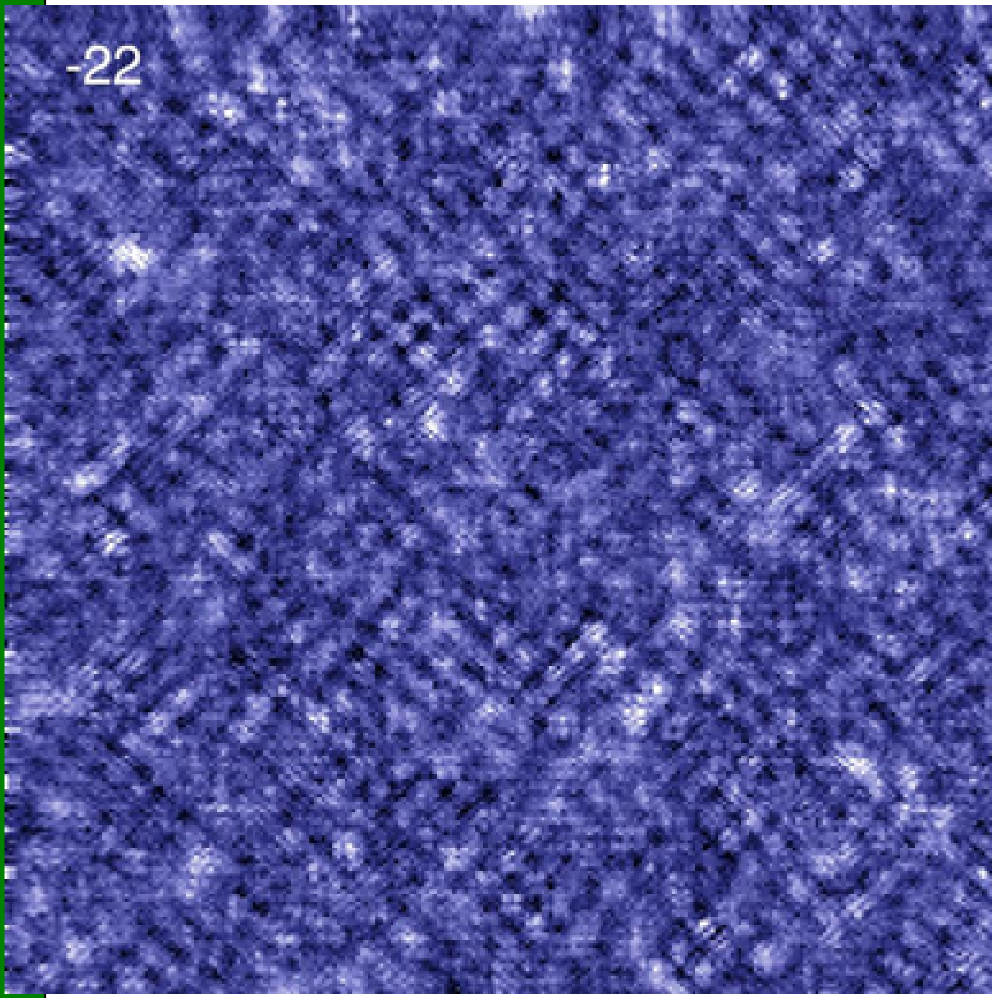
-22

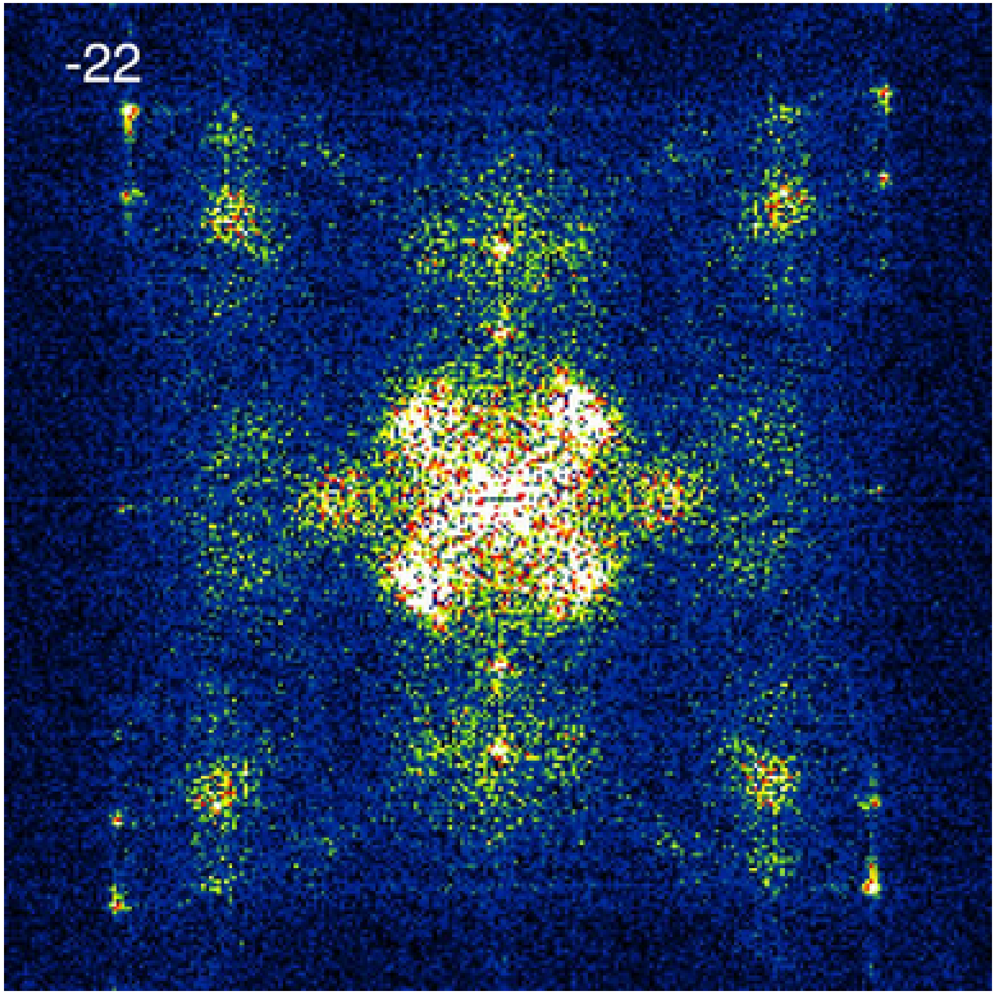
-22

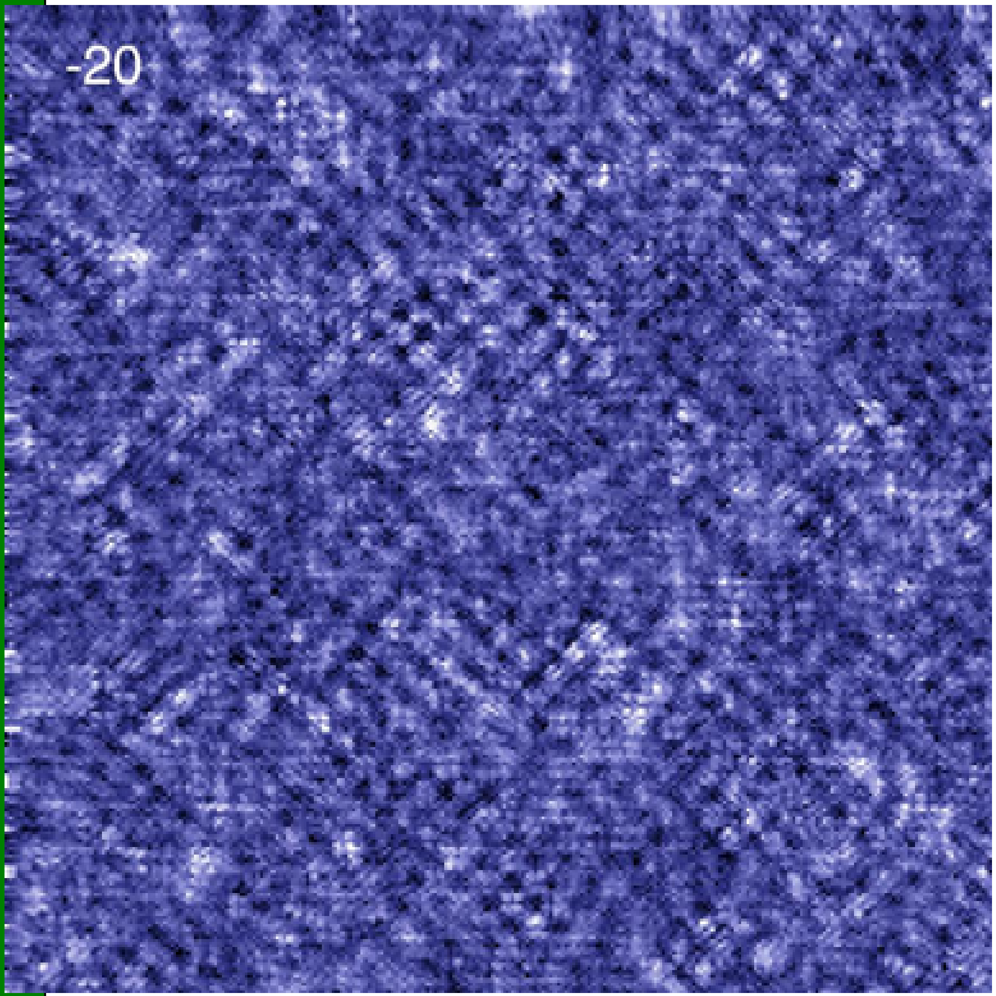
-20

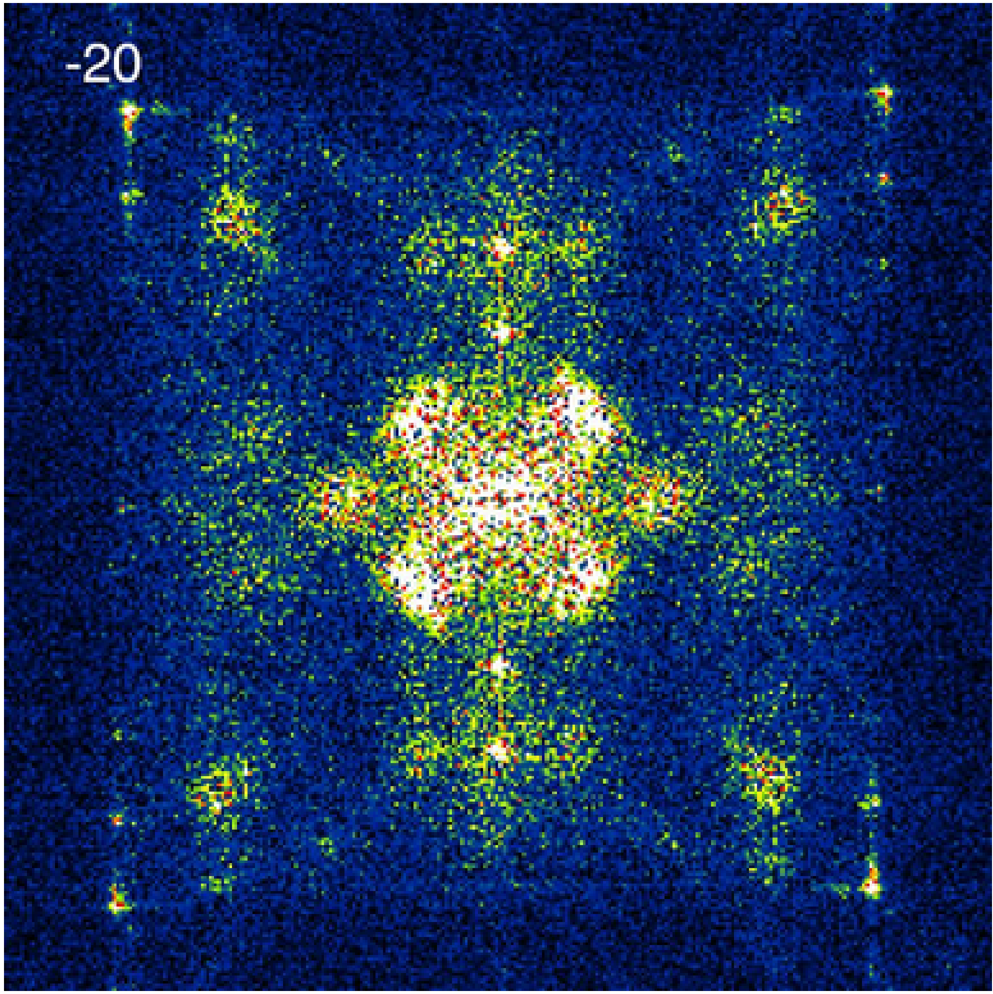
-20

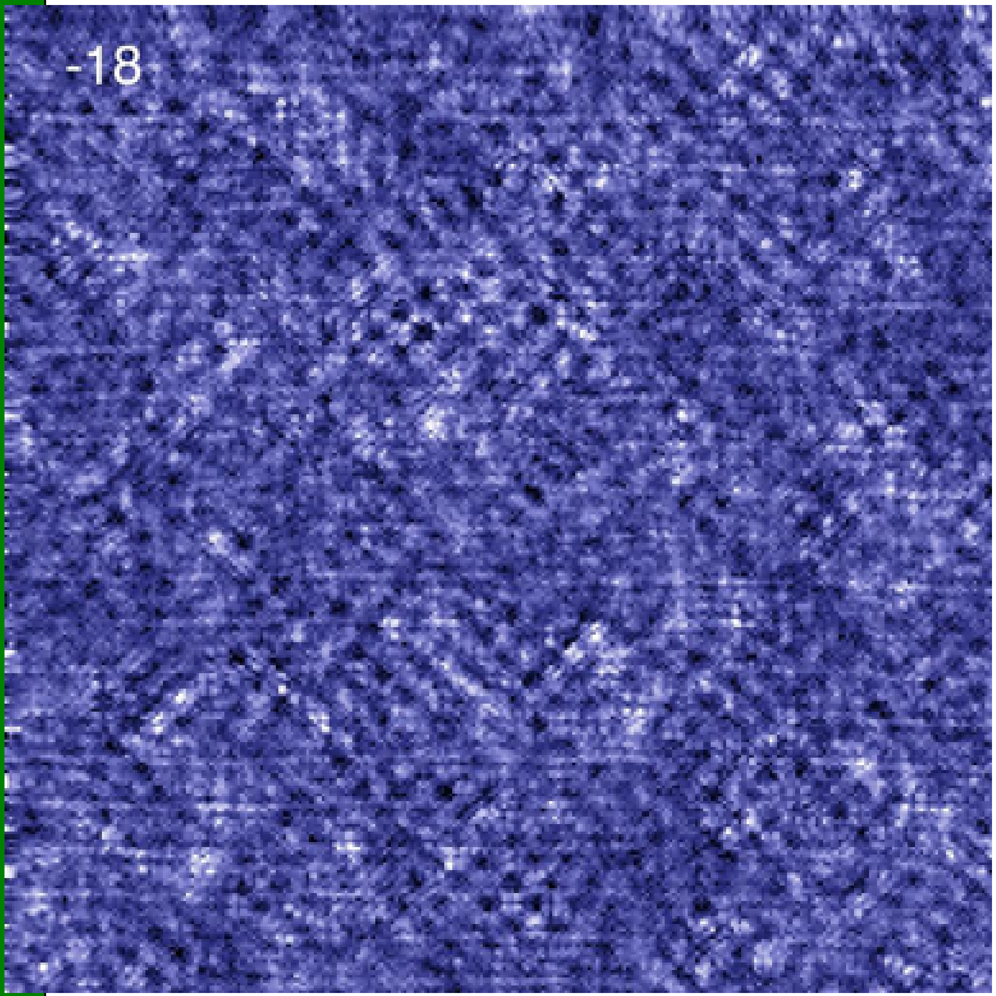
-18

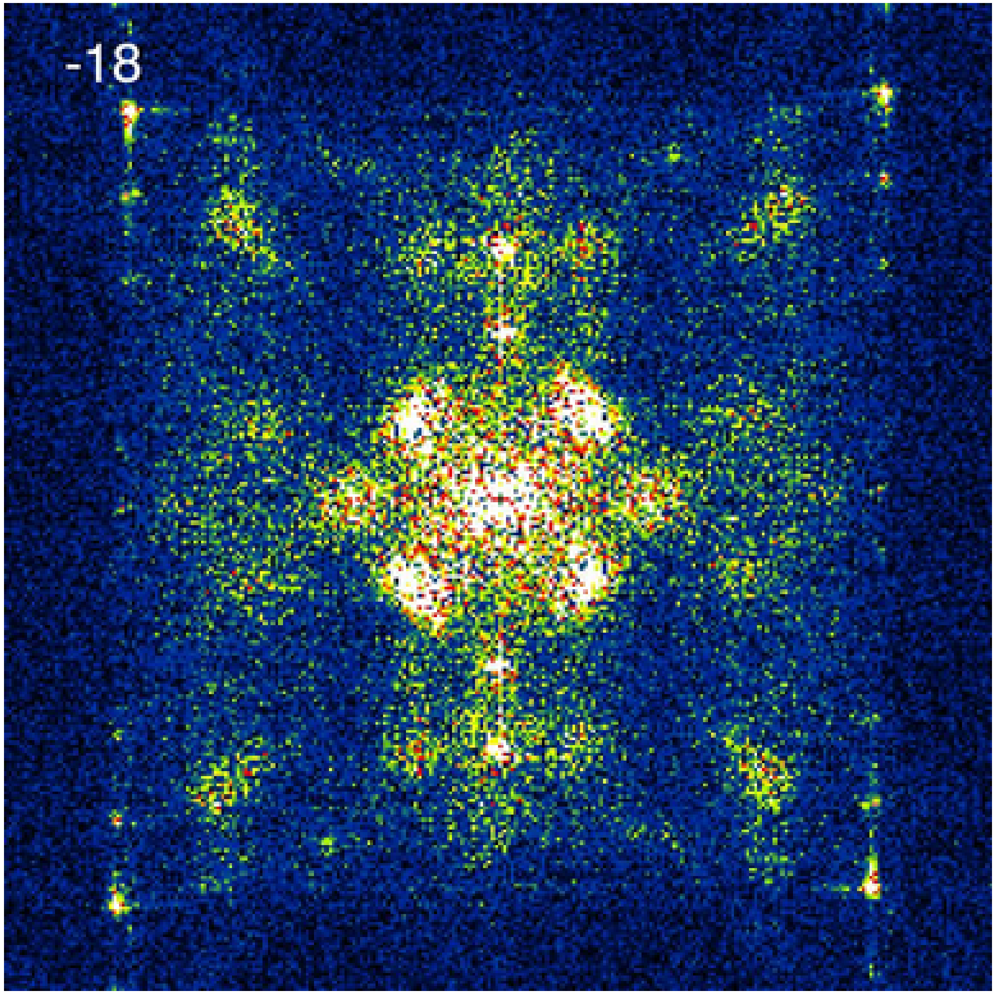
-18

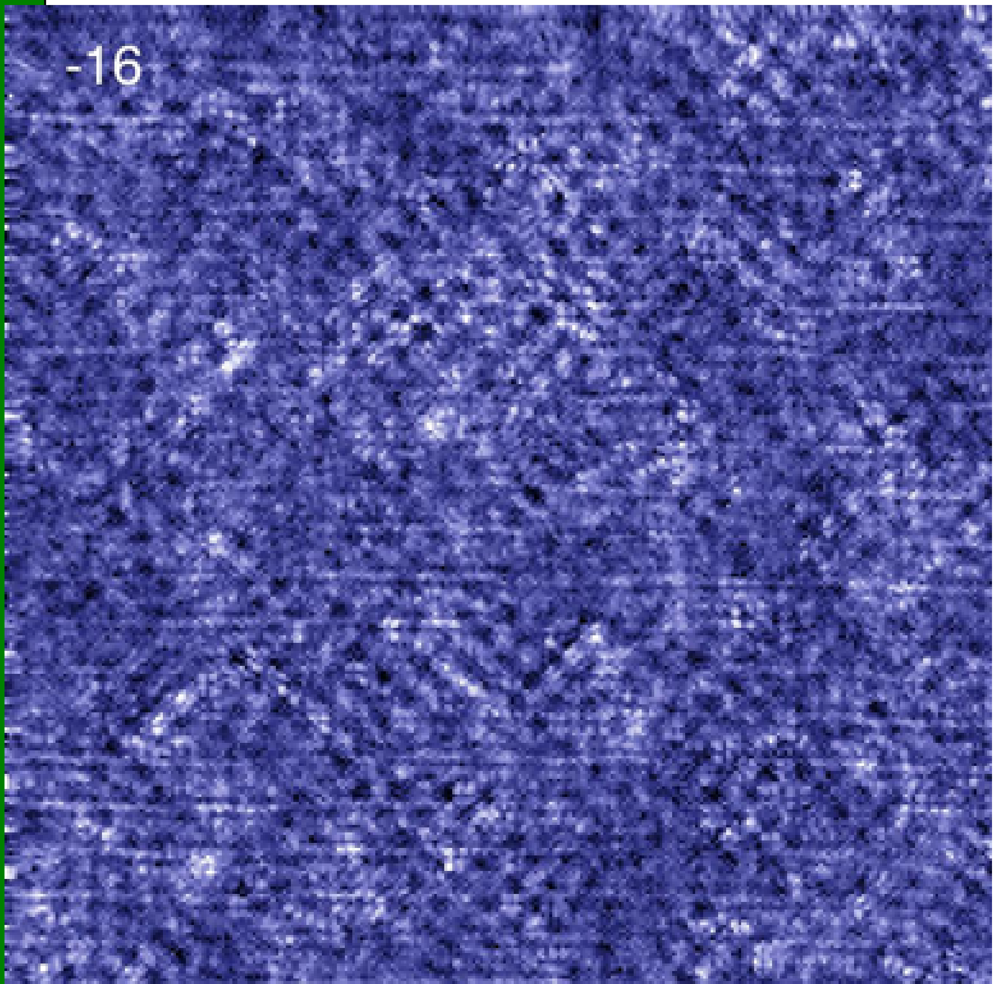

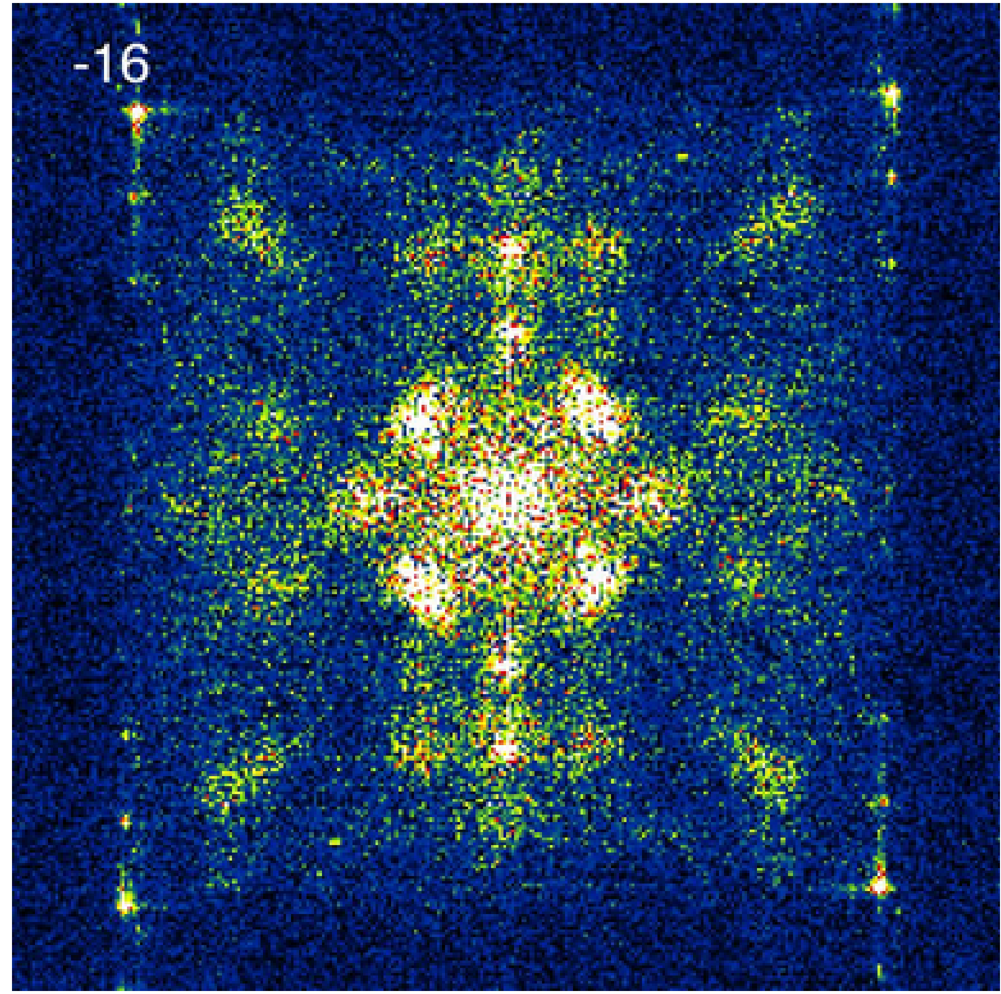

UNIVERSITÉ DE
SHERBROOKE

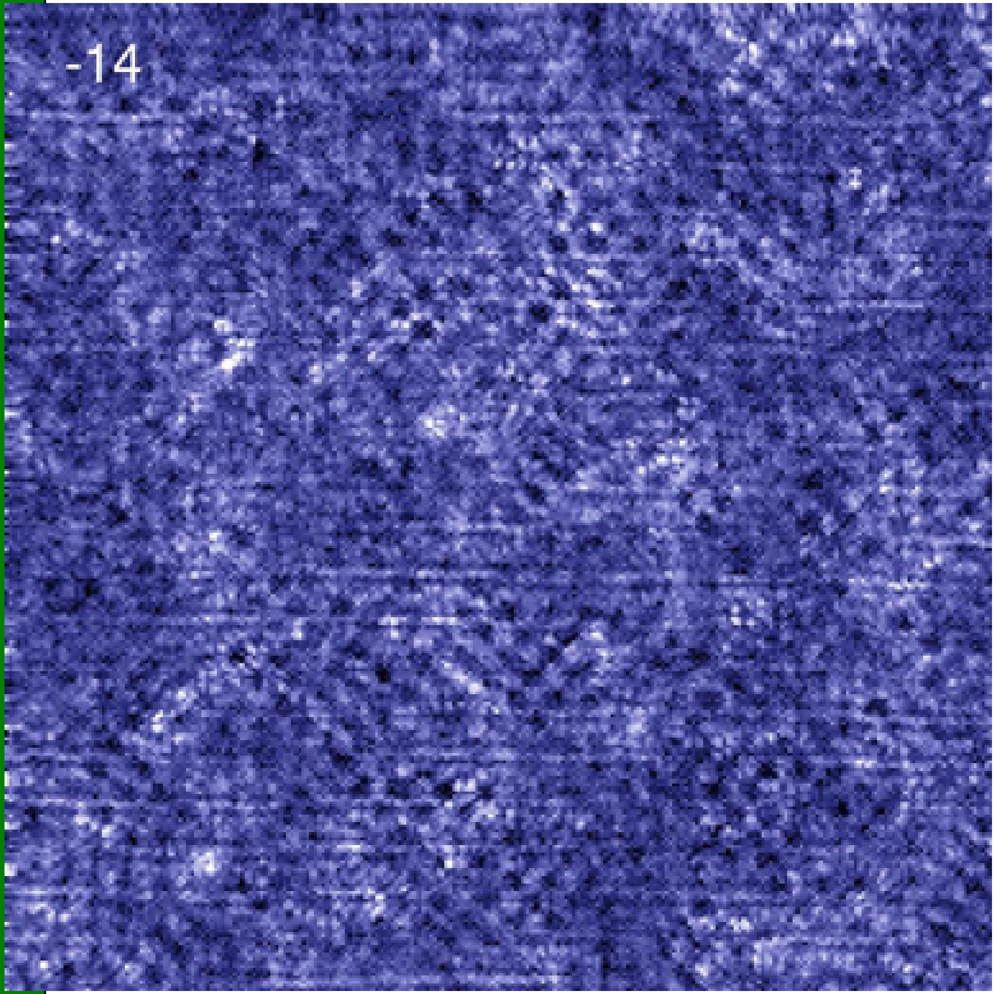
-14

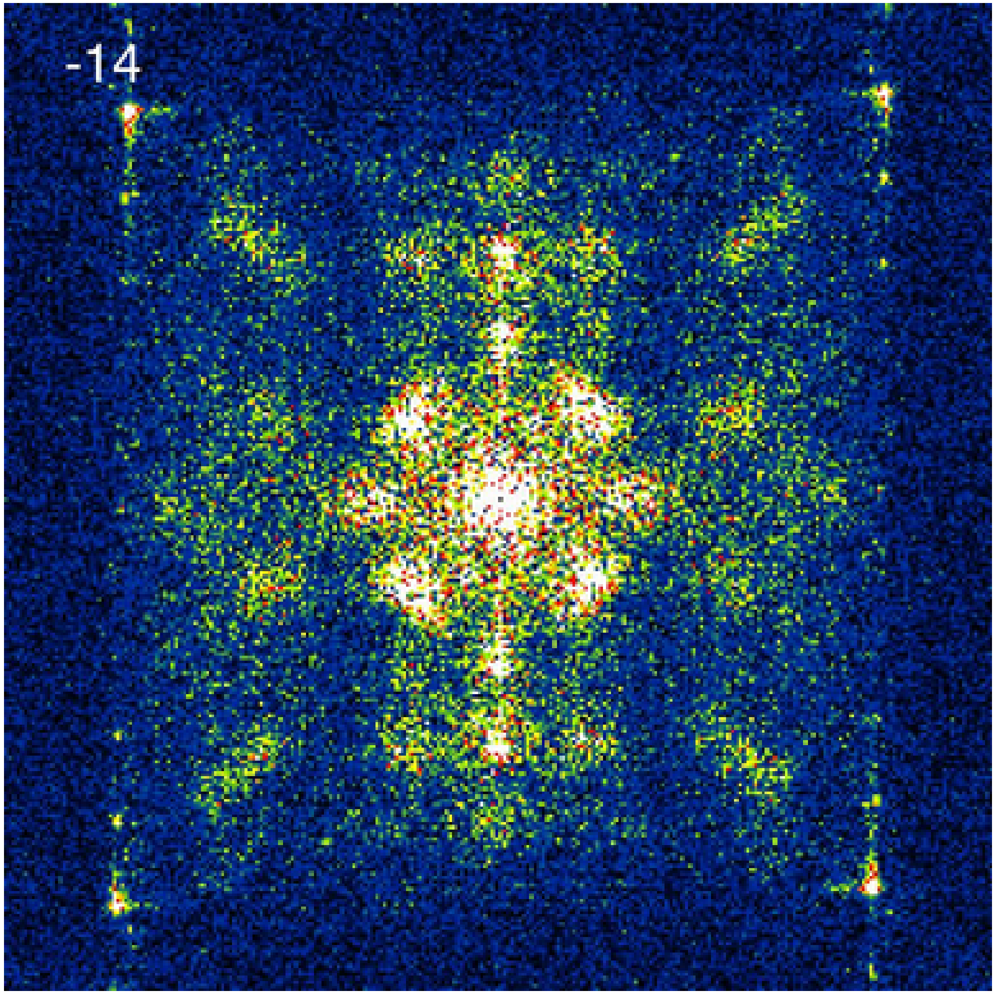
-14

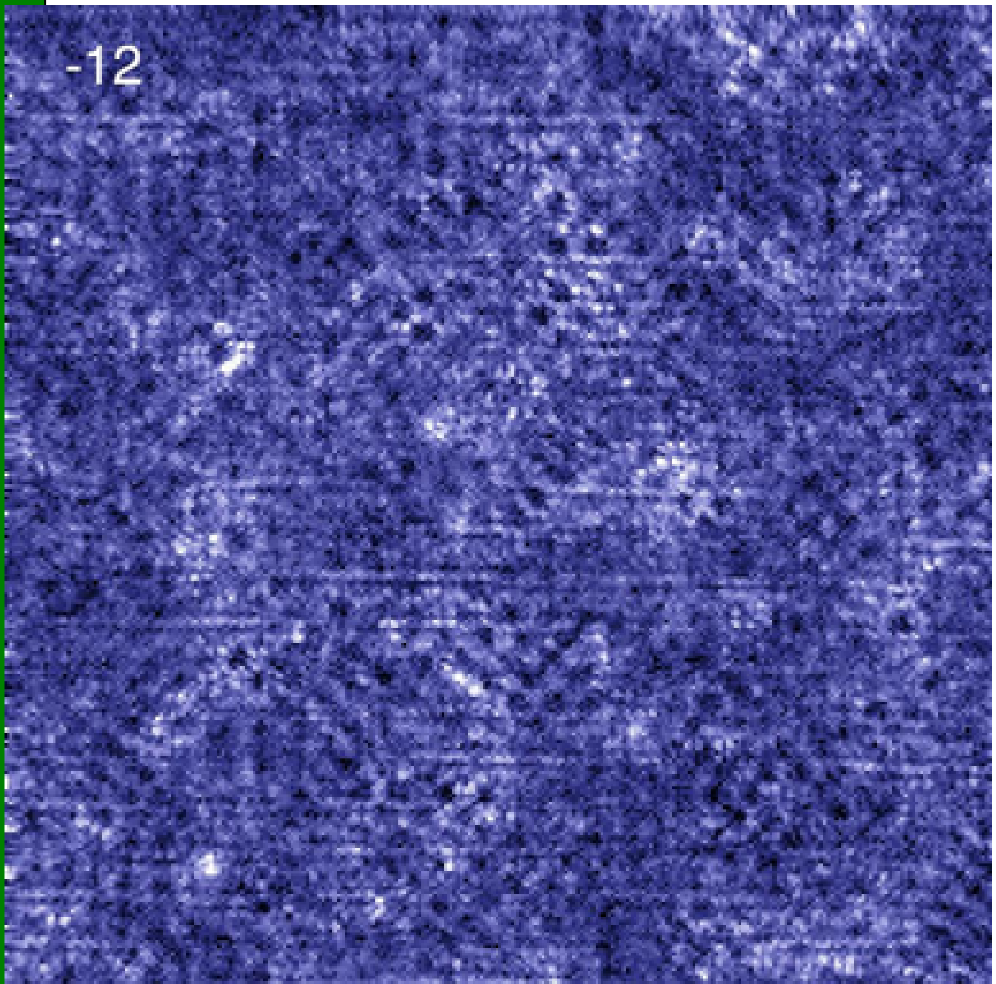
-12

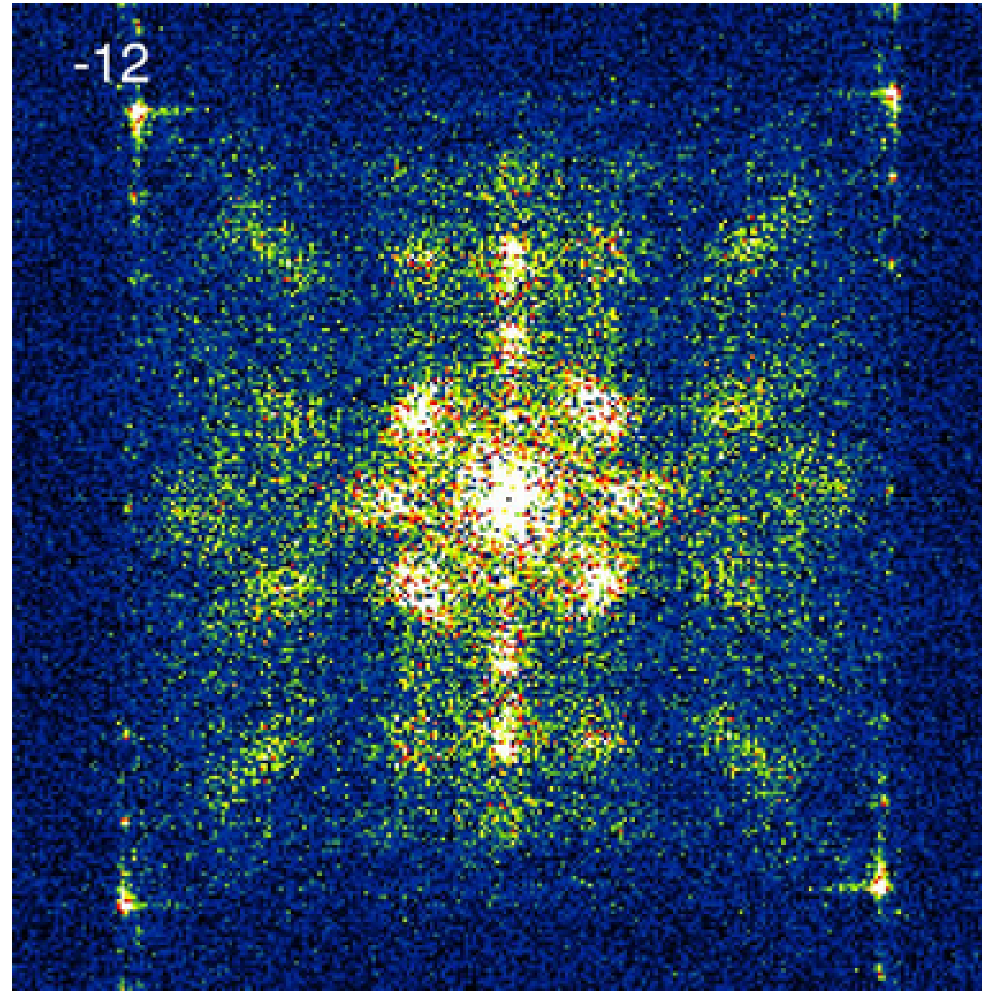
-12

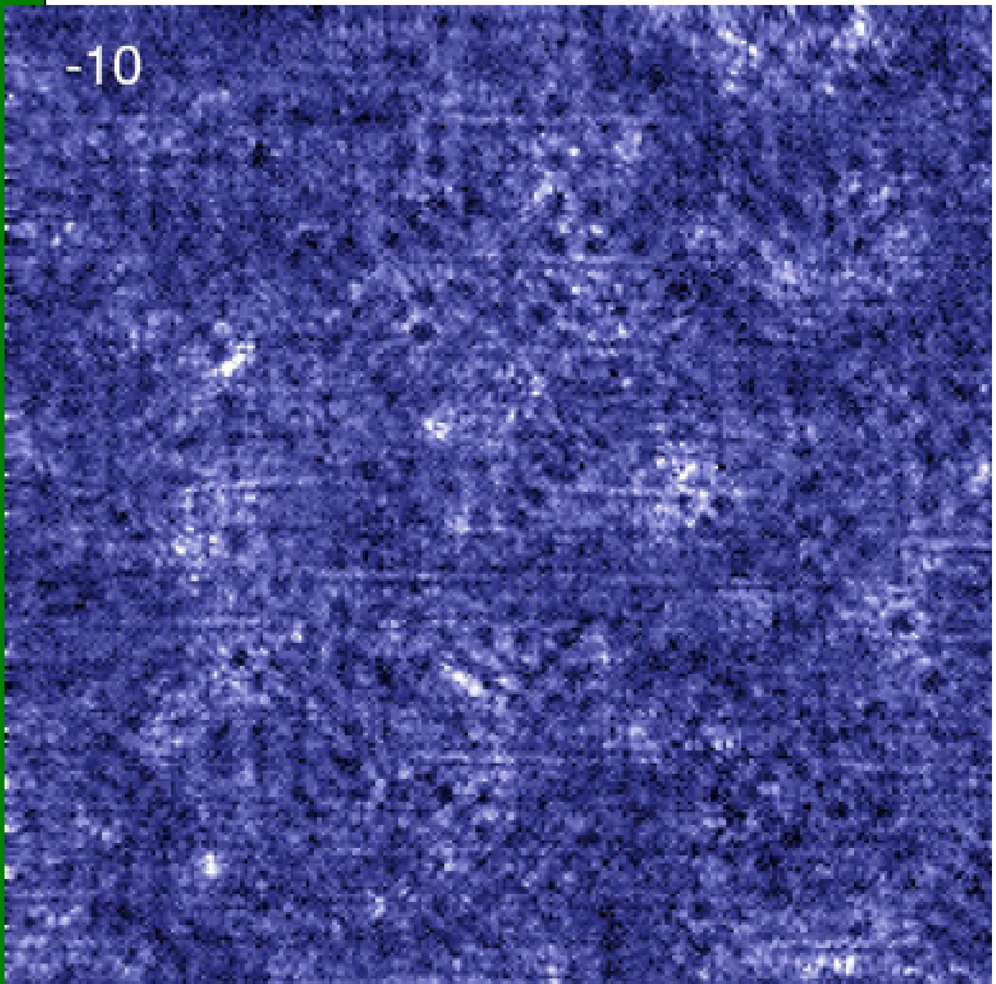

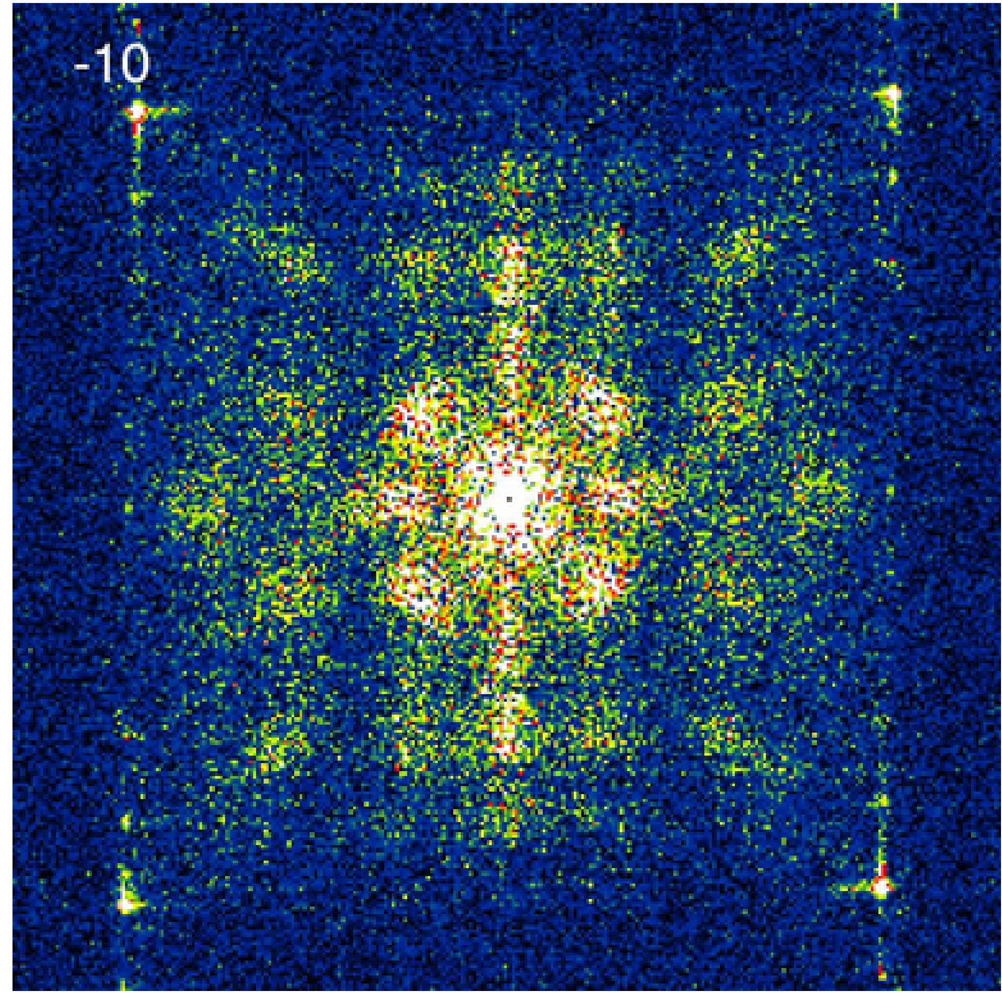

UNIVERSITÉ DE
SHERBROOKE

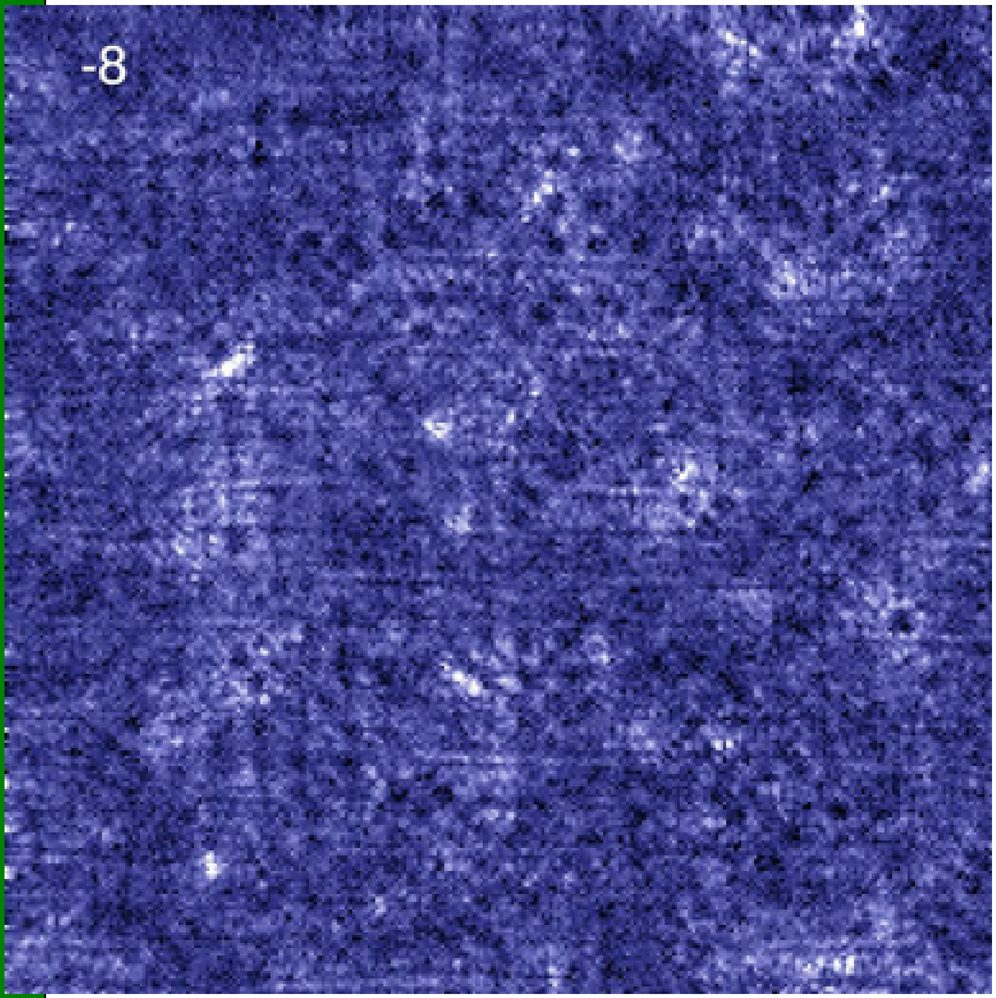
-8

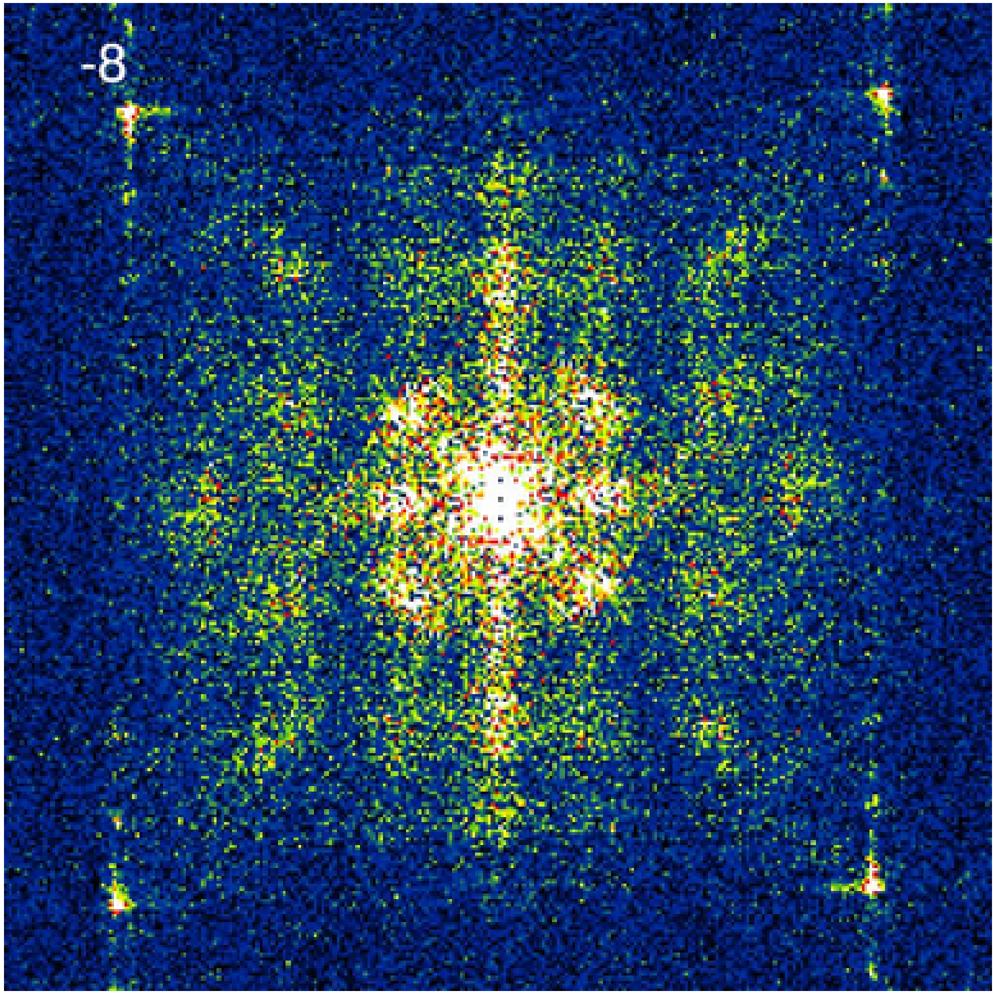
-8

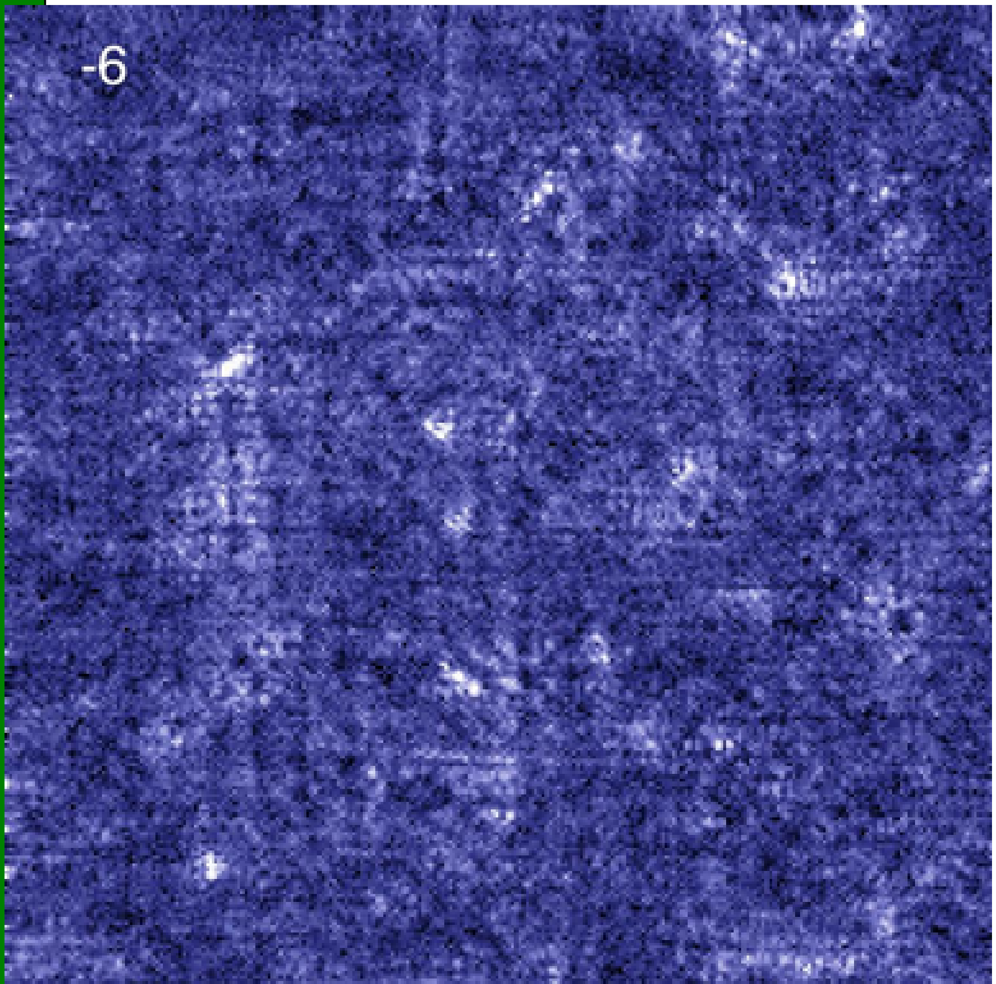
-6

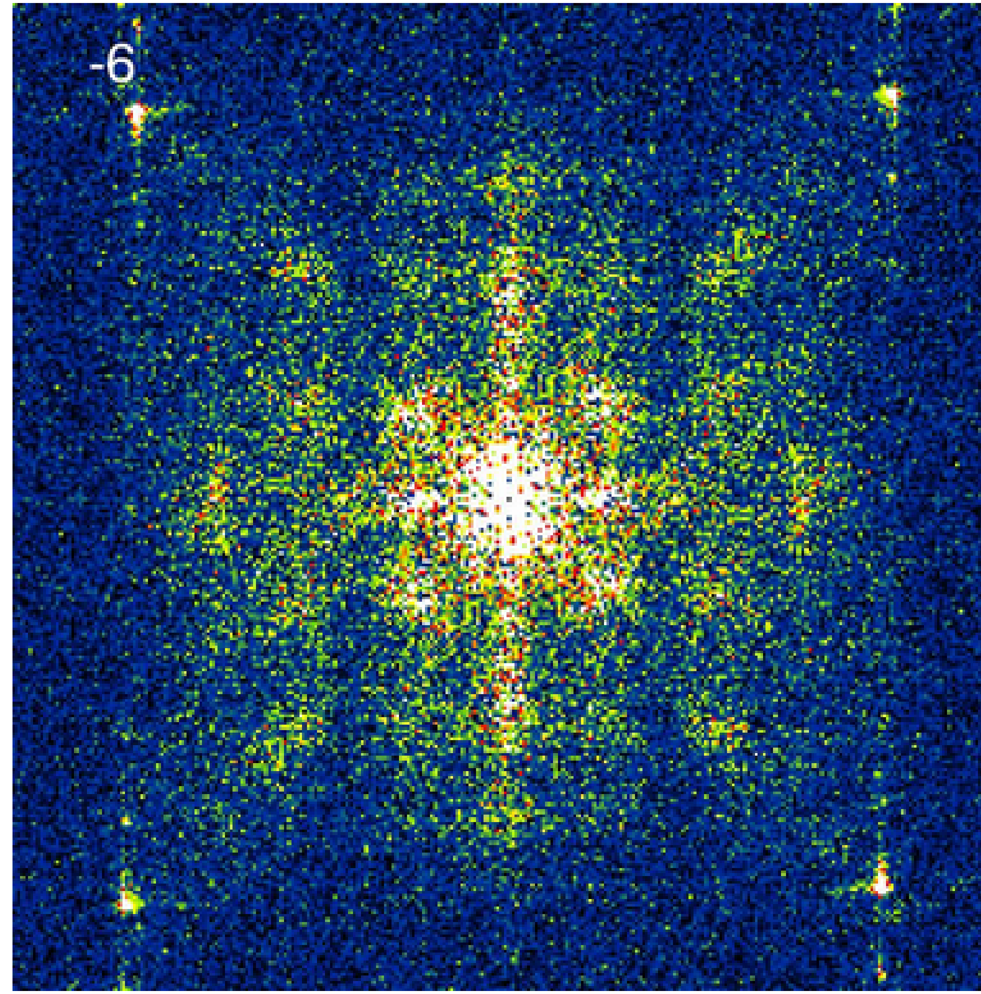
-6

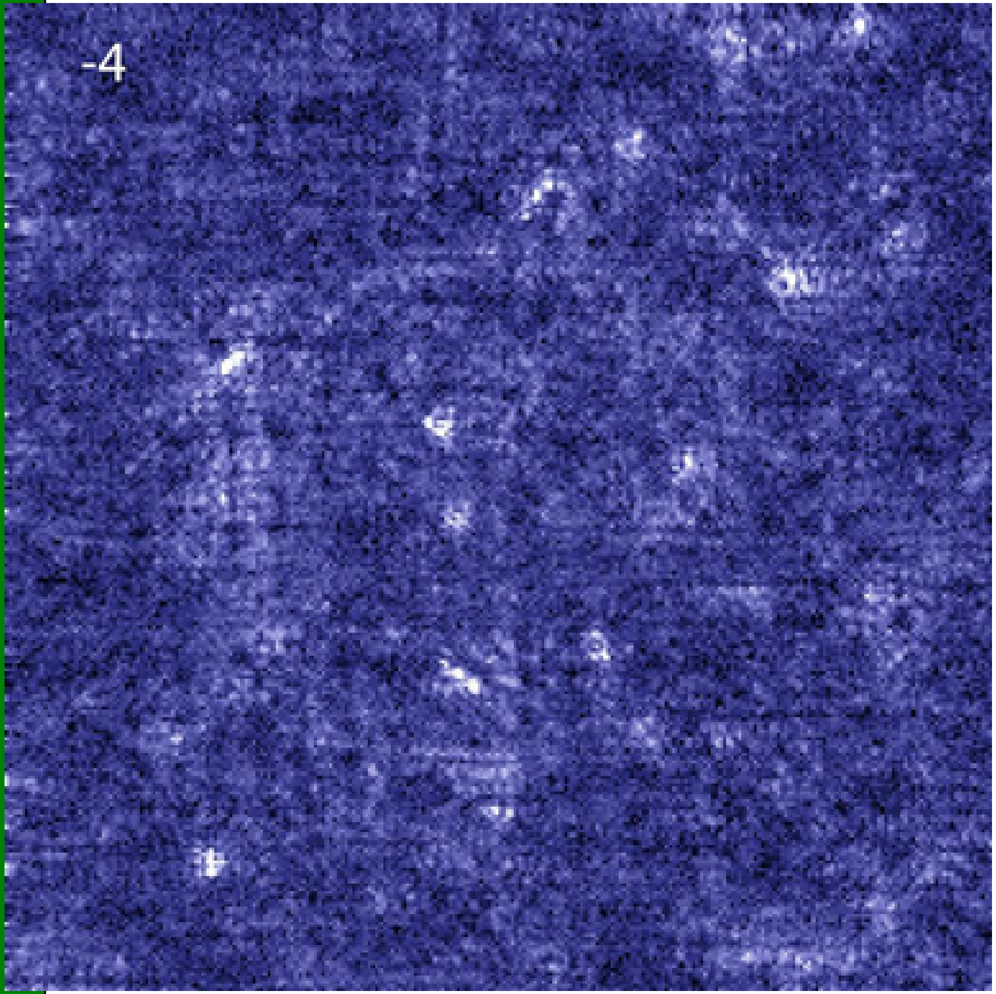
-4
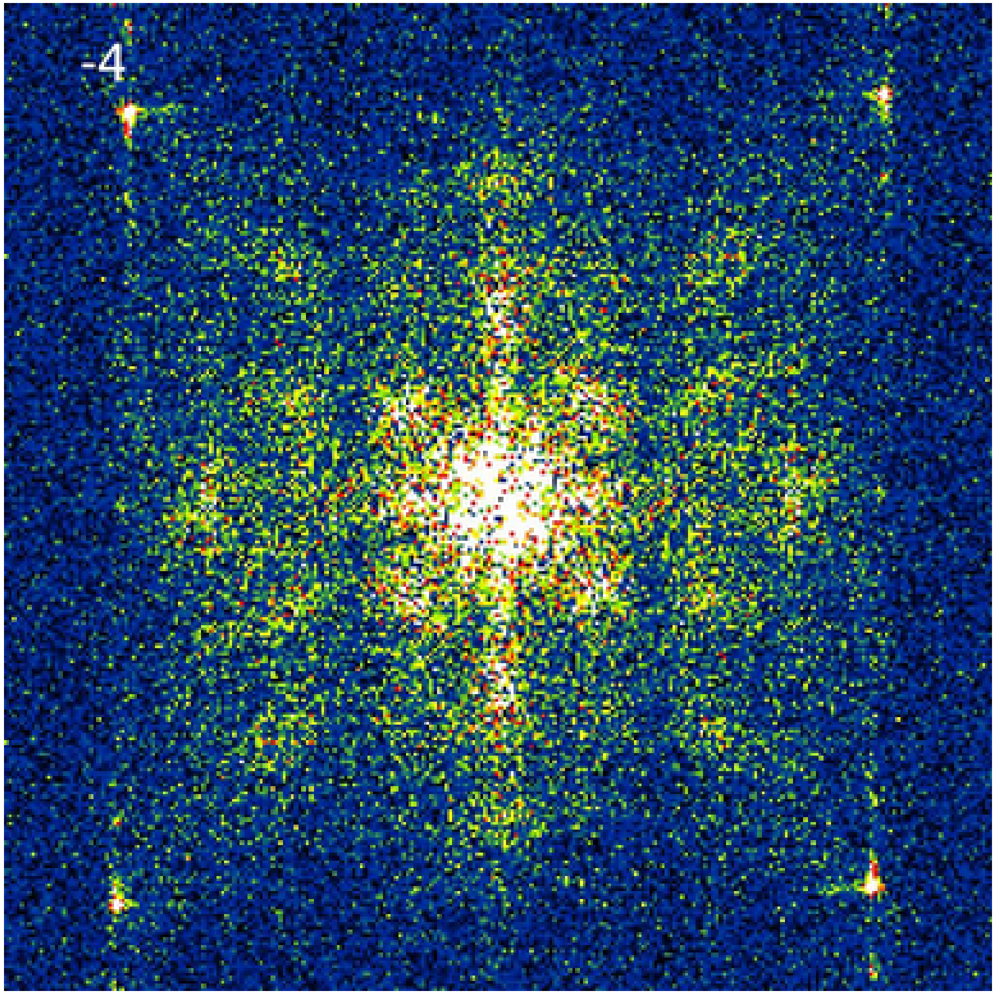
-4

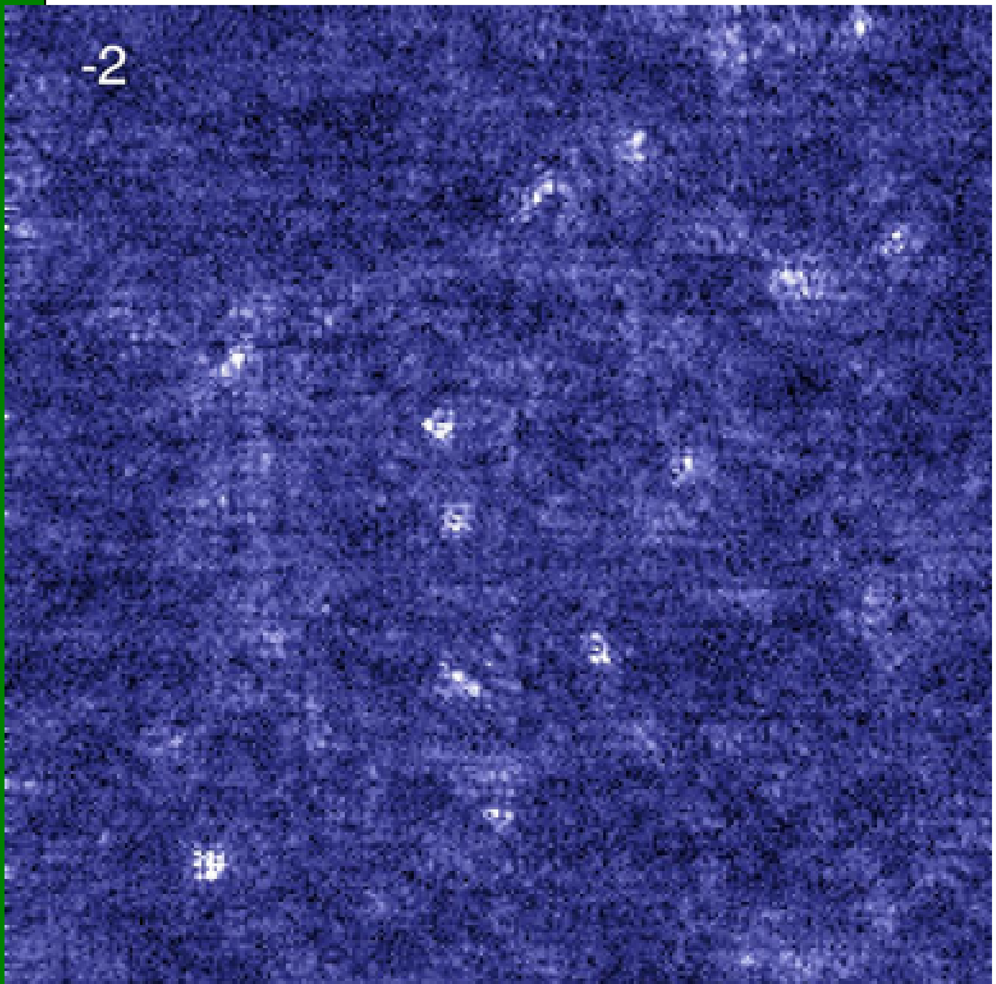
-2

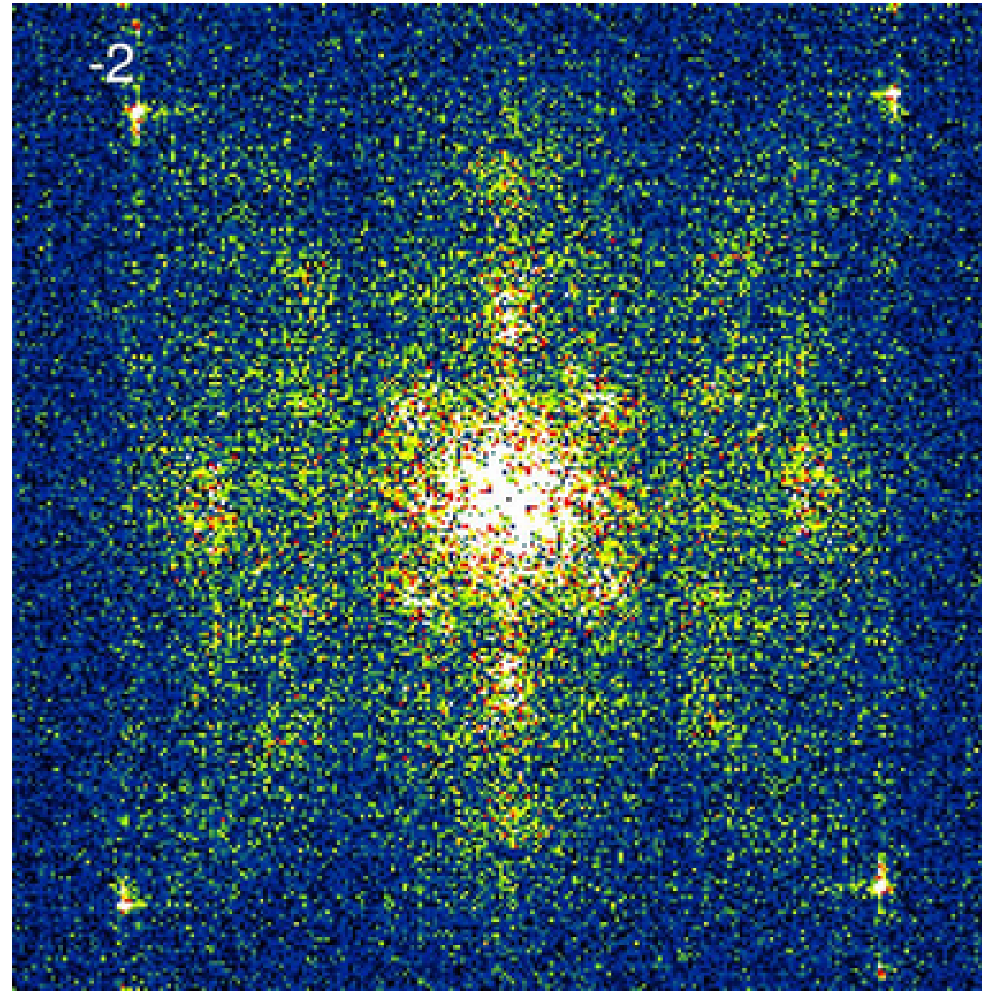
-2

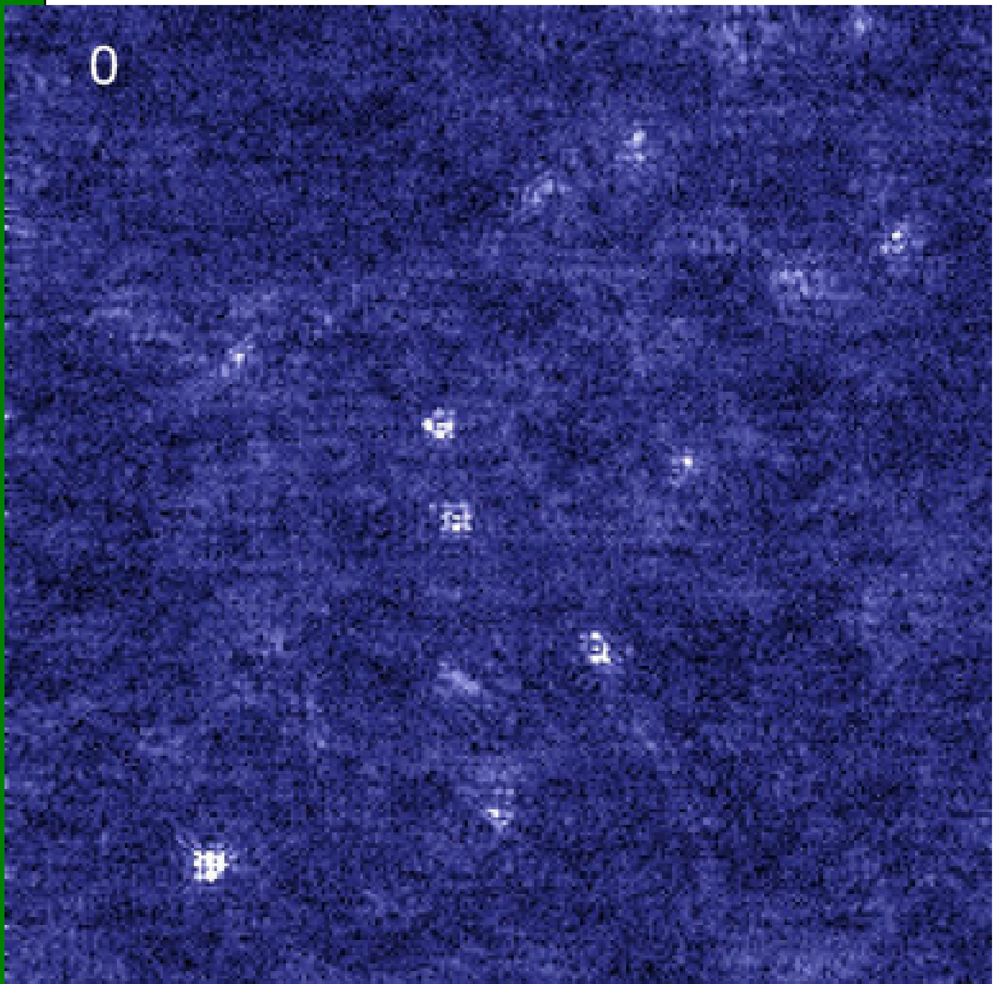

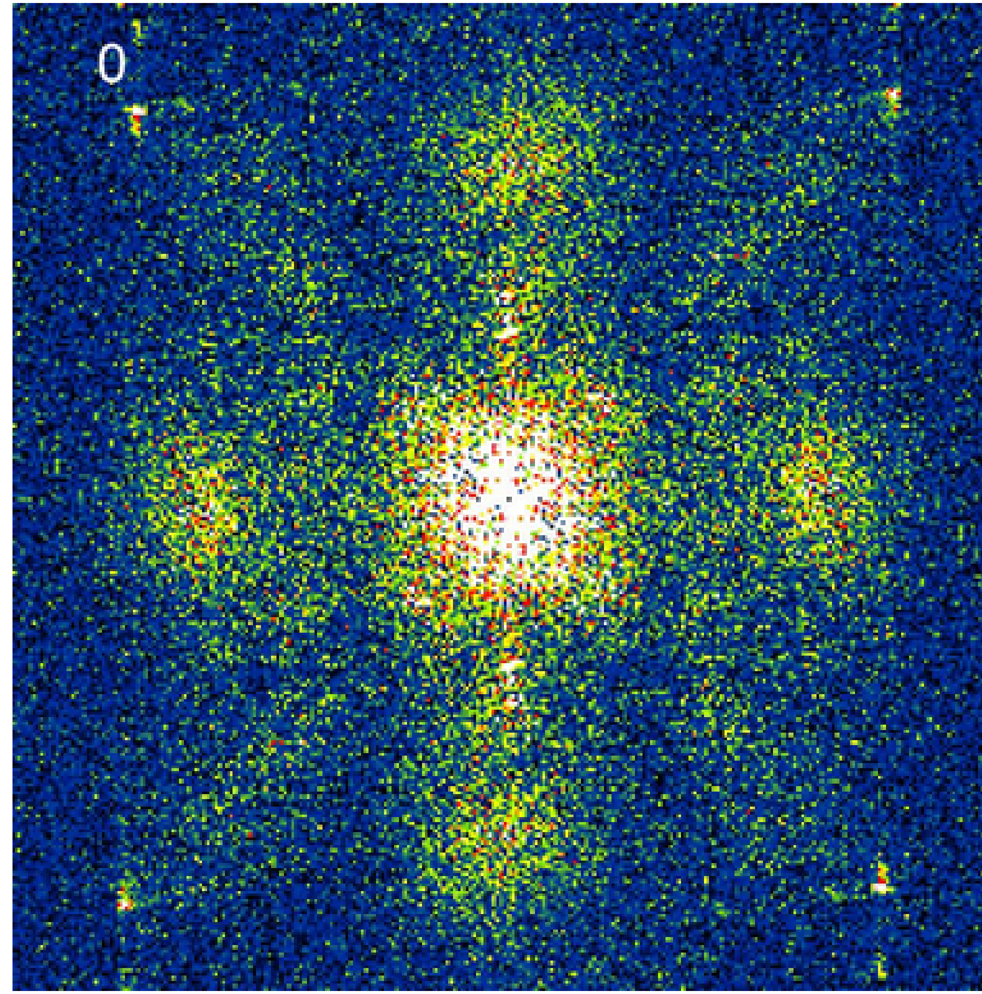

UNIVERSITÉ DE SHERBROOKE

ARPES & STM: Fermi surface comparison

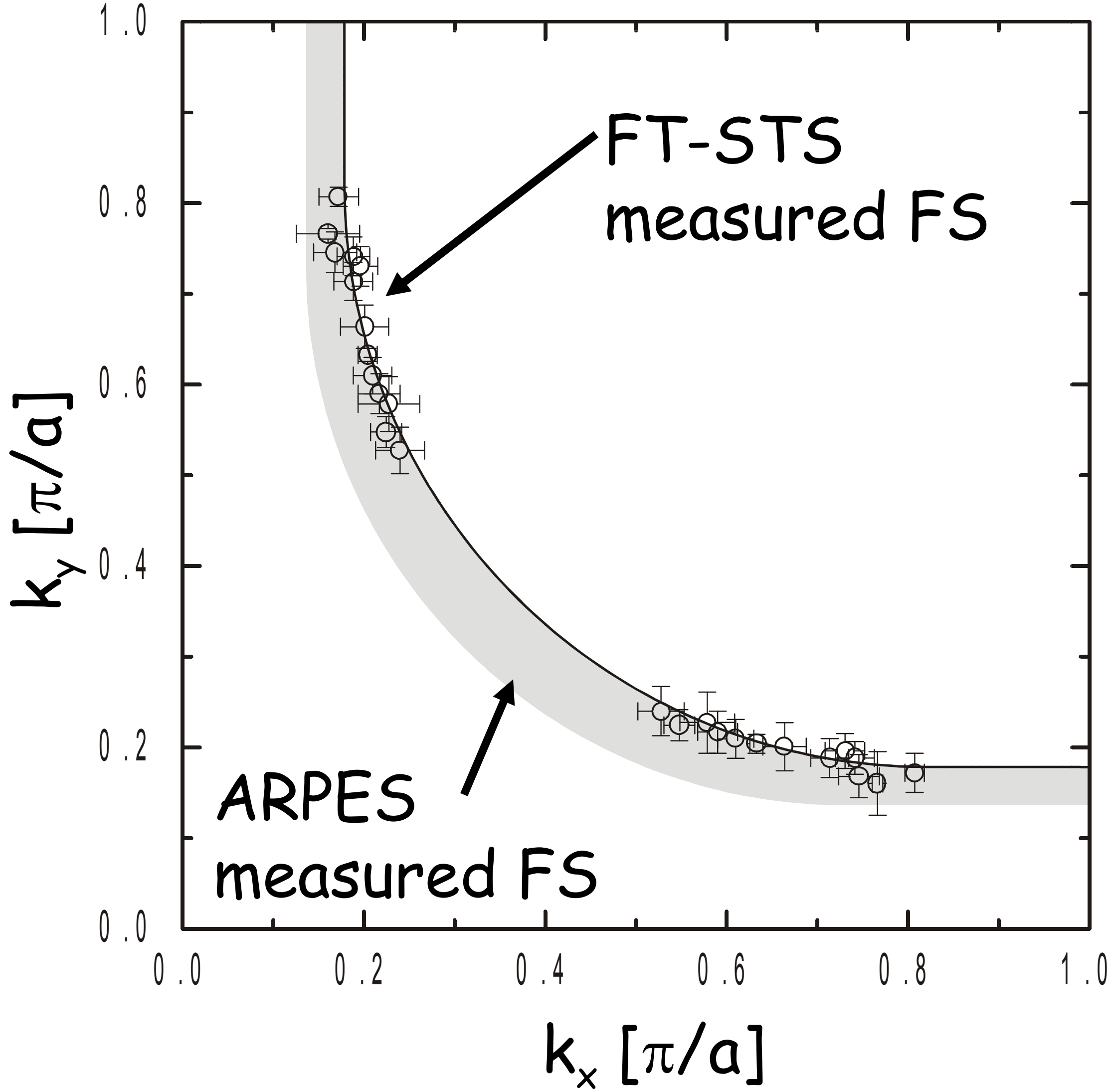

Nature, April 10, 2003

Works because
•Quasiparticle scattering
•Angular dependence of gap

FT-STS $|\Delta(k)|$: Reasonable agreement with ARPES

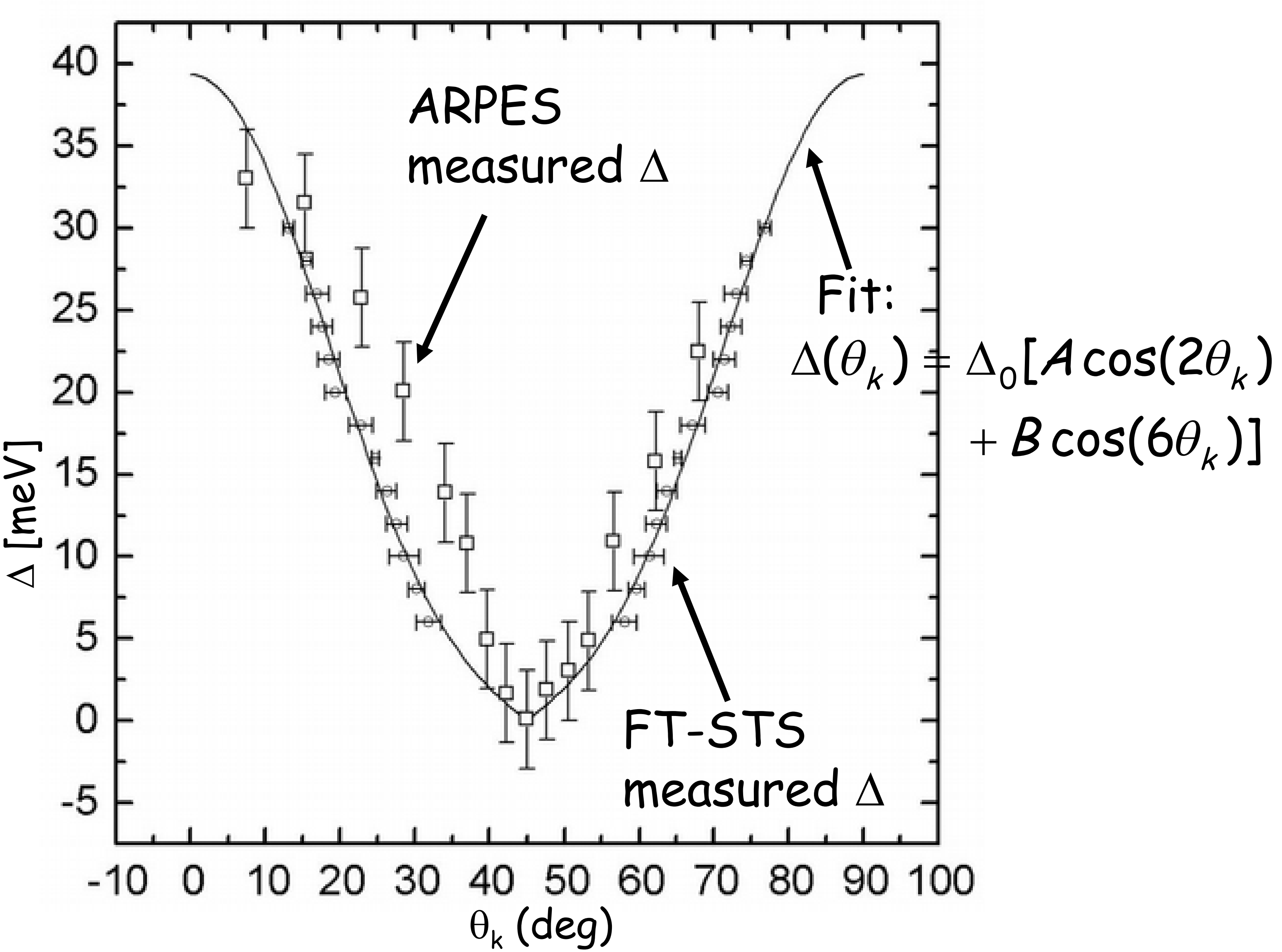

Nature, April 10, 2003

QPI et facteur cohérence

u_k et v_k

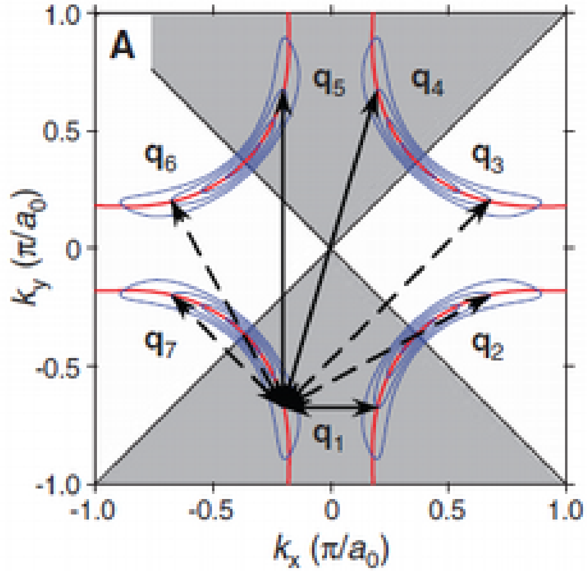

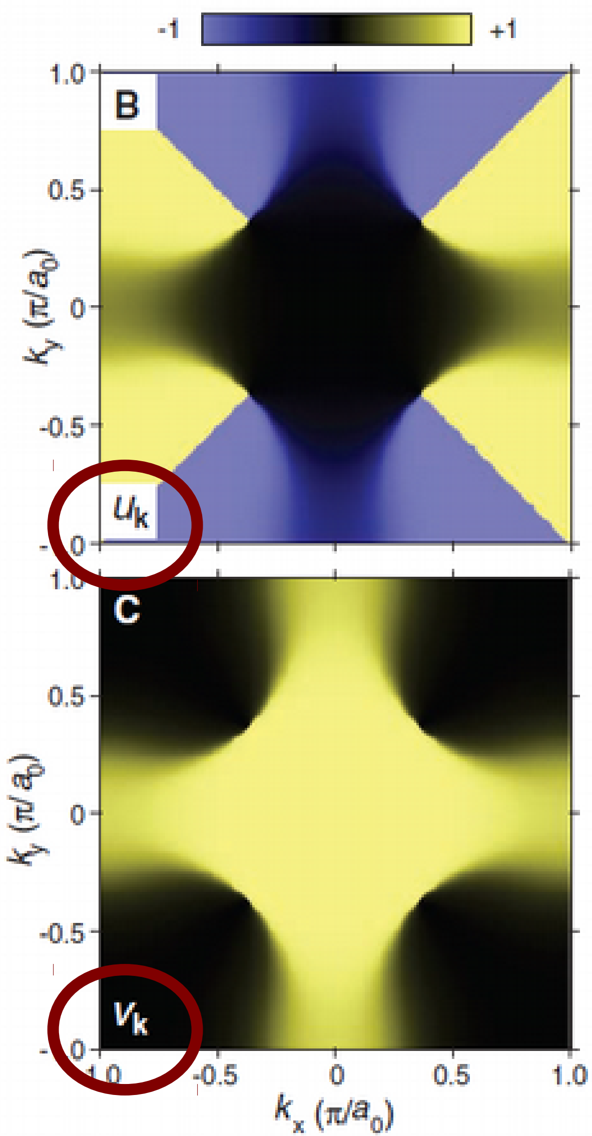

Fig. 1. Representation of **k**-space electronic states in a high-T_c cuprate. (**A**) Normal-state Fermi surface (red curves) and contours of constant energy for Bogoliubov quasi-particles (blue curves) in the first Brillouin zone. White and shaded areas represent **k**-space regions with opposite signs of *d*-wave SC gap. Arrows denote scattering **q** vectors responsible for QPI patterns. They are classified into sign-preserving and sign-reversing vectors indicated by solid and broken arrows, respectively, according to the relative signs of SC gap between initial and final states. These two kinds of vectors are associated with different coherence factors as summarized in table S1. (**B** and **C**) Bogoliubov coefficients $u_{\mathbf{k}}$ (B) and $v_{\mathbf{k}}$ (C) are mapped in **k** space. Note that $u_{\mathbf{k}}$ changes its sign according to that of SC gap, whereas $v_{\mathbf{k}}$ is always positive.

u_k et v_k se combine pour former Un facteur de cohérence.

u_k change de signe

Hanaguri et al., Science 323, 923 (2009)

Facteur de cohérence

Scatterer	Facteur cohérence	q_i augmenté
Faible scalaire	$\left(u_{k_i} u_{k_f} - v_{k_i} v_{k_f}\right)^2$	2, 3, 6, 7
Magnétique, gradient de phase	$\left(u_{k_i} u_{k_f} + v_{k_i} v_{k_f}\right)^2$	1, 4, 5
Amplitude de gap	$\left(u_{k_i} v_{k_f} + v_{k_i} u_{k_f}\right)\left(u_{k_i} u_{k_f} + v_{k_i} v_{k_f}\right)$	1, 4, 5

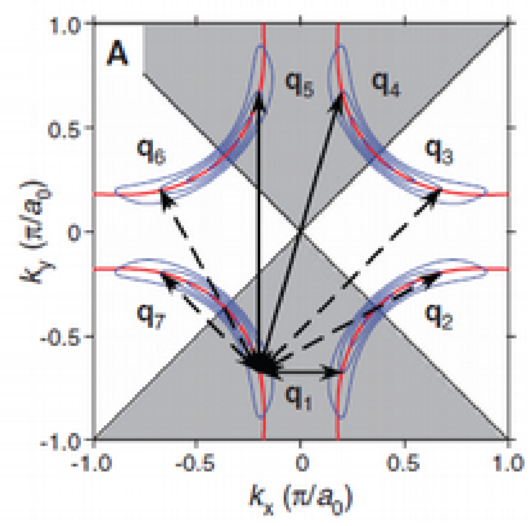

Hanaguri et al., Science 323, 923 (2009)

Effet du champ $Ca_{2-x}Na_xCuO_2Cl_2$
T= 1.6 K (x ~ 0.14 and Tc ~ 28 K)

Champ Magnétique

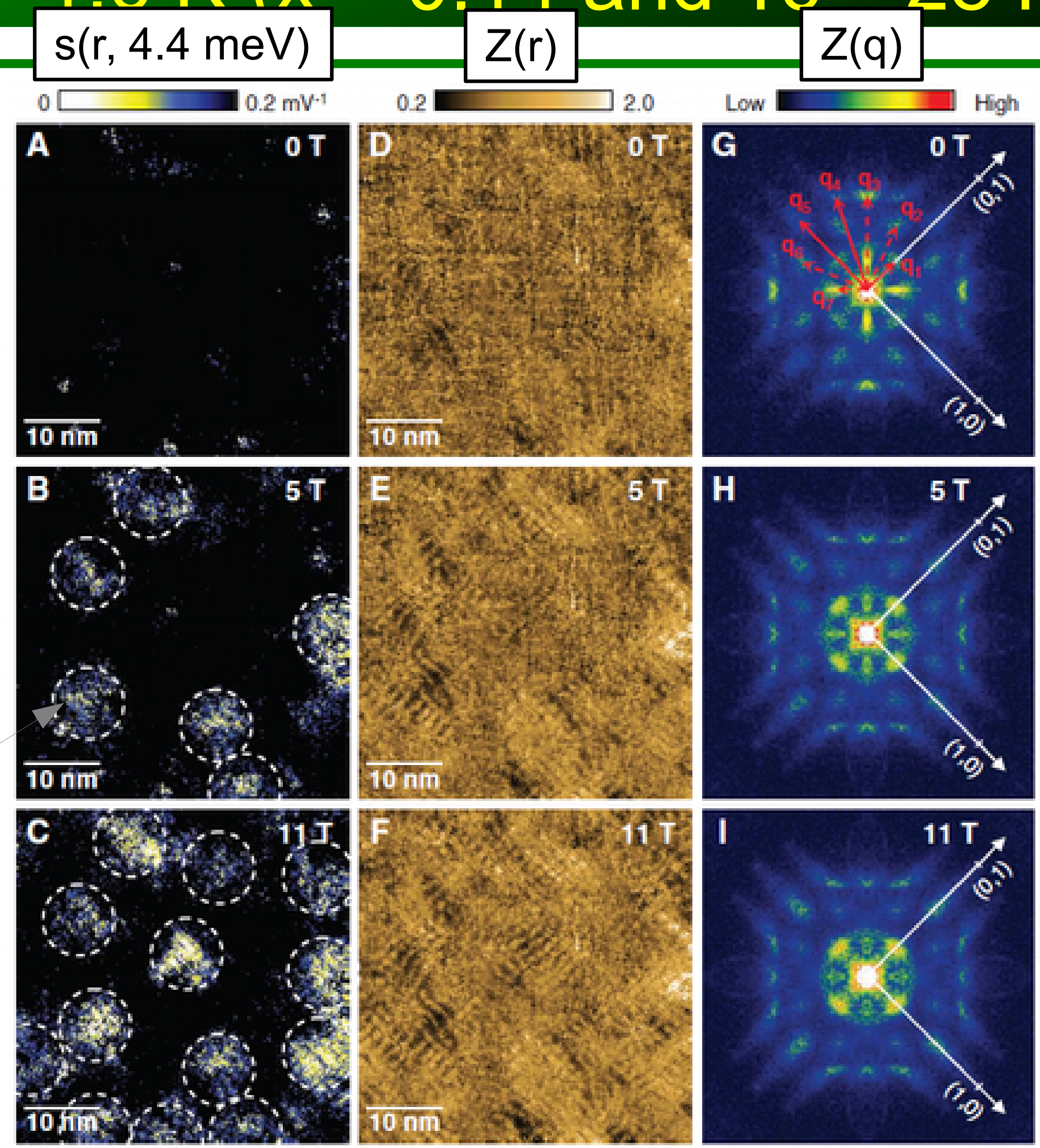

Vortex

Hanaguri et al., Science 323, 923 (2009)

Spatial effect

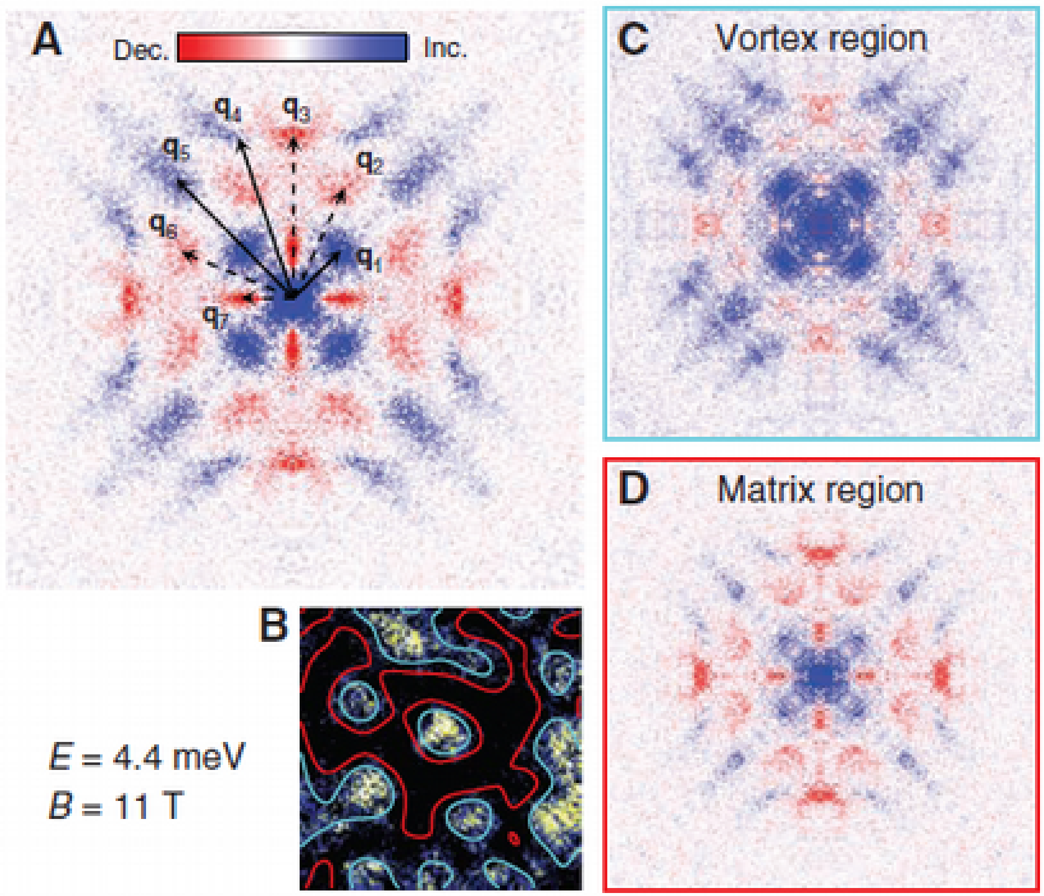

Fig. 3. Magnetic-field-induced weight transfer in $|Z(\mathbf{q}, E)|$ at $E = 4.4$ meV. (**A**) The difference map $|Z(\mathbf{q}, E, B)| - |Z(\mathbf{q}, E, B = 0)|$ for $B = 11$ T (namely, difference between Fig. 2I and Fig. 2G). Intensities of sign-preserving $\mathbf{q}$ points are field-enhanced, whereas those of sign-reversing ones are field-suppressed. (**B**) Vortex image reproduced from Fig. 1C showing the restricted field of views. Blue and red lines surround vortex and matrix regions, respectively (fig. S2). Magnetic-field-induced weight transfers are deduced separately for vortex and matrix regions as shown in (**C**) and (**D**), respectively. Intensities are normalized according to the area. Enhancement of sign-preserving scatterings at $\mathbf{q}_1$, $\mathbf{q}_4$, and $\mathbf{q}_5$ is remarkable near the vortices, whereas it is weak in the matrix region.

Hanaguri et al., Science 323, 923 (2009)

Némacité (dépendance rotationnelle)

Phase field

Fig. 2. (**A**) Smectic modulations along x direction are visualized by Fourier filtering out all the modulations of $Z(\vec{r},e=1)$ except those surrounding $\vec{S}_x$, in the FOV indicated by the broken boxes in Fig. 1B and in (C). (**B**) Smectic modulations along y direction are visualized by Fourier filtering out all the modulations of $Z(\vec{r},e=1)$ except those surrounding $\vec{S}_y$, in the FOV indicated by the broken boxes in Fig. 1B and in (D). (**C** and **D**) Phase field $\varphi_1(\vec{r})$ and $\varphi_2(\vec{r})$ for smectic modulations along x and y direction, respectively, exhibiting the topological defects at the points around which the phase winds from 0 to 2π (in the FOV same as in Fig. 1B). Depending on the sign of phase winding, the topological defects are marked by either white or black dots. The broken red circle is the measure of the spatial resolution determined by the cut-off length (3σ) in extracting the smectic field from $\tilde{Z}(\vec{q},e=1)$. We did not mark defect-antidefect pairs when they are tightly bound by separation distances shorter than the cut-off length scale.

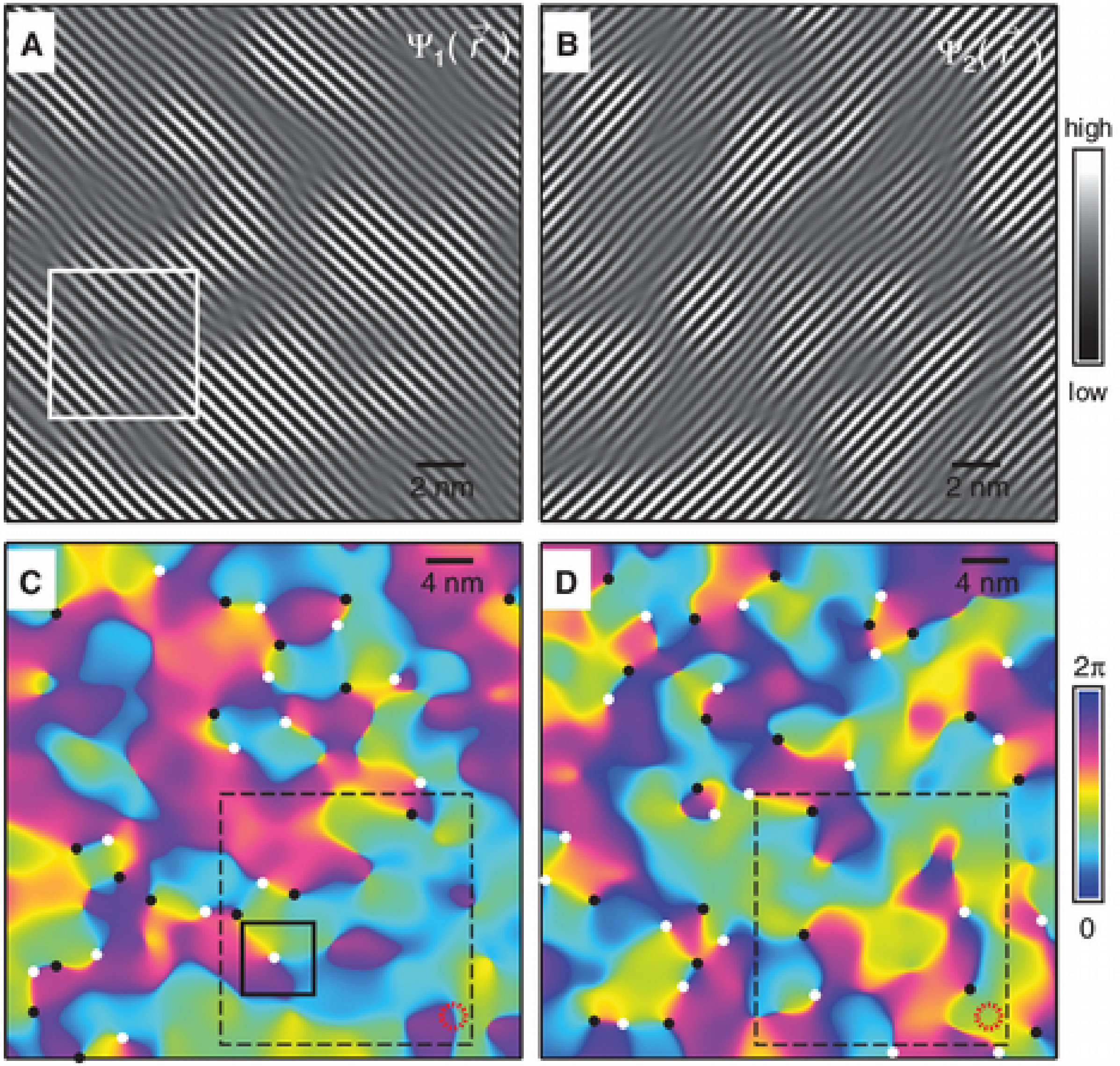

Careful about tip shape

Mesaros et al., Science 333, 426 (2011)

d-symmetry form factor density wave (dFF-DW)

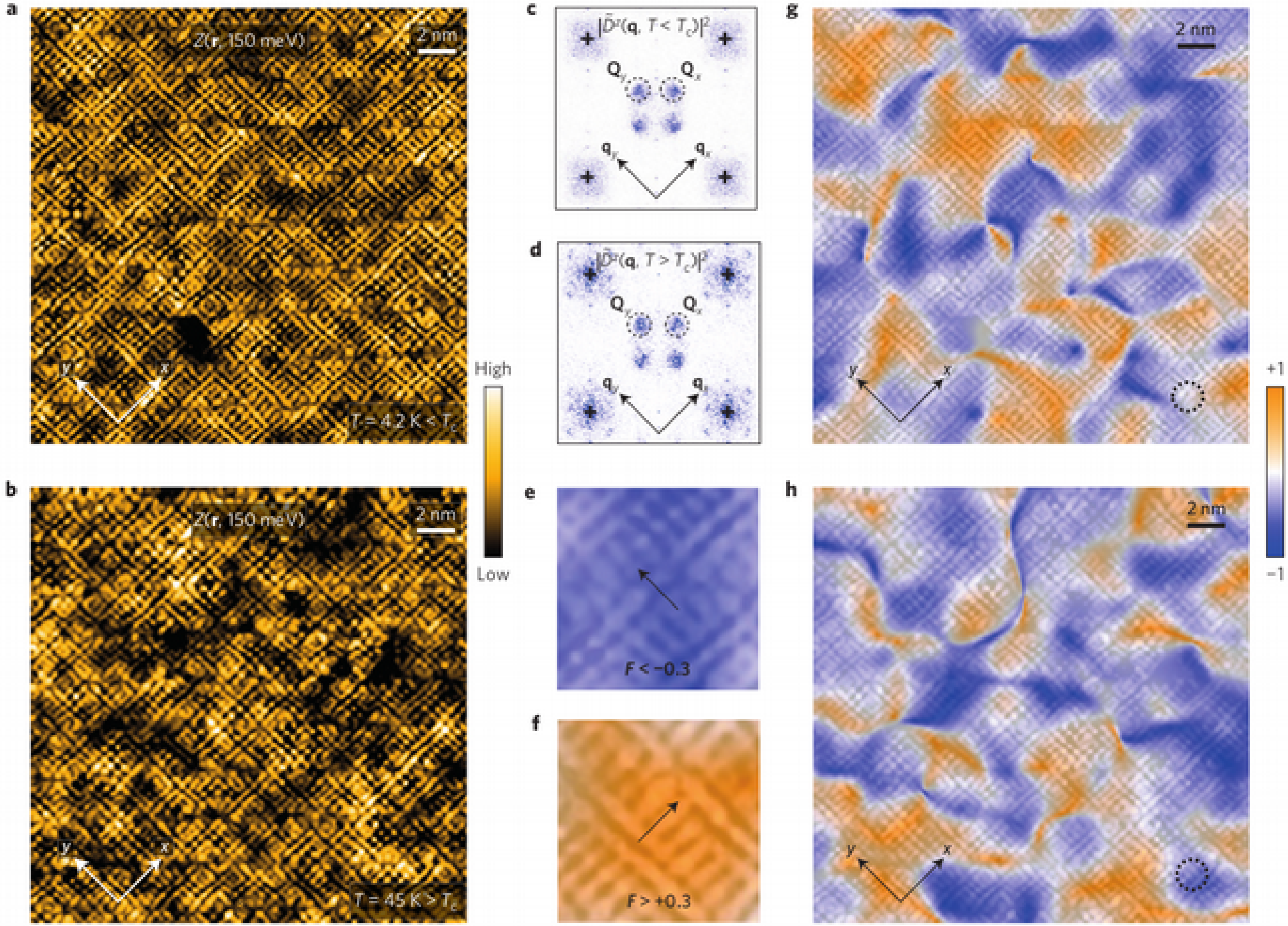

Hamidian et al., Nature Physics 12, 150 (2016)

Mesure Josephson (densité supra)

BSSCO tip

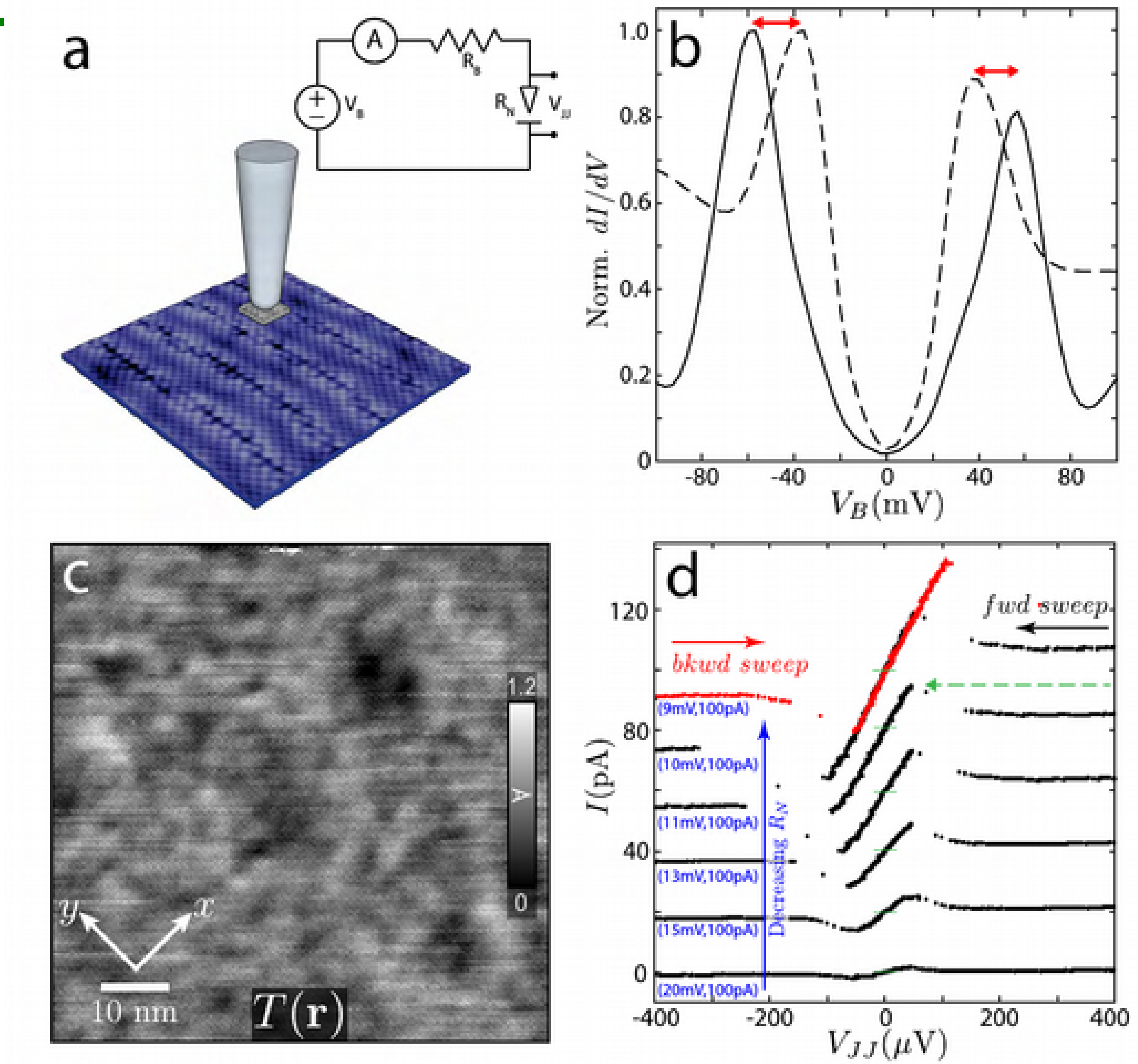

M. H. Hamidian et al., arXiv:1511.08124 (2015)

Josephson critical current imaging

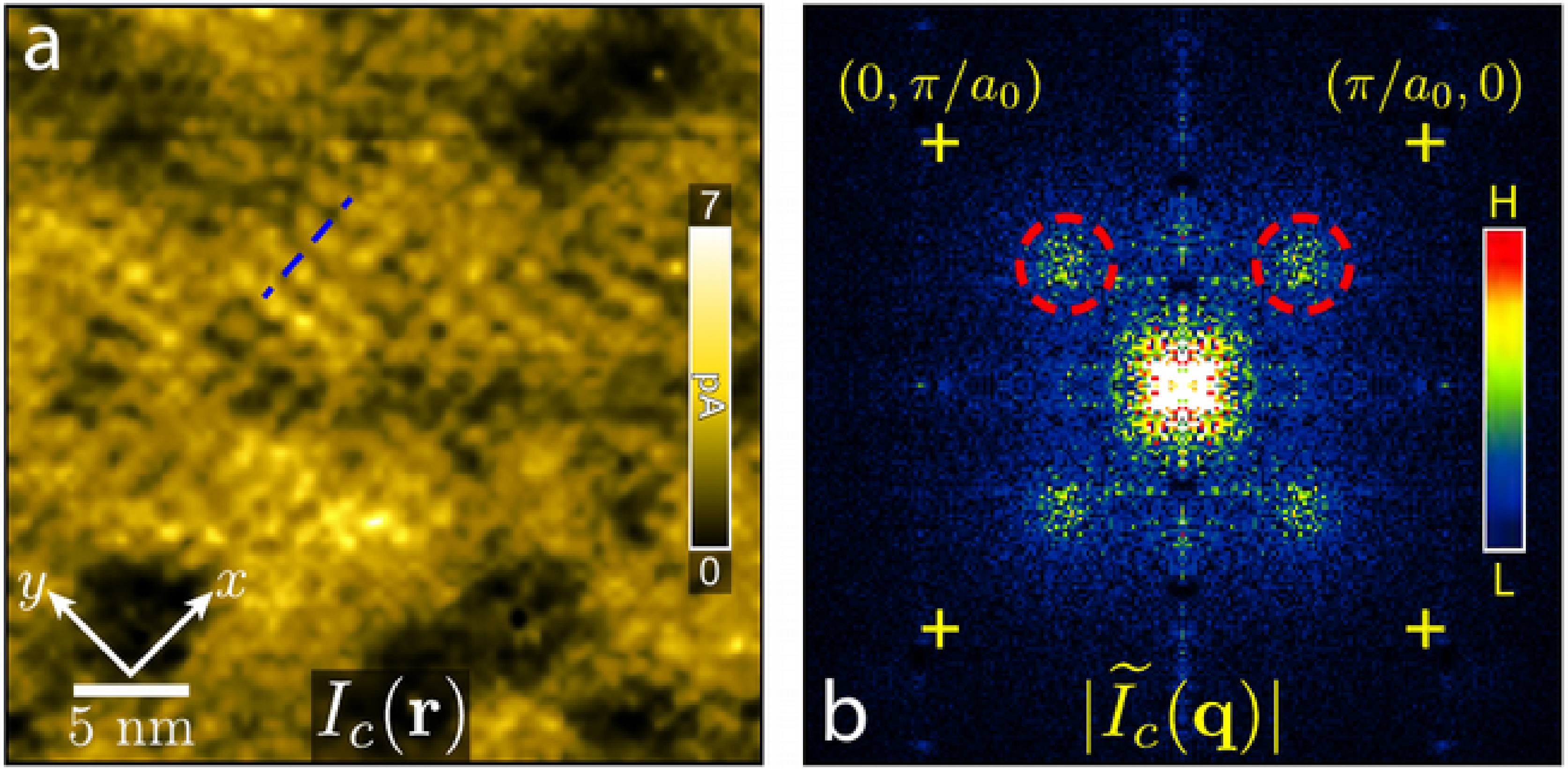

M. H. Hamidian et al., arXiv:1511.08124 (2015)

Conclusion

- STM est technique de surface puissante
- Beaucoup d'information est disponible (différentes analyses)
- Mais attention aux approximations et détails.
- Useful reference :

Spectroscopic Imaging STM: Atomic-scale visualization of electronic structure and symmetry in underdoped cuprates
K. Fujita, M. Hamidian, I. Firmo, S. Mukhopadhyay, C. K. Kim, H. Eisaki, S. Uchida, J. C. Davis
Chapter 3, Strongly Correlated Systems - Experimental Techniques by Springer (ISBN 978-3-662-44132-9)
http://davisgroup.lassp.cornell.edu/publicationPDF/Springer_SCSET_chapter3.pdf